Tailoring the performance of thin film nano composite reverse osmosis polyamide membranes for water desalination applications

By

Saba Ibrar

Department of Physics

Quaid-i-Azam University

Islamabad, Pakistan

Session (2021-2023)

Registration No.02182113008

Tailoring the performance of thin film nano composite reverse osmosis polyamide membranes for water desalination applications

A thesis submitted to the Department of Physics, Quaid-i-Azam University, Islamabad, in partial fulfillment of the requirements for the degree of

Master of Philosophy

In

Physics

By

Saba Ibrar

Department of Physics

Quaid-i-Azam University,Islamabad, Pakistan

Session (2021-2023)

Registration No.02182113008

Dedication

This thesis is dedicated to my parents and brothers for their endless love, support and encouragement. Your boundless support, both emotionally and financially, has made it possible for me to pursue my dreams and reach this academic milestone. This thesis is a tribute to your enduring faith in my potential and a reflection of the values you have instilled in me and I am eternally grateful for all that you have done.

DECLARATION

I, **Saba Ibrar,** MPhil Scholar of Quaid –i-Azam university, hereby declare that the research work entitled "**Tailoring the performance of thin film nano composite reverse osmosis polyamide membranes for water desalination applications**" done by me is original. To the best of my knowledge, it contains no material written by another person or previously published except where due acknowledgement or reference has been made. I also declare that I am aware of terms 'copyright 'and 'plagiarism', and that in case of any copyright violation or plagiarism found in this work, I will be held fully responsible of the consequences of any such violation.

Date:12/12/2023

Signature of Students

Saba Ibrar

Reg.no.02182113008

CERTIFICATE

It is hereby certified that the work presented by **Saba Ibrar** D/O **Muhammad Ibrar** in this thesis entitled "**Tailoring the performance of thin film nano composite reverse osmosis polyamide membranes for water desalination applications**" is based on results of research conducted by candidate under my supervision. No portion of this work has been formerly been offered for higher degree in this university or any other institute of learning and to best of author's knowledge no material has been used in this thesis which is not his own work, except where due acknowledgement has been made. She has fulfilled all the requirements and qualified to submit this thesis in partial fulfillment of the degree of M.Phil. in Physics, at Quaid-i-Azam University, Islamabad.

 Supervisor   _____

Dr. Naveed Zafar Ali

Principal Scientist

Department of EPD

National Centre for Physics (NCP)

Islamabad, Pakistan

Chairman Department of Physics   _____

Dr. Kashif Sabeeh

Department of Physics

Quaid-i-Azam University

Islamabad,Pakistan

ACKNOWLEDGMENTS

"If you are grateful, I would certainly give you more" *(Surah Al-Luqman)*

Thank you, my Allah, for blessing me with much more than I deserve. Your blessings are like stars that twinkle in my life, giving light to every moment. Alhamdulillah!

I want to express my gratitude to **Dr. Naveed Zafar Ali,** EPD department, National Centre for Physics, Quaid-i-Azam university campus Islamabad, for his technical support and diligent guidance. His motivating direction, insightful advice, energizing encouragement, generous assistance, politeness, courtesy, and kind nature enables me to accomplish my assignment well in time. I greatly benefited from his keen scientific insight for solving practical difficulties and the ability to put complex ideas into simple terms.

I would like to take a moment to offer a cascade of thanks to **Prof. Dr. kashif Sabeeh**, chairman of Department of Physics providing me an opportunity to work in this department. I want to express my gratitude to **Dr. Asif Mahmood** and **Mr. Zahid Mehmood** from Pakistan Institute of Engineering and Applied Science (PIEAS) Islamabad and NS&TD department of National Centre for Physics, Quaid-i-Azam university campus Islamabad, for characterizations of synthesized samples.

To my steadfast friends, **Iqra Raza** and **Sadia Alam**, your untiring support and enduring camaraderie have illuminated my journey through life's twists and turns. You have been the pillars of strength, the laughter in my darkest hours, and the constant reminders that friendship is a treasure beyond measure. I would like to acknowledge seniors and lab fellows for listening, offering me advice and supporting me through this entire process of completing my project.

I would like to express my heartfelt gratitude to my father **(Muhammad Ibrar)** and my mother **(Rehana Kousar)** for their love, constant support, and invaluable guidance throughout this journey. Their belief in me has been my driving force. This achievement is as much yours as it is mine. Lastly, a big thanks to my bloodline my brothers **Muhammad Awais, Muhammad Jawad**, who have been my safety net in my highs and lows. May ALLAH showers His countless blessings on them.

Saba Ibrar

1. Table of Contents

LIST OF Figures

List of Tables

Abstract

The development of cutting-edge technologies for effective water desalination is required due to the critical global issue of clean water scarcity. Reverse osmosis (RO) membranes made of thin-film nanocomposite (TFN) layers with incorporated nanomaterials have received substantial research as an energy-efficient material because of their flexible characteristics and improved water/salt separation abilities. Metal organic frameworks (MOFs, also known as porous coordination polymers), which are three-dimensional structures consisting of metal-containing nodes connected by organic linkers, have recently come to be recognized as a novel class of porous materials with a wide range of technological facets. **In this study**, the zeolitic imidazolate frameworks (ZIFs), a subclass of MOFs, were investigated for water desalination applications. ZIFs are an entirely novel, distinctive type of metal organic frameworks consisting of metal ions and imidazole linkers. ZIFs have many advantages, including a large surface area, tunable pore size, controlled topologies, small pore diameter, high thermal or chemical stability, and an abundance of metal as well as organic substances in their scaffolds. These features make ZIFs excellent precursors for the porous carbon and similar nanostructures that can be used as functional materials. **In the current work**, we have synthesized 3D graphene using the direct carbonization approach, as well as several classes of carbon-reinforced ZIF-based hybrid nanostructures, notably ZIF-8 and its individual composites with 3D graphene. The synthesized materials are characterized using XRD, SEM, IR, TGA, EDX, BET, and RAMAN. By employing XRD analysis, it was discovered that ZIF-8 nanoparticles have average crystallite sizes of 19.74 nm crystallizing in the cubic phase, as predicted by the Debye-Scherrer equation. SEM images of ZIF-8 nanoparticles revealed a rhombic dodecahedral geometry exhibiting an apparent uniform size around 133nm and membrane images displayed the usual ridge and valley shape of aromatic polyamide (PA) as well as BET surface area of 1242.548 m^2/g. The prepared sample ZIF-8 displays the major band at 460cm^{-1}, which is the vibration caused by the stretching of Zn-N. ZIF-8 is thermally stable up to 490ºC . The D band (1338 cm^{-1}) and the G band (1574cm^{-1}) are the two peaks of the 3D Graphene's Raman spectra, respectively. The integration of functional nanoparticles is a promising way to improve or generate unique material features, such as

the improvement of permeability or selectivity linked to water filtration and reuse. TFN-RO trilayered membranes were fabricated using top layer of ZIF-8 nanoparticles with different wt% incorporated polyamide membranes, enveloped on polysulfone (as middle layer) overlayered on PET support (bottom layer). The main goal was to examine the precise impacts of porous ZIF-8 nano structures on the separation abilities of TFN membranes. Following this, the ZIF-8 modified TFN membranes' apparent morphology, roughness, or hydrophilicity were altered, which had an impact on the TFN membranes' salt and water rejection capability. Our findings highlighted the significance of MOFs size in further research of TFN membranes including MOFs by showing that the TFN membrane containing ZIF-8 with 0.008wt% showed the best performance owing to the largest dispersion in polyamide layer. The effective incorporation of ZIF-8 nanoparticles in TFN membranes raised the water permeation of TFN-ZIF-8(0.008wt%) to 2.84 $Lm^{-2}h^{-1}bar^{-1}$, with the maximum NaCl rejection to 95.56% compared with pristine TFC and other wt% of ZIF-8/PA TFN membranes. The as synthesized membranes show the better potential for its use in water desalination applications.

Chapter 1

1.INTRODUCTION

The socio-economic well-being of a country is closely related to its resources, and water plays an essential role in its development. The issue of water scarcity is becoming more prominent globally due to factors like climate change, increased industrialization, and population growth. In 2015, the United Nations established Sustainable Development Goals (SDGs) that prioritize the availability of reliable and sufficient water as a key factor. Ensuring an adequate supply of portable water is a critical issue as population growth and rapid industrial expansion have negatively impacted both the quality and quantity of water necessary for various aspects of life[1] .The Asian Pacific regions, including Pakistan, are not exempt from the multiple challenges related to water and achieving sustainable development goals. Pakistan, specifically, is confronted with both water scarcity and water quality issues [2]. The qualitative challenges related to water encompass the presence of bacteriological contaminants, toxic metals, pesticides, and an excess of dissolved salts and metal ions. Moreover, there is a growing concern regarding water scarcity, with a current per annum availability of 1050 cubic meters of water per capita for Pakistan's anticipated population of 200 million people. However, as the population continues to increase, the situation is expected to worsen, with projections indicating a population of 220 million by 2025. This poses a significant challenge as per capita freshwater availability is estimated to decline to around 800 cubic meters by 2025, indicating a state of water scarcity. Water is an essential and renewable resource that sustains life naturally. However, it is not evenly distributed in its different forms. Saline water makes up about 97.5% of the total water on Earth, while freshwater accounts for only 2.5%. Out of this freshwater, approximately 31.1% is found in rivers, and underground aquifers, which are used for human requirements. A significant portion of the remaining freshwater is confined in ice caps, as displayed in Figure 1.1. The World Economic Forum (WEF) has identified water as the 4th most impactful and 9th most probable crisis in its global risk report. Water scarcity refers to the lack of availability or access to safe drinking water due to physical limitations or excessive demand. Over the past century, water consumption has risen at a rate more than double that of population growth. As a result, numerous regions, particularly arid areas,

are approaching the maximum sustainable limit for providing water facilities. Consequently, water is a vital resource essential for the survival of all living beings. Surprisingly, out of the global population of 7.85 billion people, only one in every nine individuals currently has access to clean water. Approximately 30% of people worldwide lack access to fresh water sources, even for elementary sanitation essentials. In the near future, it is predicted that 60-70% of the global population will reside in areas facing critical conditions of severe water stress or scarcity[3]. This situation can be attributed to either the physical unavailability of water resources or the economic inability to afford access to existing water sources. It has become a widespread issue observed in different parts of the world. Physical inaccessibility signifies insufficient water resources to address the existing challenges, while economic unaffordability refers to the absence of proper mechanisms to obtain access to water sources in the affected regions.Numerous countries, including the United States, the Middle East, North African regions, parts of Southeastern Europe, South Indian regions, Pakistan, Afghanistan, Mongolia, Tajikistan, Kazakhstan, and certain areas in Western Australia, are primarily experiencing a shortage of accessible water resources[4]. Conversely, specific regions such as Canada, several South American countries, and a few Northern European countries face minimal to no water scarcity. The demand for water in domestic, industrial, and irrigation sectors has reached a critical threshold in numerous regions across the globe. The haphazard release of untreated waste from different industries is leading to a significant global issue of heavy metal contamination.[5] This problem is expected to worsen in the future due to population growth and rapid economic development. Heavy. metals, even in small amounts, are highly toxic, non-biodegradable, and have the ability to accumulate in the environment.[6] This poses serious health risks to humans and demands immediate attention to prevent further harm to both human health and the environment.

Ensuring an adequate supply of portable water is a critical issue as population growth and rapid industrial expansion have negatively impacted both the quality and quantity of water necessary for various aspects of life[7]. The demand for water in domestic, industrial, and irrigation sectors has reached a critical threshold in numerous regions across the globe. The haphazard release of untreated waste from different industries is leading to a significant global issue of heavy metal contamination. This problem is expected to worsen in the future

due to population growth and rapid economic development. Heavy metals, even in small amounts, are highly toxic, non-biodegradable, and have the ability to accumulate in the environment. This poses serious health risks to humans and demands immediate attention to prevent further harm to both human health and the environment[8].
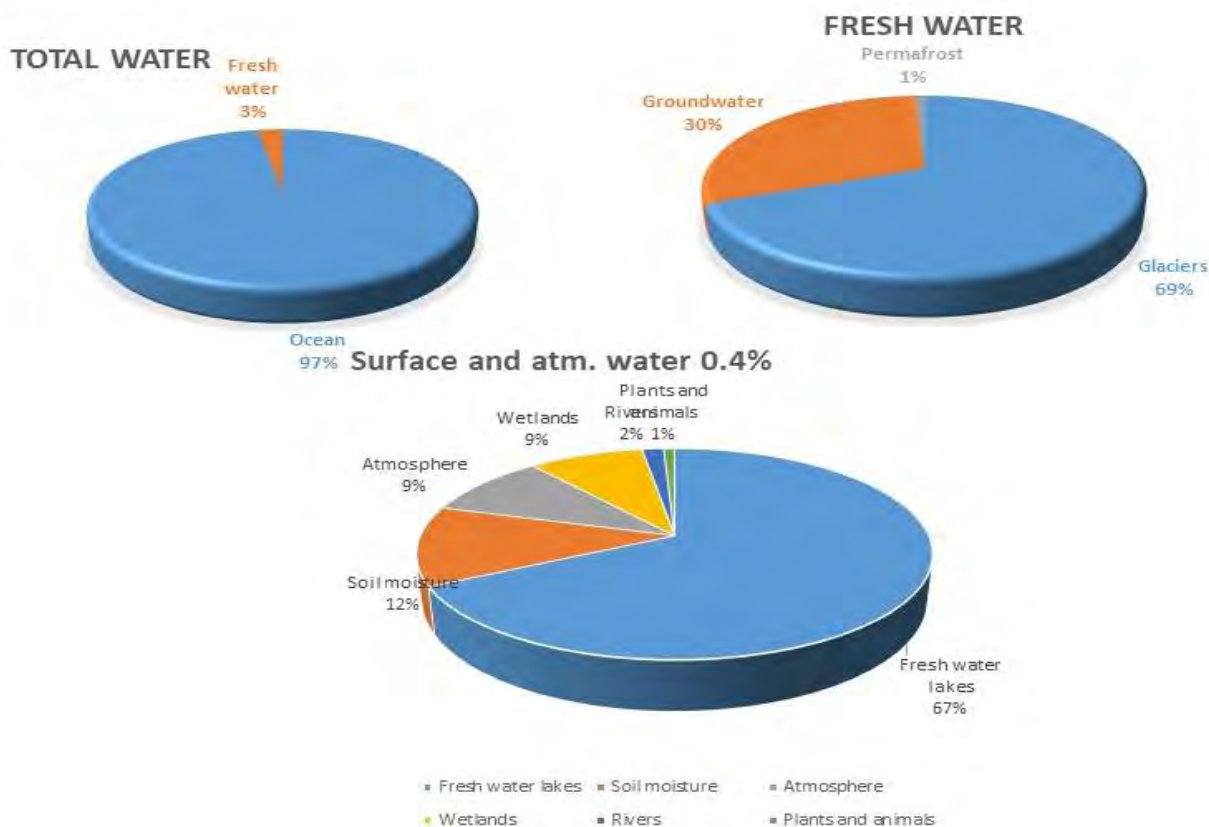
Figure 1.1:- Global distribution of total and fresh water

Saltwater, characterized by a high concentration of NaCl, is unsuitable for human consumption. The kidneys may experience stress and function impairment due to high blood salt levels[9]. Saltwater consumption in excess can result in diarrhea, vomiting, and nausea. The high salt level can cause marine organisms to disrupt their osmotic balance, which can result in death and dehydration. Because saltwater is so corrosive, it can harm metal buildings, pipes, and other infrastructure. The process of desalination, such as reverse osmosis or distillation, becomes crucial to remove salt and other impurities from seawater or brackish water, making it safe to drink[10]. Excessive salt content in water can

negatively impact plants and crops. Water with high salt levels used for irrigation can lead to soil salinization, resulting in reduced plant growth and crop yield. The removal of salt from the water aids in maintaining soil quality and prevents agricultural issues associated with salinity. By using salt-free water, manufacturing and production processes can avoid problems like corrosion, scaling, and other issues that may arise from dissolved salts. The elimination of salt from water ensures that the water quality meets the specific requirements of the industrial application. Traditional water treatment methods, such as filtration, evaporation, distillation, ion exchange, adsorption, coagulation, flocculation, chemical precipitation, and electrochemical processes, have limitations in terms of efficiency and cost-effectiveness. In contrast, membrane separation represents a state-of-the-art technology that has the potential to be applied to a diversity of separation procedures, in count to water treatment. It confers various benefits over the customary separation methods, including reduced energy requirements, lower costs, process simplicity, environmentally-friendly characteristics, hybridization, and scaling up. To this day, reverse osmosis (RO) remains the prevailing membrane-based procedure of choice for desalinating brackish water and seawater[11]. However, while RO yields pure water, it suffers from certain limitations such as a high demand for hydraulic pressure (energy), membrane scaling or fouling, and the need for widespread pretreatment of given feed [8]. As such, there exists the potential for a more energy-efficient membrane-based process to supplant RO for future desalination applications. King tides, storm surge, excessive groundwater pumping, and sea level rise are some of the main factors that contribute to saltwater intrusion. Sea level rise and climate change are frequently linked. Ice caps as well as glaciers melt as ambient temperatures rise, gradually raising the ocean's level. The over pumping of groundwater for agriculture and other urban uses (such as drinking and cleaning) in response to population growth is the other primary cause of saltwater intrusion. When the ocean's seawater level rises above the groundwater level due to rising sea levels and excessive groundwater pumping, saltwater flows towards the clean and fresh groundwater source as shown in Figure. 1.2.

1.1. Significance of Nanotechnology:

Nanotechnology involves engineering materials at the molecular or atomic level in order to create new and advanced substances[12]. In recent years, there has been a significant increase in the use of nanotechnology, resulting in the commercialization of numerous products. Nanomaterials possess unique characteristics such as enhanced strength, lighter weight, and improved efficiency due to their physical as well as chemical modifications[13].
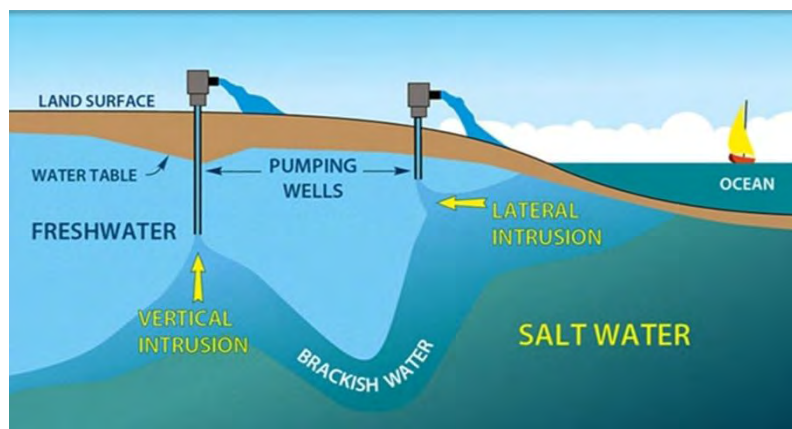
Figure1.2:-Sources of saltwater intrusion[14]

They also exhibit a high surface area relative to their volume or mass, leading to improved electrical, magnetic, and optical properties based on quantum effects. Furthermore, this high surface area allows for more functionalization sites, enhancing the materials' adsorption capabilities. Currently, there is no widely agreed-upon definition of nanotechnology. However, (NSTC) describes nanotechnology as the manipulation and comprehension of materials that exist within the range of 1 to 100 nanometers[15]. This size range exhibits unique properties that enable novel applications. People worldwide are recognizing the importance of addressing water contamination and are taking necessary actions to implement water treatment technologies and purification processes. However, the current approaches to water treatment and purification are limited and cannot provide a sufficient amount of safe drinking water to fulfill human and environmental requirements. A completely new category of functional materials created by nanotechnology need to be explored for their potential use in desalination and water purification. Hoek and his colleagues first introduced the term "TFN membrane" in early 2007[16]. In order to create

a thin-film-nanocomposite (TFN) membrane, they proposed the idea of creating enhanced RO membranes with nanoparticles embedded into the PA layer. According to reports, the innovative polyamide TFN membrane (as illustrated in Figure.1.3.) contain a variety of porous nanomaterials as nanofillers, including carbon nanotubes (CNTSs), zeolite. Through the voids that exist between nanofillers and PA, these TFN membranes quickly transport water. MOFs are highly desirable for the production of TFN membranes for the selective separation of nanoparticles[17]. This is mainly because the size of their particles can be rationally regulated by varying the reactant's composition involving inorganic metal ions as well as organic linkers.
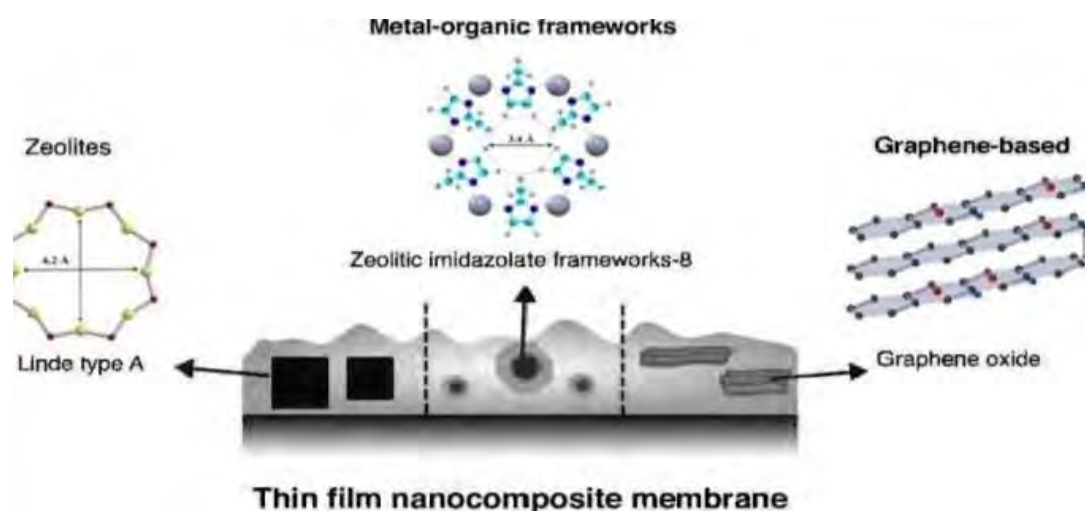
Figure 1.3:- Schematic representation of TFN- RO membranes incorporating different nanofillers in the PA layer [16]

1.2. Introduction to membrane technology:

One of the most difficult problems confronting the chemical industry is how we can separate the mixtures of different liquids and gases having high purity. This can be accomplished by using a variety of various conventional techniques that are well-known in the field of chemistry. For instance, distillation, absorption and adsorption for the separation of gases, and extraction, as well as distillation for the separation of liquids. However, compared to membrane separation, these techniques use more energy and are more expensive[18]. Additionally, some heat-sensitive components may be difficult to separate using these techniques. In recent years, membrane technology has become a crucial component of numerous critical industrial processes, including the water

purification, gas separation, dialysis, drugs and petrochemicals purification, tissue engineering. Membrane materials must be exceptionally stable provided the wide range of chemical industry uses for membrane technology. Utilizing all engineering techniques, a number of permeable membranes were developed and used to mechanically separate the   liquid streams. The effective development of some asymmetric membranes for utilization in RO by Yampol , skii   and Paul in 1994 marked a major advancement in membrane technology[19]. The membrane processes, which seek to cover a wide range of particle sizes, employ various separation principles and mechanisms. Since the membrane is considered as the core of every membrane separation process, is the characteristic that unites these processes despite all technical process variations[20]. Although there have been numerous efforts to define membranes, the following may be the most general and appropriate: A membrane can be defined as a thin, semipermeable layer used to separate solutes as transmembrane pressure is applied to the membrane or a selective barrier between two phases that permits some objects to pass through it, such as certain molecules, ions, or tiny particles under the influence of different types of driving forces[21]. The membrane's driving force comes from differences in pressure, concentration and electrical and chemical potential on both sides. [6].

Transmembrane pressure$= (P_i + P_0)/2 - P_p$ (i)

P_i represents the inlet pressure on feed side, P_0 shows the outlet pressure on feed side and P_p indicate the pressure on permeate side.
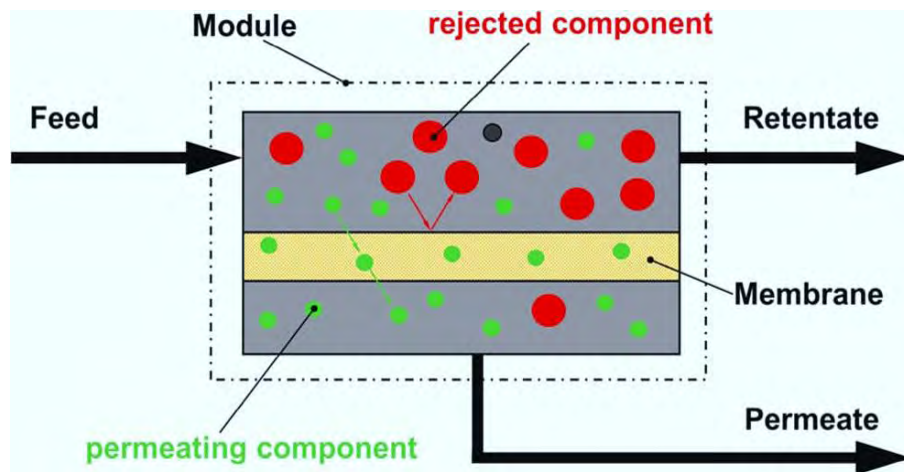
Figure 1.4:-A schematic diagram of membrane separation process

1.3. Overview of porous materials:

Due to their many applications in storage, separation, and catalysis, porous materials have attracted a great deal of interest from both the academic and industry perspectives. A solid that has pores, also known as cavities, channels, or voids whose depth is more than their width, is known as a porous material. In general, porous materials have porosity (the volume ratio of empty space over the entire volume of the material) values between 0.2-0.95[22]. Every application for porous materials should be connected to the characteristics of the pores. The most fundamental intrinsic factors—porosity, pore shape, size, and pore size distribution—have a significant impact on the characteristics of porous materials.

IUPAC divides these substances based on the size of their pores into the following categories[23]:

- Microporous materials have pores that are less than 2 nm wide, or extremely small pores. Only small molecules, such as gases or linear molecules, can pass through or be retained by them. These components are frequently employed in gas storage, gas separation, and catalysis.

- Pores in mesoporous materials range in size from 2 to 50 nm. Some large molecules, such oligomers and aromatic chemicals, can be retained by them.

- Macro porous materials consist of pores that are greater than 50 nm in width and have the capacity to hold large molecules.

- Another term for porous materials with pores between 1 and 100 nm is called nanoporous, which includes mesoporous and microporous materials.
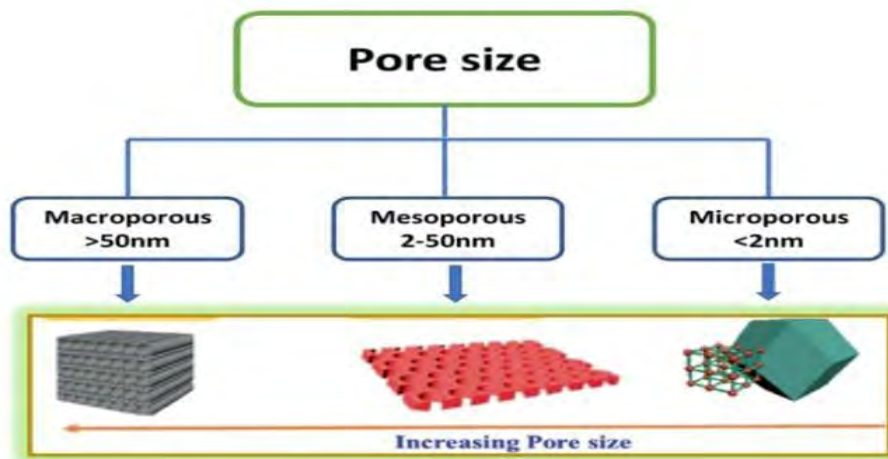
Figure 1.5 :-Classification of porous materials

1.4. Structural aspects of nanomaterial composites in membrane fabrication:

To produce a membrane with the required characteristics in separation technology, the choice of membrane material is essential[24]. The type of membrane used, the fabrication process, and the separation method are all influenced by the membrane substance. Effective separation depends greatly on the compatibility of the desired separation feature with the chosen material performance. Therefore, selecting a material is not an arbitrary process; rather, thorough study is needed based on specific polymer properties particularly structural aspects. Significant requirements for a membrane material include the following:

- Chemically resistant nature
- High flux and relatively effective separation
- Mechanical as well as thermal stability
- Engineering viability
- Reasonable production reproducibility
- Economically affordable

A chemically and thermally stable membrane may more effectively withstand the demanding operating circumstances for useful industrial separation applications[25]. The ability to retain a sufficient stiffness toward pressure gradient is essential because pressure is a major driving force for numerous membrane processes. An additional requirement is

the material's thermal stability, which enables the membrane to cope with the oppressively high temperature conditions of manufacturing operations. Consequently, the perfect material is affordable and easily transforms into an extremely effective, permeable, and long-lasting membrane. Performance, morphology, and applications of MMMs rely on the selection of the proper polymer phase, the properties of the filler, and the degree of filler material loading. These crucial factors were linked to the future growth and success of MMM's application[26]. This attribute enhances the effectiveness of MMMs, approaching the trade-off boundary set by the polymeric membrane. The filler acts as a sieve to separate one feed species while retaining the other. Some nano-porous materials that have been used to create MMMs include zeolite, metal oxides, MOFs, and CNTs. Since these conventional fillers offered improved separation for advanced application while maintaining the cost and consumption of energy in control, a great deal of attention has been placed on the successful preparation of the MMMs using them.

1.4.1. Carbon based materials:

A carbon tube having a diameter measured in nm and also have a cylinder shape (consists of rolled up sheets of single layer carbon atoms) [27]. They are mechanically strong and have a high conductivity. Hydrophobicity, non-uniformity in structure, and impurities are some drawbacks. SWCNTs are CNTs with a diameter of 0.5 to 1.5 nm and a wall structure consisting of a single graphite sheet closed in a tabular shape as shown in Figure 1.6. MWCNTs are those that have a diameter of greater than 100 nm and are made up of several graphite sheets stacked one inside the other in a tabular configuration. An allotrope of carbon known as graphene is composed of a single layer of atoms structured as a hexagonal lattice nanostructure as shown in Figure.1.6. A graphene sheet has a valence band that covers the entire surface because each atom is joined to its three closest neighbours by π-bonds and a delocalized -bond[28]. In order to understand the electrical structure of graphite, scientist Philip R. Wallace started investigating graphene theoretically in 1947. By combining the words graphite, which refers to carbon in its highly ordered crystalline structure, and the suffix -ene, which denotes aromatic polycyclic hydrocarbons in which the atoms of carbon constitute a hexagonal shape or six-sided, ring structures, scientists Hanns-Peter Boehm and Ralph Setton, as well as Eberhard Stumpp created the term

graphene in 1986. With this particular structure, it exhibits a variety of remarkable qualities, including extra high carrier mobility, exceptional mechanical durability and adaptability, high electrical conductivity, a large specific surface area, and possibly optical qualities. To be more exact, the agglomeration and re-stacking of graphene sheets significantly suppresses its inherent features because of its poor processability and unique structure, which have counteracted its practical applications when used as bulk material. One ideal approach is to engineer graphene sheets to create three-dimensional (3D) architectures (such as foam, sponge, network, aerogels, and hydrogels), preventing the re-stacking of each of the sheets, in order to maintain the special properties in bulk and increase the practical applications of graphene. Additionally, these three-dimensional graphene-based materials (3D GBMs) offer numerous novel collective physicochemical characteristics, including high porosity, low density and a large surface area, excellent mechanical characteristics, unique electrochemical performance, and so on, in addition to retaining the intrinsic properties of graphene [29]. For the desalination and filtration of water, graphene membranes have demonstrated considerable promise. Their atomic-scale pores enable the selective penetration of water molecules & preventing the passage of ions and pollutants, making it highly effective & economical for the production of clean water.

(a)   (b)
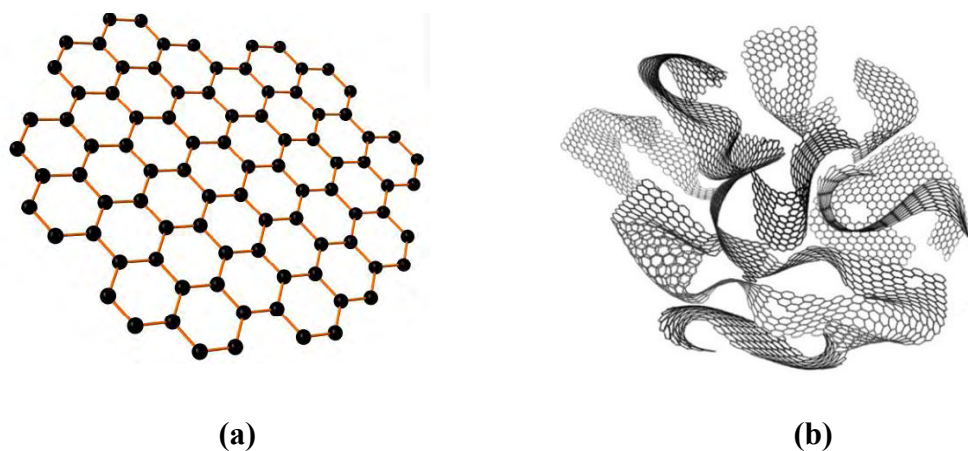
Figure 1.6 :-(a) Structure of graphene single sheet, (b) The 3D structural representation of the porous 3D graphene[30]

1.4.2. Zeolites and silica nanoparticles:

Minerals contain silicon and aluminum compounds are known as zeolites. They are divided into two categories: synthetic zeolites and natural zeolites (porous, prepared by China clay,

feldspar and soda ash)[31]. Zeolites have high melting point, resistance to environmental factors, insoluble in water, and generally used for water filtration. During the early stages of development, when rubbery polymers were utilized to create the MMM, remarkable separation efficiency for zeolite/polymer MMMs was noted. Zeolite's excellent compatibility with rubbery polymers is a result of the polymer chains' increased mobility, which effectively incorporates particles into them and reduces MMM defects. Zeolite molecular sieve is associated with considerably higher selectivity and diffusivity when compared to pure polymer. Zeolite membranes, on the other hand, are expensive and difficult to produce defect-free membranes for specific uses. Another important category of traditional inorganic fillers is silica nanoparticles, which are further divided into organized mesoporous as well as non-porous silica. The ordered meso-porous silica used in the new generation MMMs, which have various pore sizes, shapes, and configurations, has shown promise as a porous filler[32]. The high thermal as well as mechanical stability, the possibility of chemical functionalization, and the acceptable particular surface area ($>500m^2/g$) of mesoporous silica are its distinguishing characteristics. Mesoporous materials' larger pores hinder size exclusion and reduce overall selectivity, so pore structure must be chemically altered for proper separation properties. In comparison to porous inorganic fillers, nanosized non-porous fumed silica provides a unique set of properties for silica/polymer MMMs[33]. .

1.4.3. Covalent organic framework (COFs) and metal organic framework (MOFs):

 The lighter elements (H, C, and N) that make up covalent organic frameworks are highly porous organic solids that are extended in two or three dimensions and joined by covalent bonds. The covalently bound framework is limited to 2D sheets in 2D COFs, whereas in 3D it is only allowed in 3D sheets with a large surface area. COFs have an ordered, porous structure with great surface area and stability. In contrast to MOF, non-metal nodes like boron and nitrogen are used in place of metal nodes. MOFs are organic-inorganic hybrid materials with crystalline pores that are made up of a regular arrangement of metal ions that are positively charged enclosed with organic "linker" components[34]. These metal ions act as nodes, connecting the linkers' arms to create a repetitive, cage-like framework as illustrated in Fig.1.8. MOFs have such an exceptionally vast internal surface area

because of its hollow nature. MOFs provide unparalleled structural diversity due to their consistent pore structures, customizable porosity, and flexible network architecture[35]. - Their atomic-level morphological uniformity and varied chemical functionality make them unique among all other porous substances. Researchers can successfully manage the morphology, porosity, and functionality of the framework. With extremely high porosity (close to 90 percent free volume) and massive interior surface areas, exceeding 7800 m^2 /g[36]. MOFs, have become a distinct group of crystalline substances. These qualities make MOFs intriguing for potential uses in renewable energy, particularly as media for storage for various gases like as methane and hydrogen and also large-volume adsorbent substances to encounter diverse separation requirements. These characteristics, along with the extraordinary range of variability for inorganic and organic parts of their frameworks, also make MOFs interesting[37].

organic linkers   metal ions or clusters   metal organic frameworks
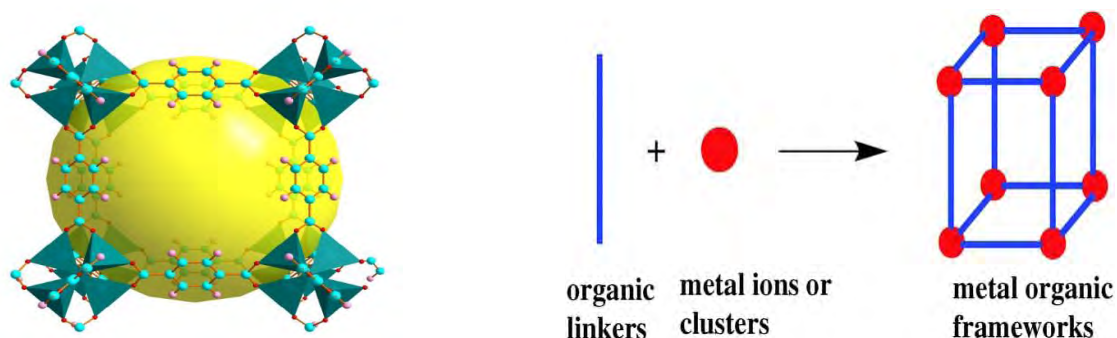
Figure 1.7:- Schematic representation of structure of typical MOFs[38]

We now have MOFs, crystalline hybrid materials produced by molecular self-assembly from both inorganic and organic components. Initiated by Prof. Omar Yaghi at UC Berkeley in the late 1990s ("Design and manufacture of an extraordinarily stable, highly porous and permeable metal-organic framework"), MOFs have developed into a quickly expanding study area. There have been reported over 90, 000 various MOF structures so far, and the number is increasing every day. MMMs possess outstanding characteristics such as controlled porosity, high absorption capacity, improved selectivity, and exceptional adhesion with polymers [39]. These features are attributed to their large surface area and the integration of organic linkers into their structural framework. Although there are some preliminary understandings of the properties and transport processes in MOFs, more extensive study in this area is still required to resolve many unanswered questions. The

choice of an appropriate polymer/MOF pair and an effective MOF with greater selectivity is a significant challenge in the production of technologically appealing MOF/MMM. Because there are so many MOFs accessible, it seems like this is a necessary requirement for effective MMM production. Many applications in many domains are being developed that utilize MOFs' cage-like structure, including as gas separation and storage, liquid purification and separation electrochemical energy storage, sensing and catalysis and removal of heavy metal ions from water[40].

1.4.4. Zeolitic -Imidazolate Frameworks (ZIFs):

Zeolitic imidazolate frameworks (ZIFs), which have structures comparable to common aluminosilicate zeolites, are a novel and distinct class of metal organic frameworks made up of imidazolate linkers and metal ions. Transition metal ions like Co^{2+} and Zn^{2+} serve as the metal source for ZIFs, and imidazole or imidazole derivatives, which are comparable to the ligands of the aluminosilicate zeolite, serve as the organic linker. ZIFs produce a metal-imidazole-metal (M-Im-M) structure, similar to the Si-O-Si link in conventional silica-based zeolites, when the transition metal ion and the ligand come into contact[41]. ZIFs are able to possess the porous structure and high surface area of MOFs as well as the adjustable characteristics and excellent stability of the conventional zeolite structure. Many ZIF materials offer a wide range of possible applications due to their inherent porous properties, diversity of functions, and remarkable thermal and chemical stabilities.

ZIF-8s are a well-known and recognized subclass of MOFs that have been extensively examined for numerous applications. Among the wide variety of ZIFs, ZIF-8, which is the most common one[42]. It was first created by Chen's group, and Yaghi's group gave it a systematic designation[42]. The sodalite (SOD) structure of 2-methyl imidazole and zinc metal ions can be used to create zeolitic imidazolate framework-8 having a ZnN_4 cluster with four and six rings, respectively. ZIF-8 nanoparticles' exceptional stability, which allowed for long-term use, is one of their advantages. ZIF-8 offers two important benefits. First off, there is a wide range of potential applications due to its simple fabrication, customization, and stability. Secondly, its crystallographic pore size, which is 3.4, is between that of CO_2, which is 3.3, N_2, which is 3.64, and CH_4, which is 3.8, offering a good sieving window for CO_2 gas separation. These factors have made ZIF-8 one of the

most widely used ZIF materials at the moment, especially in the area of CO_2 gas separation membranes. In addition to having superior compatibility between nanofiller and polyamide, ZIF-8 has 3.4Å pore size, making it perfect for separating salt from water. Furthermore, ZIF-8 has exceptional chemical stability towards hydrocarbons like benzene and alkanes, which are frequently present in water. Therefore, there is a good chance that ZIF-8 will be employed as a nanofiller to create a TFN membrane with increased chemical stability for the water treatment. Due to its advantageous characteristics, such as low tortuosity nanochannels for quick water transport, pore sizes appropriate for molecular sieving, better compatibility with polyamide, and superior chemical stability against hydrocarbons, ZIF-8 was chosen as the nanofiller in this work to create the TFN membrane. Incorporating ZIF-8 particles whose size is less than the thickness of the polyamide film is particularly desirable. This is done to make sure the ZIF-8 particles may fit appropriately inside the polyamide film and prevent the formation of TFN membrane defects. ZIF-8 crystal structure is comparable to that of zeolite (as shown in Fig.1.9.), and its pore size is 0.34 nm, making it useful for separating water (0.28 nm) or hydrated sodium and chloride ions (0.6–0.7 nm)[43] .
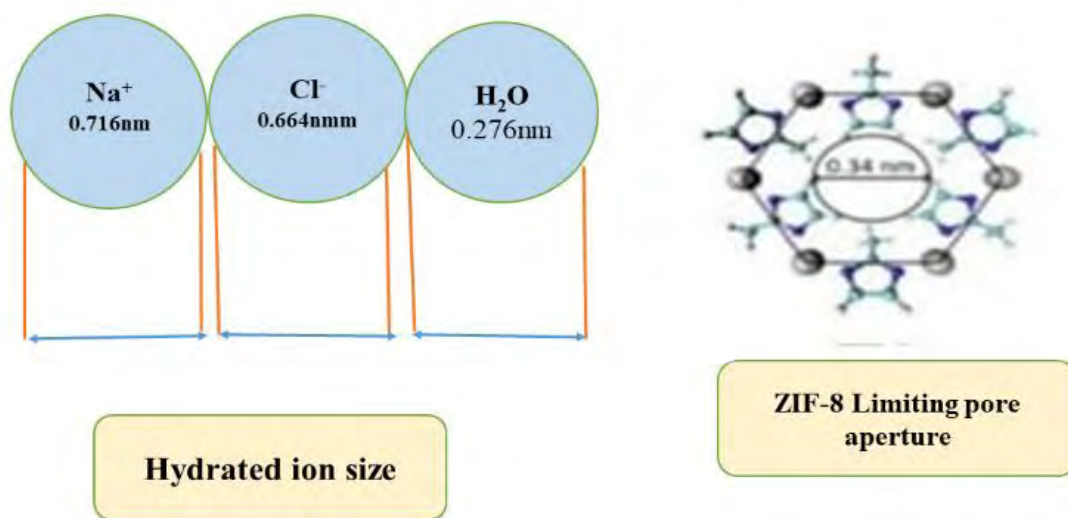
Figure 1.8:-ZIF-8's relative pore size relative to the of Na^+, Cl^-, & water molecules.

Another subgroup of MOFs is zeolitic imidazolate frameworks -67, or ZIF-67. Similar to ZIF-8, its structure is created by linking 2-methyl -imidazolate anions, and cobalt cations,

resulting in a sodalite (SOD) shape. ZIF-67 and ZIF-8 almost share the same synthesis mechanism due to comparable organic ligands and structural similarities.ZIF-67's nanostructures as well as mean particle sizes can be altered by carefully varying the experimental conditions[44]. The subsequent ZIF-67 has an extremely unwavering structure, an adaptable pore aperture, catalytic activity, and supplementary properties.ZIF-67's advantages can also be coupled with other substances or building blocks to make compounds that might function more effectively than pure ZIF-67. Scientists are interested in ZIF-67 as well as its derivatives because they can be employed in processes including gas adsorption, molecular separation, electrochemistry, catalytic processes, and other related activities [44]. The superior stability and large surface area (1240 m^2/g) were factors in the selection of ZIF 67.
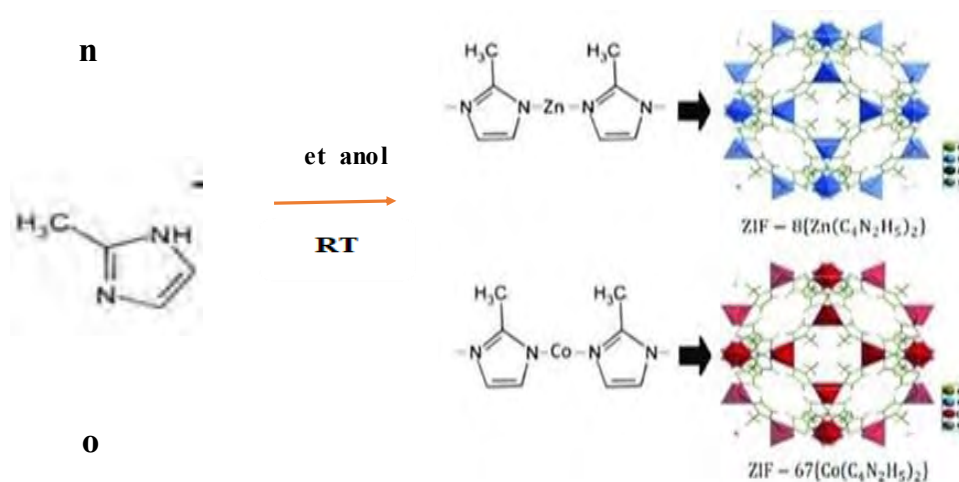
Figure1.9:-display a representative diagram of ZIFs with metal centers linked by imidazolate linkers that are tetrahedrally coordinated.

1.5. Customary protocols chemical mixtures separation:

The separation of chemical mixtures is non-spontaneous process and requires energy to separate the chemical mixtures into their constituent parts. Usually, there are one or more phases in a combination. In the case of a multiphase mixture, the phases must first be separated. The products may vary depending on whether the feed mixture is solid, liquid, or gaseous[45]. Each separation process involves the components of a mixture moving to

various, distinct spatial locations or phases. By using **separation by phase creation** technique, a second phase that is not miscible with the feed phase is produced. Crystallization and distillation are two typical processes that involves the transfer of species between the liquid and vapor phases and **Separation by phase addition** technique produces a new fluid phase that selectively absorbs, strips, or removes a certain species from the feed. Liquid-liquid extraction is one of these procedures that is most well-known. **Separation by solid agent** approach involves contacting a vapor or liquid feed with a solid material (adsorbent) that has a large surface area and porosity. Then it makes use of variations in a species' capacity to absorb for that particular adsorbent. **In separation by force field or gradient** ,fluid feeds are subjected to centrifugal, electrical, thermal, and other external forces, with electrophoresis particularly useful for separating proteins by altering their electric charge and diffusivity[46]. **Separation by barrier** method uses a barrier, usually a membrane, and analyzes differences in species permeability via a barrier. There are two general requirements for the separation process: Technically, separation must be possible as well as economically, separation must be feasible. The purpose of the separation can be categorizing as:

- Concentration
- Purification
- Fractionation
- Reaction mediation

1.6. Polymeric membranes:

Polymeric membrane is a semipermeable filter media composed of polymers. The part of feed that may pass through polymeric membrane is known as retentate, while the part of feed that cannot pass through membrane is known as permeate. Polymeric membranes based on organic polymer chains that have been cross-linked to create open space for molecules to diffuse. Polymeric membranes offer strong thermal stability and are inexpensive, but they compromise on selectivity and permeability, and they have poor mechanical stability and fouling issues. In order to manage the selective movement of ions,

polymeric membranes are primarily utilized in batteries, gas separation, and water purification[47].

- **Permeability:**

The permeability is a measure of a membrane's permeability to molecules.

Permeability= P= DS

Diffusivity (D) = measurement of a molecule's ability to move through pores in a polymer chain.

Solubility coefficient (S)=The amount of gas that may dissolve in a unit volume of solvent.

1.6.1. Rubbery polymeric membrane:

Rubbery materials can be used at temperatures above the glass transition, the polymer chains have plenty of time to rearrange and maintain thermodynamic balance. Silicon rubber, polyethylene glycol, and polydimethylsiloxane (PDMS) are common examples of rubbery plastics that are primarily used for membranes. The degree of selectivity with in rubbery membranes can typically be predicted by the solubility difference of various gases, regardless of the size of permeate[48]. Therefore, it is uncommon that larger molecules frequently diffuse more readily than smaller ones. When it is necessary to separate nitrogen from organic molecules, rubbery polymers primarily permeate organic vapours. The separation of different solvents from nitrogen or air has been extensively researched using a representative example of rubbery polymer, PDMS. Blume and colleagues used PDMS to examine the gas separation capabilities of various gases. They noted that the concentration of the solvents has a significant impact on their permeabilities and that solvent sorption into the polymer's structural framework is a necessary condition for solvent penetration. Silicon rubber is another instance of a rubbery polymer. Silicon rubber-based polymer membranes can be used in virtually every vapour separation equipment because they have excellent selectivities and are highly permeable to most gases.

1.6.2. Glassy polymeric membrane:

Glassy polymers have exceptional mechanical qualities and high selectivity, which is why they are used in the majority of commercial gas separation operations. Smaller molecules have been found to be more permeable. Size restriction is typically the basis for selectivity in glassy polymers. Chain rearrangement takes an extremely long time in glassy polymers compared to rubbery polymers because they can operate far below the T_g. As a result, thermodynamic equilibrium is never attained in terms of membranes. Polymer chains that are not precisely packed result in extra free volume in the form of tiny spaces all over the polymer material. The glassy polymers such as polysulfones, polycarbonates, cellulose acetate, and polyimides are frequently used for gas separation process. The membranes of this material are controlled by diffusivity selectivity due to micro voids in the polymeric matrix. Due to the stiff molecular chains of polymers, sufficient free volume (up to 20%) can be produced by fast cooling and careful solvent removal. These non-interconnected micro voids can produce an open surface area that can be based on the gas absorption method[49].

Table1.1: Examples of rubbery and glassy polymers

Rubbery polymers	Glassy polymers
Polydimethylsiloxane	Polysulfone
	Polycarbonates
Ethylene oxide or propylene oxide-amide copolymers	Polyimides
Silicon rubber	Cellulose acetate

1.7. Porous and dense membranes:

There are two main types of membrane structures: porous membranes and dense membranes. The construction of the dense membranes lacks any distinct, well-defined pores or spaces. A gradient in pressure, or electrical potential   and concentration drives

the diffusion process that transports a combination of molecules through dense membranes[50]. The construction of dense membranes can be symmetric or asymmetric. The use of an electron microscope is useful in identifying voids and holes as well as differentiating between porous and dense arrangements. Most uses for porous membranes involve ultrafiltration and microfiltration. The size, distribution, and molecular weight of penetrating species all affect the separation performance. Fouling and the concentration polarization effect, which lower the flux, are a disadvantage of porous membranes[51]. To prevent fouling, material selection is therefore essential. Some membranes have straight pores, while others have interconnected pores with curved channels, known as tortuous porous membranes. In Figure 1.10, the dynamic parameters relevant to membranes utilized in water filtration procedures are highlighted.
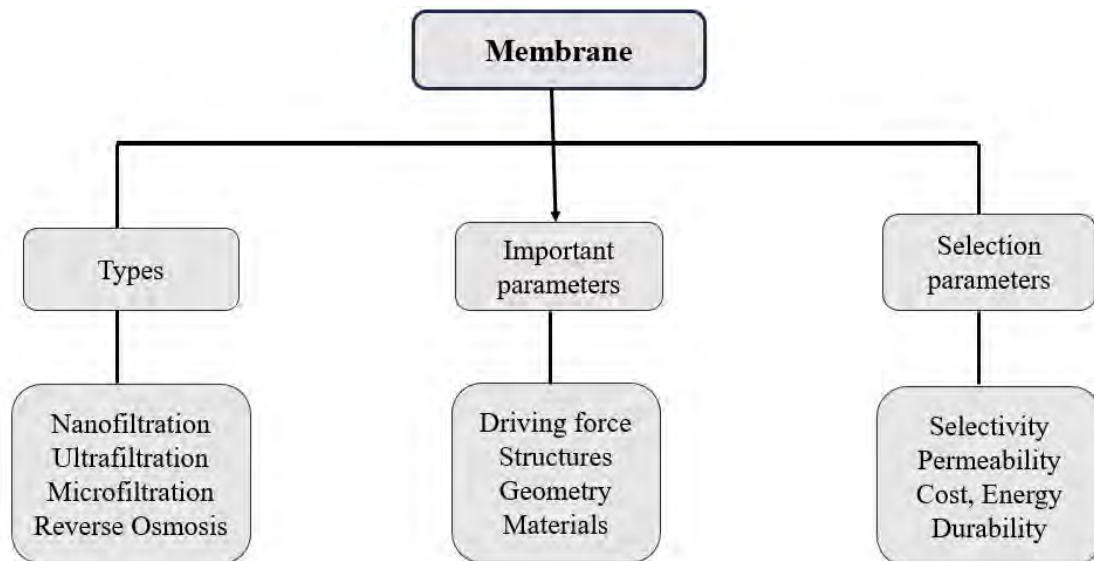
Figure1.10 :-Dynamic parameters for membrane selection

1.8. Symmetric or Asymmetric membranes:

A symmetric membrane contains a uniform structure all the way along. Two common types of symmetric membranes are homogenous dense and porous membranes as shown in Figure.1.11. The separating and bulk support layers are considered a single unit in the isotropic membrane structures. It is preferable to have a thin uniform layer to accomplish greater separation because the rate of flux via polymeric membranes has an inverse relationship to the thickness of the membrane[52]. The range of symmetric membrane

thicknesses (whether porous or nonporous) is around 10 to 200 nm, with the overall membrane thickness dictating the barrier to mass transfer. A breakthrough to industrial applications was the creation of asymmetric membranes. They are made up of a very thick top layer or skin that ranges in thickness from 0.1 to 0.5 nm, which is supported by a porous sublayer that is between 50 and 150 nm thick. While an asymmetric composite membrane consists of two or more separate layers created through a variety of procedures[53]. The porous support layer offers mechanical support without contributing to membrane separation, while the thin layer separates species.
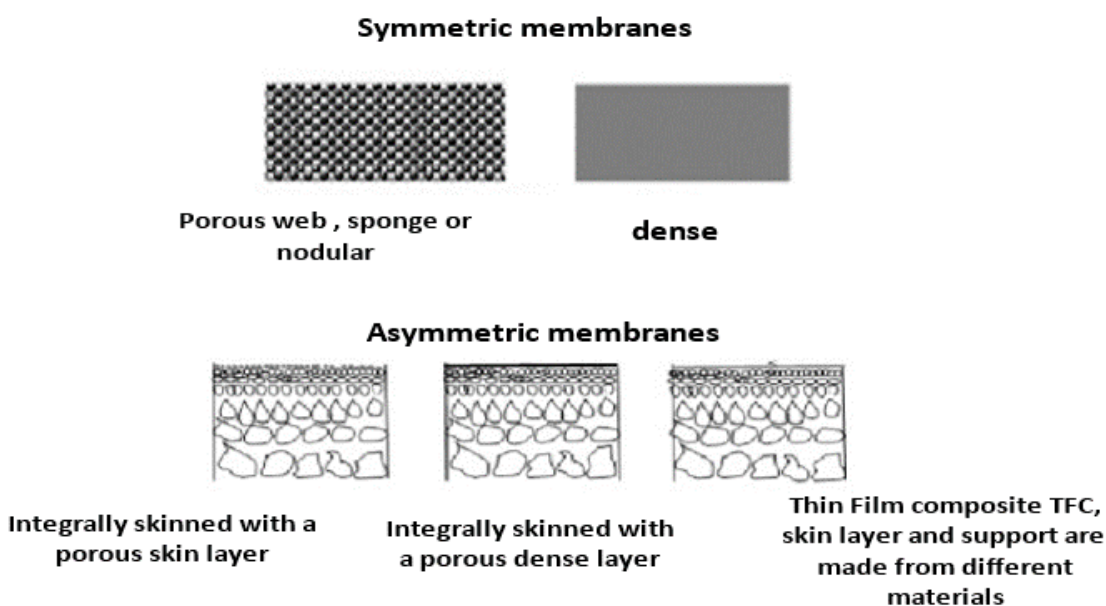
Figure 1.11: Schematic representation of symmetric and asymmetric membrane[54]

1.9. Polyamides:

Numerous studies have been conducted with the primary goal of prolonging the operational life of components exposed to severe environments, searching for organic polymers that are resistant to high temperatures as the main focus. Polyamides (PAs) are the most well-known organic polymers that are formed through polymerization reaction of TMC with MPD as shown in Figure.1.12. Polyamides are resistant to various chemicals including bases, acids and oxidizing agents and highly thermally stable due to their strong thermal stability, polyamides can survive high temperatures without experiencing

considerable damage[55]. Polyamides are well suited for use in high-pressure water treatment applications because of their great tensile strength and endurance. Several commercial nanofiltration (NF) and reverse osmosis (RO) membranes have been successfully produced using PA, which has good hydrophilicity, mechanical strength, and thermal/chemical stability. The two crucial properties of the perfect membrane are high permeability and selectivity. High water permeability is a characteristic of polyamide membranes that makes them ideal for effective water filtration. The permeability of these membranes does, however, have a practical limit, beyond which it becomes challenging to maintain an adequate rejection of solutes. Due to issues with the membrane, fouling, and concentration polarization, it is difficult to attain 100% rejection of all solutes. In 1990, Robeson developed a model for membrane performance. It is known that selectivity decreases as the permeability of the more permeable component increases. Although polyamide membranes offer an acceptable level of fouling resistance, they are not completely immune to it. Due to the high degree of crosslinking and low free volume of PA, the cross-linked PA membranes, particularly the aromatic cross-linked PA membranes, exhibit high selectivity but slightly low permeance. The membrane's permeability reduces with increased fouling, which may also have an impact on rejection performance. Using over 300 permeation data results, a trend was created by plotting membrane selectivity against permeability of the more permeable component[56]. This allowed for the clear distinction of rubbery and glassy polymers through specific data points. The data plots illustrated the balance between selectivity and permeability and raised the performance limit of the membranes studied.

It has been reported that adding inorganic porous materials to PA to create thin film nanocomposite (TFN) membranes can increase the membrane's permeance. Examples of such fillers include silicas, zeolites, metal oxides, MOFs and   CNTs, or graphene. The thick PA layers of thin-film nanocomposite   membranes can have more transport channels created by inorganic "fillers" with porous structures and appropriate pore size[57]. This results in increased permeance without a reduction in selectivity. Because of their superior separation capabilities, polyamide membranes can efficiently filter out pollutants, salts, and other impurities from water. These membranes can produce clean, filtered water and have high rejection rates. Salt as well as other dissolved solids can be eliminated from

water by RO membranes made up of polyamide, resulting in freshwater that is appropriate for a variety of uses. Although the polyamide TFC membranes surpass other polymeric materials in terms of increased water flux , salt rejection, as well as operational stability over an extensive pH as well as temperature range, the desalination market is still looking for high-performance RO membranes in order in order to further reduce the energy utilized by RO processes[58].

Polyamide network
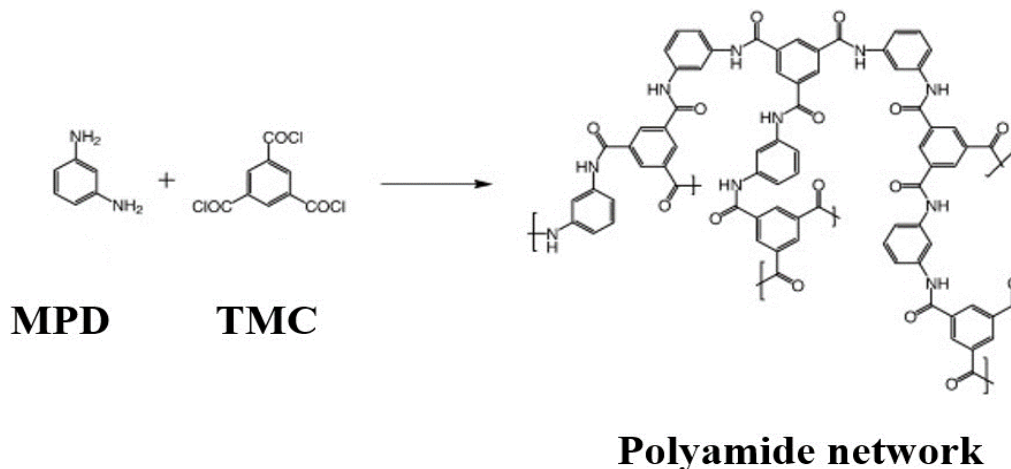
Figure 1.12: Structure of polyamide [59]

1.10. Mixed matrix membrane (MMMs):

The integration of a solid phase (MOFs, zeolites, carbon nanotubes, COFs) in a continuous polymer matrix is known as a mixed matrix membrane. By combining the simple processing of polymers and the higher selectivity of inorganic materials, mixed-matrix membranes (MMMs) improve the properties of polymeric membranes. Through the utilization of MMMs, the production of costly inorganic membranes can be eliminated by employing polymers as the continuous phase and inorganic particles as the dispersed phase. Mixed-matrix membranes are constructed using either traditional porous fillers like zeolites, porous silica, and porous carbon molecular sieves, or nonporous fillers like graphene oxide, which can change the molecular packing of the polymer chains in the membrane to change the free volume of a polymer[33]. Because of their stability, surface charge, surface-area-to-volume ratio, and other common characteristics, nanoparticles are

great candidates to be added to polymers for both the environmental and biomedical applications including traditional water-treatment methods.
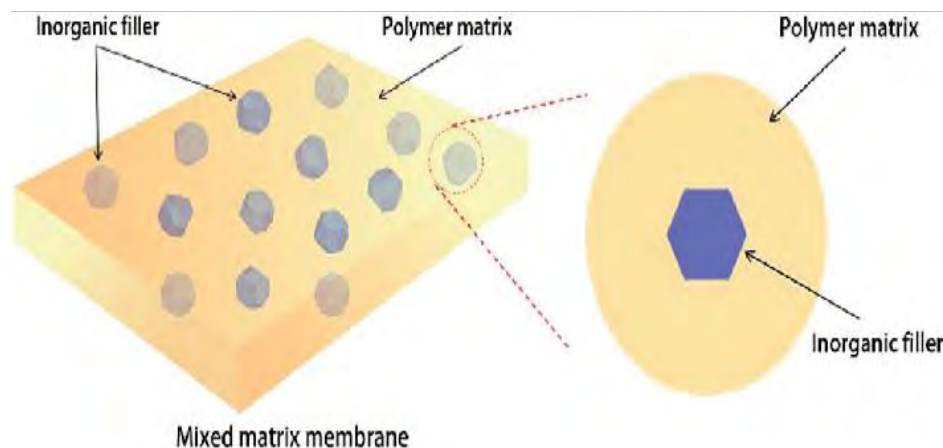
Figure1.13:- Schematic representation of MMMs

In 1970, the first research on mixed matrix membranes was conducted, with the addition of 5A zeolite as a nanofiller into the polymer matrix demonstrating the best gas separation performance in comparison to polymeric membrane. The main separation mechanisms of biological systems, like blood purification, require numerous selective membranes. As a result, it was the initial factor that attracted natural scientists to membrane technology. Later, the industrial implementation of the membrane method made a breakthrough due to the need for sea water desalination through an energy-efficient process. In all the highly technological different countries, research on the production of high-performance membranes has become mainstream with the creation of the reverse osmosis method for desalination. Recent studies on the membrane process have demonstrated that it can outperform traditional separation techniques like filtering, absorption, adsorption, and distillation on the basis of energy efficiency, compactness, usability, and environmental friendliness.

1.11. Applications of mixed matrix membranes (MMMs):

Due to competition in selectivity and permeability characteristics, inorganic and polymeric membranes have faced difficulties. The efficiency of inorganic and

polymeric membranes in separation processes can be improved by combining nano fillers inside the polymer matrix. The separation industry has given (MMMs) some consideration because of their excellent mechanical, physicochemical, and transport qualities[61]. Gas separation, hydrogen storage, water desalination, pervaporation are the common applications of mixed matrix membranes (MMMs).

1.11.1. Waste water treatment:

70% of the earth is covered in water, and 97% of that is sea water, which is worthless because of its high salt content. According to the WHO, 1.1 billion people lack access to clean water, which endangers humans, plants, animals, and humans by containing poisonous metal ions and causing diseases like malaria [62]. ZIF-8 has become a subject of significant interest as a potential nanomaterial for polyamide TFN membranes. This is mainly due to its impressive characteristics, such as its excellent water permeability (approximately 5.0 liters per square micron per hour per bar), high specific surface area (around 1400 square meters per gram), narrow pore size (3.4Å), and remarkable stability in aqueous environments. A major cause of heavy metals (toxic substances) in surface and groundwater is wastewater produced by mining, battery manufacturing, and metallurgical processes. Thus, heavy metals must be removed from wastewater before it is released into the environment. Some researchers have also created high-flux MMMs for heavy metal removal from a mixture of polymer and nanofillers. The membranes which are produced from polysulphone and zeolites nano particles have the capacity to remove the Pb and Ni from synthetic solutions. During filtering, the PVDF alpha-ZrP membrane with a 1.00 wt% alpha- ZrP content was able to remove 42.8% (Cd^{2+}), 44.4% (Ni^{2+}), 93.1% (Cu^{2+}),91.2% (Pb^{2+}), from an aqueous solution. A useful adsorption material for treating wastewater is alpha -ZrP because of its extraordinary qualities, including high ion-exchange capabilities, high biocompatibility, and capacity to trap different kinds of molecules with different sizes between their layers.

1.11.2. Olive oil/water separation:

Eliminating pollutants has become a difficult problem in the modern day due to the growth of environmental contaminants and their hazardous problems[63]. In addition to limiting the growth of animals and plants, toxic substances found in oily effluents are harmful to

people. Examples include phenols, polyromantic hydrocarbons. Oil separation has recently caught the interest of many researchers for the aforementioned causes. One of the most significant traditional foods around the globe is olive oil. Over 2.5 million tons of olive oil were produced globally in 2017, and 87% of that was done so in Mediterranean nations. Production of olive oil is a valuable resource for many countries, both commercially and in terms of health. Due to its cholesterol-depleting, and anticancer and advantageous effects on the brain, heart, and nerves, olive oil is regarded as the major nutrient in the well-known Mediterranean diet. Oil combustion, oil collectors, bio-combustion, are examples of traditional technologies for the purification of oily wastewaters. In addition, there are certain novel techniques, such as membrane technology, cyclones, electrostatic deposition, gravity or centrifugal deposition, and absorption. Membrane technology, which is typically successful for the separating of the oils having size smaller than 10 micro meter, is one of the methods described that is most successful for the removal of oil and dissolving oil emulsions. For oil/water separation, for instance, mixed matrix membranes containing HMO (hydrous magnese oxide) and TiO_2 nanoparticles were created. Their findings demonstrated a reasonable balance between oil rejection effectiveness and pure water flux. By increasing the nanoparticle loading in membranes, researchers discovered the greatest pure water flux of 1194 L/m^{2}h, while flux of pure polysulfone membranes having the pure water flux was 151L/m^{2}h. Since the nanoparticle-containing membrane had an oil rejection performance of almost 100%. ZIF-8 metal-organic framework impregnated polyacrylonitrile-based membranes demonstrated exceptional hydrophilicity and the high oil total rejection effectiveness in the addition of ZIF-8 particles.

1.11.3. Pervaporation:

Metal-organic frameworks (MOFs) & polymer-based MMMs provide a lot of prospects in pervaporation separation due to the ease of creation and modification of MOFs as well as their compatibility with polymer matrix. In recent years, biofuel has drawn a lot of attention as a potential green energy source to solve the world's energy issues. As The pharmaceutical, fine-chemistry, and chemical industries are highly relevant economically to alcohol dehydration processes. Applications of PV can be categorized into 4 primary groups: separation of the organic-organic mixtures, dehydration of the organic solvents

mixtures, and removal of diluted organic molecules from aqueous streams and reversible process. Polymer membranes have now been widely used in the PV process, although the plasticization effect caused by the swelling of polymeric material typically results in a decrease in selectivity. As a result, it was suggested that mixed matrix membranes (MMMs), which consist of inorganic fillers and a polymer, could improve PV performance by increasing selective sorption, diffusion, and stability by the addition of the suitable fillers. The pervaporation process is a very promising technological advancement because it may be used in reasonable working conditions. With potential energy savings of up to 50% compared to the conventional distillation separation, it has proven to be one of the most effective separation technologies for the purification of bioalcohols. Water permeates preferentially via hydrophilic membranes like poly (vinyl alcohol), chitosan, and polyacrylonitrile (PAN), hence these materials are frequently used. Hydrophilic membranes interact via dipole-dipole interactions, hydrogen bonds, or ion-dipole interactions with water. Polyimide is the most popular polymeric substance among those used for pervaporation. It has excellent mechanical, chemical, and thermal stability needed for liquid separations. ZIFs have shown permanent porosity and much better thermal and chemical stabilities as compared to others MOFs.ZIF-8 has been widely employed in MMMs for n-butanol pervaporation at a high flux and selectivity due to its permanent porosities and strong hydrophobicity.

1.12. Membrane process:

Depending on the driving forces, a variety of membrane processes can be used in industry, including microfiltration (MF), an ultrafiltration (UF), reverse osmosis (RO), Nanofiltration (NF), gas separation (GS), pervaporation (PV), and vapour permeation (VP).

1.12.1. Microfiltration:

Microfiltration is a technique for removing microscopic particles, including microorganisms yeast cells, colloids, as well as smoke particles, from solutions or gases. The technique makes use of membrane filters having pores which are accessible to liquid yet retain the particulates, leading to separation, and have a size range of roughly >0.1

micro metre. Microfiltration employs porous membranes and operates at low pressure. Various materials, including ceramics and stainless steel, can be used to produce filters for microfiltration, such as those made from polymers.

1.12.2. Ultra filtration:

The process of ultrafiltration (UF) involves passing a semipermeable membrane through a separation caused by factors like pressure or concentration gradients. The so-called retentate is where suspended particles and solutes with a high molecular weight are kept, whereas the permeate is where water and solutes with a low molecular weight pass through the membrane (filtrate)[64]. Sugars and other tiny molecular weight molecules can pass through ultrafiltration membranes while larger substances including colloids, particulates, lipids, germs, and proteins can be separated from them. Ultrafiltration membrane pore diameters range from 0.1 to 0.01 micrometers, which are in between nanofiltration and microfiltration. Additional properties of polymeric ultrafiltration membranes include strong chemical and temperature resistance, as well as low fouling propensities with the right pretreatment.

1.12.3. Nanofiltration:

Between RO and ultrafiltration (UF) membranes, the NF membranes are a comparatively recent form of pressure-driven membrane[65]. The definition of an NF membrane is based on two approximations: (1) pore sizes of 0.01 to 0.001, and (2) the passage of a significant number of monovalent ions (> 30%) across the membrane and multivalent ions are significantly rejected (by > 90%). The increased permeability, lower energy use, and lower capital cost of the NF membrane make it more desirable in a variety of industries, including the pretreatment of desalination plants, wastewater treatment, food, beverage, and pharmaceutical industries.

1.12.4. Reverse osmosis:

A semi-permeable membrane is employed in the reverse osmosis method to cleanse drinking water by removing unwanted compounds, larger particles, and ions. Reverse osmosis is used for both industrial and potable water production due to its proficiency in eliminating a broad range of bacterial and chemical species from water. The energy-

efficient, high pressure reverse osmosis process, also known as hyper-filtration, is used to concentrate low molecular weight compounds in solution, to dewater process streams, or to purify wastewater. Due to its capacity to concentrate both suspended and dissolved particles, this method has been applied to the desalination of brackish water. The Reverse Osmosis (RO) phenomena is depicted in Figure. 1.15. Desalination is done in a way that creates a flow across a membrane, allowing water that comes from the salty side to enter the salt-free side. This is only possible if sufficient pressure is applied to the water column in the area where salt is present. In order to forcefully drive water across the membrane, this is carried out in order to first reduce the osmotic pressure that is naturally there and then to provide the pressure that is needed. It is essential to be familiar with the osmosis phenomenon in order to fully comprehend the RO process. The solvent is allowed to move through the membrane, but the solute is trapped on the pressurized side selective membrane must allow smaller components, like water molecules, to pass through without obstruction. Larger molecules or ions cannot pass through due to the small pore size. Osmotic pressure across a layer of membrane can be decreased to prevent the natural process of osmosis as the direction of flow is normally towards the concentrate from the diluted. In this case, more salt must be added to the cell in order to produce more clean water. Figure 1.16 presents the basic elements of the RO procedure. We need to increase the pressure applied to the membrane's salty side in order to drive the water through. The fundamental determinant of pressure is the salt concentration; when water is driven out, the salt concentration rises and more pressure is needed to obtain more clean water.

Reverse osmosis works by employing a high-pressure pump in order to increase pressure on the salt portion of the RO and drive the water over the semi-permeable RO membrane, leaving nearly all (between 95% and 99%) of the dissolved salts left in the reject stream. The pressure needed varies depending on the level of salt concentration in the incoming water. If the feed water has a higher concentration of salt, a greater amount of pressure is necessary to surpass the osmotic pressure[66]. If the hydraulic pressure is higher than the total of both the osmotic pressure differential as well as the pressure loss of diffusion across the membrane, the water can diffuse in the opposite direction. The name "reverse osmosis" refers to this procedure. When the other parameters are kept constant, the water flow rate becomes proportional to its total pressure since diffusion will occur more quickly if the

pressure being applied is higher and vice versa. We can concentrate various solutes that are distributed or mixed in a solution using the RO technique. The water flow across a RO membrane is seen in the diagram below.
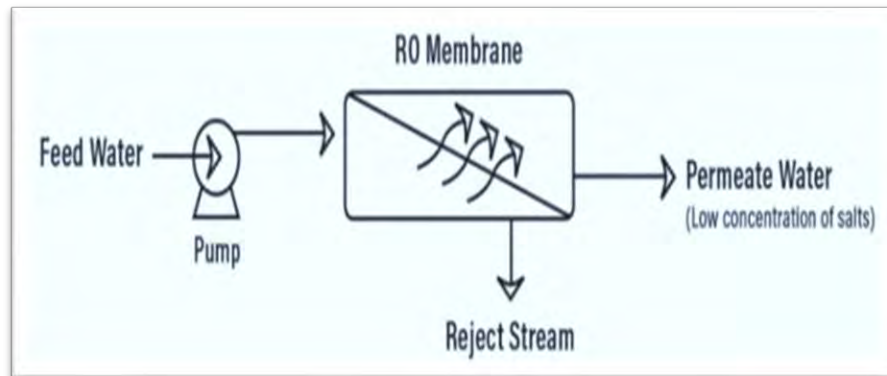
Figure 1.14:-Rejection mechanism of RO membrane [66]

Reverse osmosis is the opposite of the natural process of osmosis. While osmosis happens spontaneously without requiring energy, reversing the process requires the application of energy to more concentrated solution. A RO membrane is a special type of barrier that allows water molecules to pass through but restricts the movement of dissolved salts, organic sub stances, bacteria. Although both FO as well as RO membranes have a dense thin film selective layer and a porous support layer, their constructions are different. In pressure-driven membrane-based procedures like RO, the feed mixture flows against the selective layer and the permeates accumulate on the support layer. Because high pressure is used in these processes, it is necessary for a pressure driven membrane to have a narrow   or thin selective layer for increased water flux with salt rejection on a thick or dense porous substrate to give sufficient mechanical strength.
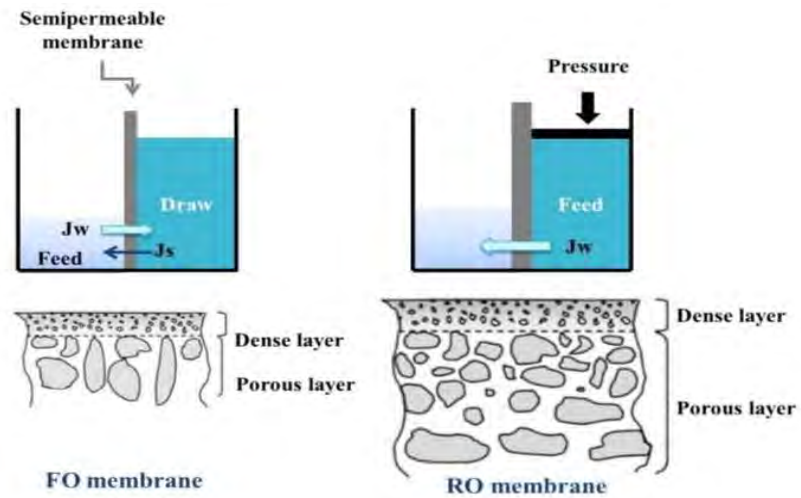
Figure 1.15:-Comparison between the morphology of both FO and RO [67]

Overall, membrane processes are influenced by a number of variables, including the pore size, pressure range, flux range, permeate and membrane type and structure as shown in Table 1.3.

Table 1.2:A brief summary of membrane process

Membrane process	Pore size	Pressure (bar)	Flux range	Membrane type	Structure
Microfiltration	>1μm	1-2	>50	Porous	Symmetric or Asymmetric
Ultrafiltration	0.1-0.0μm	2-5	10-50	Porous	Asymmetric
Nano filtration	0.01-0.001μm	5-40	1.4-12	Porous	Composite
Reverse osmosis	<0.001μm	15-1	0.05-1.4	Porous	Composite or Asymmetric

Regarding the history of membrane technology, there have been two distinct developments: the scientific development and the commercial development. Already in the middle of the eighteenth century, membrane phenomena were seen and investigated, although more for the purpose of understanding the barrier qualities and associated phenomena than for the purpose of creating membranes for technical and commercial uses. Research on membranes has traditionally included work by biologists, biochemists, biophysicists, and zoologists in addition to chemists and physicists. Before 40 years ago, membrane filtration was not thought of as a technically significant separation method. Today, a variety of applications utilize membrane processes. From an economic perspective, the current state of membrane processes is somewhere between first generation (MF, UF, NF, RO) and second-generation pervaporation (PV) and gas separation (GS) processes.

1.13. Pressure requirement for RO process:

The process of reverse osmosis (RO) is based on a phenomenon known as a liquid driven membrane, which enables membranes to flow water while rejecting micro-solutes like salts and less molecular weight organics. In order to offset the effect of osmosis that drives water to flow towards a very concentrated feed form dilute permeate, pressure-driven force—the second sort of driving force needed—must be applied. The total amount of pressure that needs to be used is determined by the salt solution concentration on the concentrated side of the membrane. For instance, applying more than 200 psi of pressure is necessary for a system to operate at 1100 ppm to the concentrate side. Typically, the system requires >800 psi of pressure or more to operate at saline concentration >33000 ppm. For domestic appliances, 50 to 70 psi of pressure are required. Osmotic pressure consideration is a key element in the high-pressure osmosis process. Typically, the high-pressure RO process includes feed side operating pressures more than 100 bar. For waste water treatment systems to achieve high water recoveries, functioning at trans-membrane pressure differences between 120 and 200 bars must be established. The separation of water from the solution of salt will be sufficiently driven by this type of pressure differential. When high separation of both salt as well as low molecular weight organic solutes from solutions is needed, the low-pressure RO technique is used to prepare electronic grade water.

The RO method is popular and considered to be the most important when it concerns purifying brackish water. When the high flux asymmetrical cellulose acetate (CA) membrane was created using the technique introduced by Sourirajan and Loeb, it was first used commercially in the late 1960s. The RO method has the following benefits:

- Since the process is pressure-driven, no possibly costly solvents are required.
- It is an easy technique with an extremely simple structure and operation.
- It can be employed in conventional procedures as well as hybrid processes.
- Inorganic as well as organic substances can be separated and concentrated simultaneously.

1.14. RO membranes:

The permeability of a membrane is just as crucial as its ability to selectively separate different solutes. When a specific material is chosen for its inherent separation properties, the permeability of the resulting membrane can be enhanced by decreasing its thickness. The rate of substance flow through the membrane is almost inversely proportional to its thickness. To maximize performance, most reverse osmosis membranes are designed with an asymmetric structure. They consist of a thin, dense top layer (thickness <1μm) supported by a porous sublayer (50-150 μm thick). There are two types of reverse osmosis membranes that are most frequently used.

- **Asymmetric membranes**
- **Thin film composite membranes**

Reverse osmosis membranes of the asymmetrical varieties have a thin skin layer that is supported by a porous sublayer made of a related type of polymer. The dense skin layer defines the selective characteristics of the membrane along with fluxes, while the porous layer serves as a mechanical support for the skin layer above it. This thick layer restricts the movement of very tiny solute molecules. Typically, phase inversion techniques are employed to prepare these types of asymmetric membranes. Since the majority of polymers can be dissolved in one or more solvents, it is possible to manufacture asymmetric membranes from nearly any type of material. Cellulose esters, such as cellulose diacetate

and cellulose triacetate, are a significant type of asymmetric reverse osmosis membrane created through phase inversion. These membranes are highly suitable for desalination due to their excellent water permeability and minimal solubility towards salt. However, their resistance to chemicals, temperature, and bacteria is notably low. To maintain their performance, these membranes are typically operated within a pH range of 5 to 7 and at temperatures below 30°C, preventing polymer hydrolysis

Thin film nanocomposite membranes made up of a thin polymeric barrier layer produced on one or more support layers that are never identical to the surface layer above them. Similar phenomena occur in these types of membranes where the surface layer controls the flux and the porous layer acts as a mechanical support[67]. The barrier layer is quite thin, allowing for quick water flux. Such membranes are created using an interfacial polymerization technique, in which extremely porous poly-sulfone is covered with a polymer solution in water, followed by a cross-linking agent reaction in a non-water solvent as shown in Figure 1.19. Aromatic polyamides are commonly utilized as alternative materials for reverse osmosis membranes. These materials exhibit strong salt selectivity, although their water flow rate is slightly lower. A notable advantage of polyamides is their ability to function effectively within a broader pH range, spanning approximately from 5 to 9.
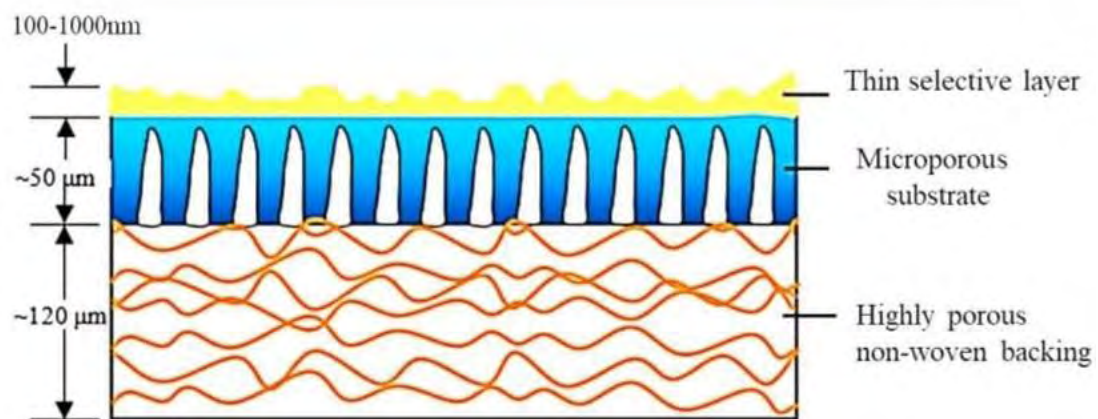
Figure 1.16:-Schematic cross section of the typical thin-film composite (TFC) membrane, displaying the functionality of each layer[68]

Reverse osmosis has a broad range of potential uses, which can be categorized into two main types: purifying solvents to produce a permeate as the desired outcome, and

concentrating solutes to obtain the feed as the desired product. Reverse osmosis (RO) differs in their ability to retain substances. RO has varying retention characteristics for different types of solutes as shown in table 1.4.

Table 1.3:Retention characteristics of   reverse osmosis (RO)

Solute	RO
Monovalent ions	>98%
Bivalent ions	>99%
Bacteria and viruses	>99%
Micro solutes	>90%

Reverse osmosis, also known as RO, membranes constitute a crucial part of the   RO process, that is frequently employed for desalination, water filtration, and other industrial uses. To achieve best performance and efficiency, RO membranes are chosen based on a number of factors such as quality of water, membrane material, permeability, fouling resistance etc. The overall quality of the feedwater must be considered while selecting the proper RO membrane. Important factors include the amount of dissolved solids, the presence of organic components, scaling potential, or suspended solids. A thin-film composite (TFC), polyamide, and cellulose acetate are just a few of the materials that can be used to create RO membranes. The material selection is influenced by the particular use, the operational environment, and the feedwater compatibility. The size of particle or solutes that may penetrate through the membrane is determined by its Molecular Weight Cut Off (MWCO). To reject impurities and let desired molecules, such as water, pass through, it is essential to choose the proper MWCO. The rate at how quickly water may pass through the membrane is referred to as its permeability. High permeability is preferred because it boosts the effectiveness and productivity of the RO system. The percentage of solute still present within the feed stream is known as solute rejection. Removing dissolved salts along with other impurities from water is the main goal of RO. Therefore, while choosing a membrane, the salt rejection rate becomes crucial. A higher salt rejection

suggests improved performance. Over time, system performance may suffer from membrane fouling, which is a collection of particles or pollutants on the membrane surface. Longer membrane lifespan and improved system efficiency can also be achieved by choosing membranes with superior fouling resistance.

1.15. Design and operational criteria for the RO process:

Since water flow is a function of the *pressure* differential that exists between the applied hydrostatic pressure and the osmotic pressure across the membrane, pressure plays a significant role in both the design and operating circumstances. While osmotic pressure is considered to remain constant, the flow of water increases as the pressure being applied rises. Due to an increase of solvent flux or no change in solute diffusion, the rejection of the solute rises with pressure.

In addition to a decrease in viscosity, the solvent flux rises with *temperature*. The rejection of solutes also increases with temperature because of the rise in osmotic pressure and the fact that solute transit requires a larger activation energy than solvent passage. The flux decreases when the *solute concentration* rises as a result of a rise in the osmotic pressure difference. The solute is polarized at the membrane when the feed velocity is lower, but as the feed velocity increases, the mass transfer re-disperses more of the polarized solute, decreasing the actual concentration of the solute at the membrane.

The *recovery factor*, which measures plant capacity, typically ranges from 75 to 95 percent with a practical maximum of roughly 80%. If the recovery factor is high, the salt concentration in the process water will be higher, and vice versa. If the concentrations are significantly higher than they typically are, the separation efficiency will decline. The effectiveness of separation processes is impacted by this issue. The term *Concentration polarization* refers to the depositing of the undesirable solute at the membrane's surface, which raises the amount of solute at the membrane's wall over that the of a bulk feed solution. Understanding surface fouling and predicting its performance are crucial for designing the reverse osmosis process. When a solvent exits the solution and enters a membrane during the desalination process, a localized concentration of the solutes builds up. This results in the formation of a rather stable boundary layer near to the

membrane[69]. Overall driving force will decrease because boundary layer concentration has a negative impact on osmotic pressure. Due to this, the water flux will significantly decrease. In simple terms, the concentration polarization can result in the following:

1. A significant reduction in flow
2. Fouling has increased
3. A rise in Solute transport
4. At the membrane surface, film resistance against mass transport into the liquid may be greatly increased.

1.16. Membrane filtration and water Desalination:

Membrane filtration technology emerged in the 1970s as a means to produce effective and high-performing membranes. This method offers superior separation efficiency, lower energy requirements, and greater environmental friendliness compared to traditional treatment methods. Reverse osmosis (RO), ultrafiltration (UF), and nanofiltration (NF) membranes are commonly utilized for separation and purification processes. Desalination is a method used to produce freshwater by removing salts as well as metal ions, and various minerals from naturally saline water. There are two ways to desalinate water: thermal and membrane-based methods. Thermal desalination processes can be further divided into multi-stage flash and multi-effect distillation processes. These processes involve heating the salty water to its boiling point and gradually condensing it to separate unwanted salts (in their ionic form) from the water. On the other hand, membrane-based desalination processes like reverse osmosis (RO) and electrodialysis utilize semipermeable films or membranes to separate dissolved solids (DS) from the water. Figure1.20 illustrates the global distribution of desalination capacities based on the technology employed. Regardless of the specific method used for desalination, energy in the form of heat or electricity is essential and plays a crucial role. Separation through membrane is widely recognized as a highly adaptable method for desalination of water. Researchers are actively seeking advancements within the membrane field, focusing on chemical modifications, nano-scale fabrication techniques, and the utilization of biodegradable materials to enhance sustainability. Four distinct separation modes are illustrated in Figure 1.21. The first two, ultra-

filtration and micro-filtration, operate based on the size of their pores, while nano-filtration and reverse osmosis employ dense or non-porous membranes, enabling molecular diffusion through concentration gradients. Reverse osmosis membrane-separation is a technology that relies on the energy provided by difference of osmotic pressure. These membranes have extremely small pores at the nanometer scale and work based on the principle of hydraulic pressure, allowing them to separate both multivalent as well as monovalent ions[70]. In a study conducted by Malamis et al, they developed RO systems with metal components that achieved an impressive 98.4% removal of heavy metal ions from wastewater. This advancement significantly enhances the effectiveness of the RO membranes for the purification of wastewater.
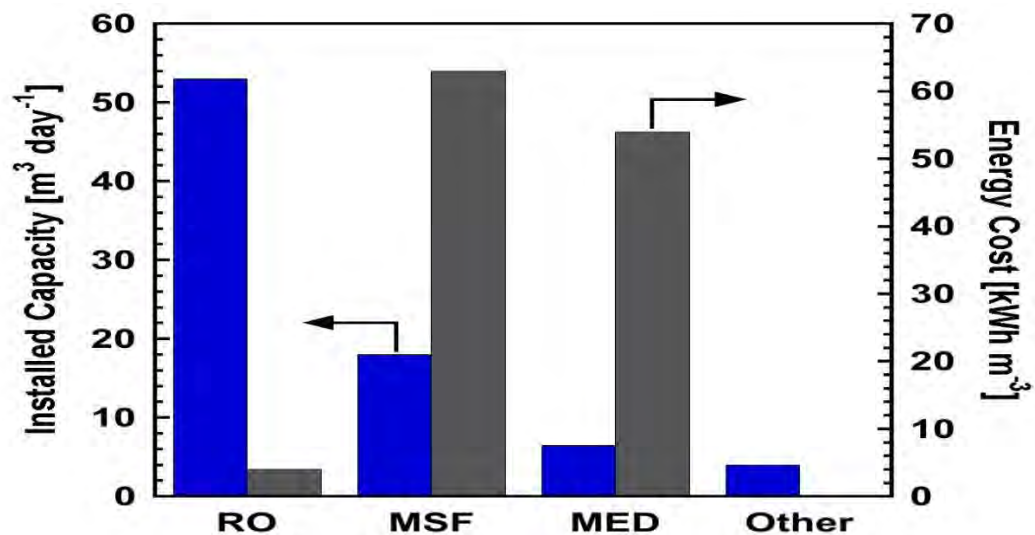
Figure 1.17:-Global distribution of desalination capacities based on the technology employed [70]

The majority of early water desalination techniques relied on the evaporation and distillation of seawater to supply fresh water. For many centuries, these techniques have been in use, and they have been created to match the requirements of modern living. The multi-effect distillation (MED) process, which involves heating the seawater in stages with hot steam, is still a common desalination technique. Despite the efficiency and simplicity of distillation, other desalination techniques have been developed in parallel with recent technological advancements[71]. Reverse osmosis (RO) emerged in the late 1950s through financial support from the U.S. Government, with the aim of desalinating seawater.

Presently, reverse osmosis has gained recognition as the most efficient and effective technique for water filtration, offering convenience and a comprehensive purification process. Among the most widely used methods are electro-dialysis (ED), which involves converting seawater in hot steam via a process called multi-stage flashing (MSF), desalination by freezing, and extracting particles that dissolve from ice crystals. The most promising approach for desalinating water today is reverse osmosis (RO), that depends on a specific permeability characteristic of membranes. Membrane-based desalination techniques have become increasingly important in the desalination industry over the past few decades. Reverse osmosis is a highly effective process for eliminating various substances from water[72]. It has the ability to remove a significant amount, typically ranging from 95% to 99%, of dissolved salts, particles, colloids, organics, bacteria, and pyrogens present in the feed water. This is achieved through the use of an RO membrane, which selectively blocks contaminants based on their size and charge. In general, any substance with a molecular weight above 200 is supposed to be rejected through a properly functioning reverse osmosis system. Additionally, contaminants with higher ionic charges are unable to flow through these RO membranes.

1.17. Membrane modules:

Various kinds of membrane modules are designed to meet industrial requirements depending on the type of membrane and its shape. The commercial availability of hollow-fiber (HF), spiral-wound (SW), plate-and-frame, and tubular modules has recently increased. Due to their high membranes area to volume ratio, the SW as well as HF modules are the ones most often used. Although the SW module has the two primary issues of high concentration polarization (CP) and fouling , it is nevertheless employed for commercial RO to UF systems since, according to research, the water flow has increased[74]. The primary uses of the SW module are the desalination of seawater, treatment of water and wastewater, water reclamation, product treatment for the dairy industry, and the recovery of valuable commodities for the pharmaceutical business.
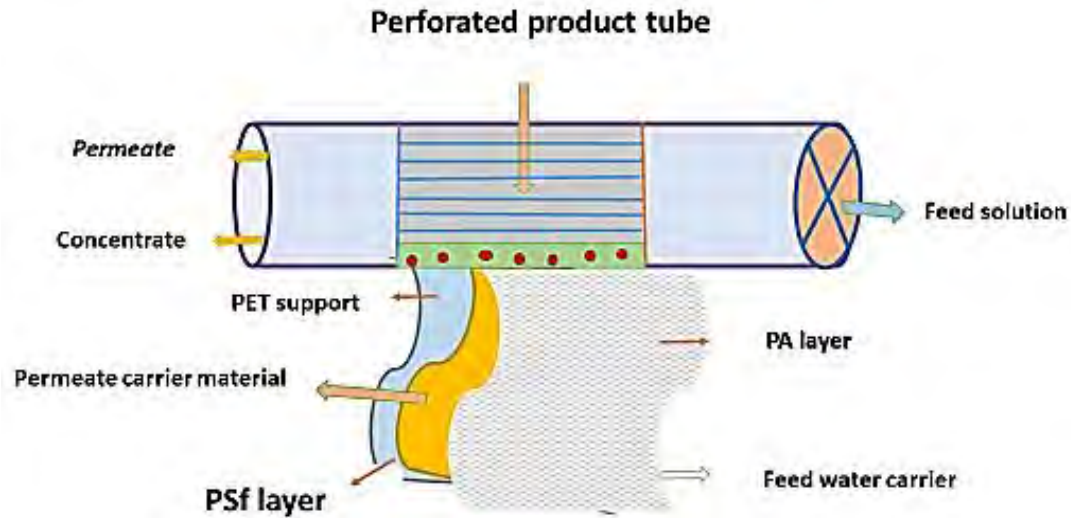
Figure 1.18 *:* Schematic representation of a spiral wound membrane module

A sequence of thin sheet membranes and a fine mesh spacer material are used to create spiral coiled modules. Figure 1.23 illustrates how these sheets are encircled around a tube with a central perforation. A feed tube, membranes, and a permeate tube, or perforated product tube are the basic components of a spiral wound module[75]. Water flows across the membrane surfaces because of the feed spacer. Here, the technique of cross-flow filtration is employed, and the feed runs perpendicular to the surface. On the industrial level, many spiral-wrapped structures can be connected in a certain order depending on the need[76].

1.18. Synthesis techniques for RO membranes:

Various methods, including phase inversion, electro-spinning, track-etching, and interfacial polymerization, are used to create membranes in literature. However, porous layer preparation and selective layer formation are mainly accomplished using PI and IP, respectively.

1.18.1. Phase inversion (PI)-based support layer synthesis:

PI is one of the regularly used techniques for creating membranes from a range of polymeric building elements. The procedure comprises the carefully regulated transition of a material such as polymer from its solution state to its solid state. Several techniques

are categorized as "PI" methods, including immersion precipitating, thermal precipitation based on the vapour phase, as well as controlled evaporation precipitation[77]. The fabrication of membranes frequently uses the immersion precipitation technique. The polymer must be dissolved in an appropriate solvent, cast on an appropriate support, and submerged in a coagulation bath free of solvents. The coagulation bath and casted polymer solution's interchange of solvent with non-solvent causes the polymer to precipitate. Various types of polymers such as PSf , PVA, PES, PVDF, PAN, serve as substrate materials. DMSO, DMF, and NMP are the commonly used solvents in phase inversion.

1.18.2 Interfacial polymerization (IP) for selective layer synthesis:

The quality of TFC membrane is affected by the ultra-thin selective layer's chemical and preparation parameters. A new technique creates a PA layer over a substrate using two monomers. One monomer is organic and the other is aqueous. The technique forms a crosslinked layer. Figure1.23. displays the most commonly utilized amine and acyl chloride monomers in literature. When MPD and TMC are combined, a ridge as well as valley structure results, however when PIP and TMC are combined, a globular surface shape results. The monomer plays a key role in the thin selective layer of PA composition .The ridge-and-valley structure of PA layer over globular PA structure is good at rejecting NaCl[78]. Primarily, the composition of piperazine (PIP) is subject to fluctuations ranging from 1 to 2wt.% in the production of NF membranes, whereas the content of m-phenyldiamine (MPD) is conventionally acknowledged to be 2 wt.% in the creation of RO membranes.
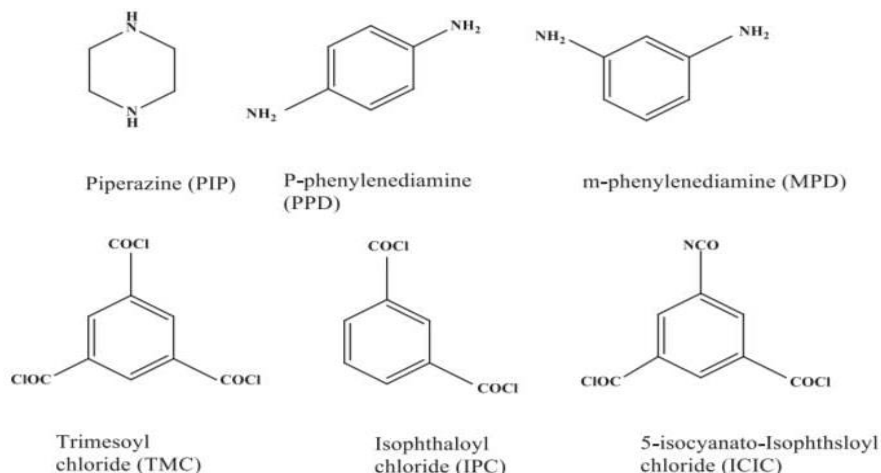
Figure 1.19: List of some of the monomers commonly employed to create the PA active layer [78]

For the fabrication of RO and NF membranes alike, it is customary to maintain a modest amount of TMC concentration within the secondary monomer solution, typically ranging within the lower bounds of 0.1 to 0.2 wt.%. to ensure a thorough polymerization of monomer and prevent the hindrance of amide bond formation, it is recommended to maintain a higher ratio of amine-to-acyl chloride. Furthermore, this approach will also hinder the hydrolysis of acyl chloride, thereby maintaining a higher degree of crosslinking within the polymer network.

1.19. Calculations for RO membranes:

The following operational characteristics are required in order to accurately measure a RO system's performance:

- **Salt Rejection(R) %:**

The following equation can be used to calculate the NaCl rejection:

$$R = (1- C_p/C_f) *100\% \qquad\qquad (i)$$

where C_p is the permeate solution's NaCl concentration and C_f is the feed solution's NaCl concentration. The performance of the system improves with increasing salt rejection. Low salt rejection may indicate that the membranes need to be cleaned or replaced.

- **Water Flux:**

Water flux was calculated by using equation (ii)

$$J_w = \Delta v / \Delta t. A \qquad\qquad\qquad (ii)$$

Eq. (iii) was used to determine pressure-normalized water permeation:

$$J_w = \Delta v / \Delta t.A. \Delta P \qquad\qquad\qquad (iii)$$

where Δt is the measurement's time (h), Δp represents pressure at which the device operates (bar), and ΔV is the volume of permeate (L). A is the actual membrane area (m^2). The electrical conductivity of both the feed or permeate solutions were compared using a conductivity meter to calculate the amount of NaCl rejected.

1.20. Objective of study:

The objective of this project is to synthesize the different nanomaterials such as ZIF-8 and its composite with 3DG and H-BN using solvothermal technique, synthesis of 3DG using direct carbonization method and also create Thin-film nanocomposite (TFN) membranes using ultrathin polyamide layers embedded with nanomaterials. These membranes are known for their energy-efficient properties and have been widely investigated for their potential in (RO) desalination. Thin-film nanocomposite membranes incorporating zeolitic imidazole frameworks, such as ZIF-8 and its composite with graphene, have demonstrated enhanced performance in reverse osmosis (RO). This improvement can be attributed to the membranes' inherent microporosity and significant surface area. The performance of thin-film nanocomposite (TFN) membranes in reverse osmosis is influenced by the interaction between the polyamide matrix and ZIFs nanoparticles. The selective layer and polymeric sub-layer will be created using the interfacial polymerization and phase-inversion process respectively. The effectiveness of the developed membrane will be evaluated using a standard reverse osmosis (RO) setup. Additionally, the RO membranes and synthesized materials will be analyzed using techniques such as X-ray diffraction (XRD), Fourier transforms infrared spectroscopy (FTIR), and scanning electron microscopy (SEM), RAMAN spectroscopy and TGA, BET.

1.21. Thesis layout:

Chapter 1 covers the background and overview of water purification technologies and their limitations and advantages, an overview of nanotechnology as well as membrane technology, and an overview of porous materials, different types of materials for membrane preparation, various separation modes and methods for separating the mixtures, Reverse osmosis's fundamental principle, membrane modules, classification of membranes and various applications of mixed matrix membranes.

Chapter 2 describes the experimental work and provides information about the methods and materials used.

Chapter 3 compiles all the results as well as discussion.

Chapter 4 summarizes the project conclusions and future suggestions.

1.22. Plan of work:

1. Synthesis of ZIF-8 and its composite with 3Dgraphene using solvothermal approach.
2. Synthesis of 3DG by direct carbonization method.
3. Synthesis of PSf@PA-ZIF-8 and PSf@PA-ZIF-8-3DG based MMMs membranes with different wt% for water desalination applications.
4. Surface morphology, phase purity, thermal stability, and structural characterizations
5. Performance testing of membranes by using RO membrane permeation tester.

Chapter 2

Experimental techniques and materials:

This chapter explains the details of numerous experiments performed for the production of ZIFs materials as well as their composites with 3D graphene and ZIF-8 incorporated polyamide based MMMs for water desalination. An overview of various characterization techniques utilized to analyze the samples is also provided.

2.1. Synthetic procedures:

Nanomaterials are used in a variety of applications, and their performance is greatly influenced by their size and shape. In this way, an effort to manage the production of nanomaterials has been made. The controlled production of ZIF-67 as well as ZIF-8 nanomaterials has become very important due to the wide variety of applications for these materials. ZIF-67 and ZIF-8 have been combined in a variety of nanostructures, including hollow spheres, nanowires, and nanotubes, although each of these courses has some drawbacks. The potential for these nanoparticles to grow into large, irregular particles is one of these challenges and pure phase of the final product presents the scientists with their next problem. In order to overcome these challenges, it is necessary to promote a more consistent and easy preparation technique to obtain pure nanomaterials. Simple mixing techniques (stirring and sonication) were used in the current work. This method is quick, uncomplicated, and doesn't need a lot of expensive toxic materials or a catalyst. As a result, it is the most effective method for producing nanomaterials at a low cost.

2.2. Instruments and materials used:

Instruments which are used for the synthesis of materials are weighing balance, heating oven and magnetic stirrer, ultrasonic bath sonicator and tube furnace, casting blade, rubber wiper, centrifuge machine and conductivity meter. Using superior synthetic chemicals and solvents for the synthesis of materials. Cobalt nitrate hexahydrate ,2 –methyl imidazole and zinc nitrate hexahydrate, m-phenylenediamine (MPD), trimesoyl-chloride (TMC), polysulfone (PSF) pellets were obtained from Sigma –Aldrich. Methanol was used as the solvent for the fabrication of the nanoparticles and was obtained from Sigma Aldrich.

Hydro chloric (HCL) acid was obtained from BDH and was 99% pure. The laboratory's deionizer was used to obtain deionized water. Triethanolamine (TEA), Camphorsulfonic acid (CSA), Dimethyl sulfoxide (DMSO), Dimethylformamide (DMF), maleic acid and sodium carbonate were purchased from (Sigma –Aldrich).

Figure *2.1*:Experimental instruments utilized (NCP**)**

2.3. Solvent drying:

Ethanol, methanol, and deionized water were the solvents employed in the synthesis process. Before usage, they were dried   to remove any moisture or contaminant from the solvents in the following ways:

2.4. Drying of ethanol and methanol:

Ethanol and methanol were first distilled, refined, and then further purified by reflux drying and Mg turnings were used as a drying agent while. Crystals of iodine were used as an indication.

2.5. MOFs synthesis methods:

In general, both conventional hydrothermal/solvothermal procedures and unconventional approaches can be used to synthesis MOF as shown in Fig.2.1. For the manufacture of MOF, the most conventional and fundamental method is the solvothermal approach.

2.5.1. Conventional hydrothermal/solvothermal methods:

The processes of hydrothermal and solvothermal synthesis are comparable. The precursors or reactants are dissolved in water in the hydrothermal production method while non-aqueous solvents are used in the solvothermal synthesis method. Similar to the solvothermal method, the hydrothermal method's fundamental concept is to heat the reactants inside a closed vessel utilizing water as a medium and allowing both the pressure as well as temperature to rise rapidly. Hydrothermal/solvothermal synthesis is the process of crystal growth or synthesis under extreme conditions of temperature and pressure. Depending on the temperature range, a Teflon-coated autoclave, or a bottle of glass is used to heat the solvent in which the organic linker and metal ions are mixed. To create a certain structure, a number of variables must be controlled, including temperature, pressure, solvents composition, reagent quantity, etc. The temperature of the reaction mixture is the key factor for the manufacturing of MOFs. The advantages of using hydrothermal/solvothermal synthesis techniques include (1) producing powder directly from solutions, (2) controlling particle size and form by using hydrothermal circumstances, and (3) the highly reactive nature of the powder that is created.

2.5.2. Non-conventional methods:

2.5.2.1. Mechanochemical method:

Using a ball mill or a pestle and mortar, this method involves grinding a combination of metal salts as well as organic linker which require no additional solvent The mixture is progressively heated after being milled to evaporate any remaining water or additional volatile byproducts. The method is referred to as a mechanical-chemical process. The bonds between molecules are mechanically disrupted during this process, and a chemical reaction occurs. When a smaller quantity of solvent is added at first, liquid aided grinding

happens. This procedure is very environmentally beneficial because it uses no solvents and yields more product. MOF crystals with small pore diameters are able to create in about 10 to 60 minutes. However, utilizing this method leads to large, amorphous particles with irregular morphologies.

2.5.2.2. Microwave-assisted synthesis:

In this approach, the energy required for the reaction is created using microwave radiation (MW). The use of this technique has a lot of benefits include a rapid crystallization process, strong morphological control, and a small and homogeneous particle size distribution. Cr-MIL-10 is the first MOF made using this method. Using this microwave technology method, MOF, that includes Fe^{3+}, Al^{3+} and Cr^{3+}, was also created[79]. In the process of synthesis utilizing the microwave approach, the sample, that takes the shape of a mixture consisting of the substrates and the solvent that is used, will be placed inside a Teflon vessel, closed snugly, and then heated for the required period of temperature and time. When using a microwave approach, a permanent dipole molecular moment and an electric field that oscillates create molecular rotation, which quickly heats up the liquid phase.

2.5.2.3. Electrochemical synthesis:

The electrochemical production of MOFs takes place with metal ions which are continuously supplied via an anodic solvent rather than employing metal salts as a metal source[80]. This solvent will interact with the conduction salt and the dispersed link molecule in the reaction media. The aprotic solvent used in this approach prevents the deposit of metal on the cathode, although H_2 is generated in the process. Continuously electrochemical synthesis can produce more products with a higher solid content than batch processes.

2.5.2.4. Sonochemical synthesis:

The sonochemical method functions by exposing a solution to ultrasonic waves at extremely high frequencies. When a solution is exposed to ultrasonic vibrations, the solution's component particles collide under intense pressure. Homogeneous and fast

nucleation techniques can result in far smaller decreases in crystallization time as well as particle size than conventional solvothermal synthesis. This method uses ultrasonic radiation having frequency between 20 KHz -10MHz to produce MOF, which can accelerate the process of crystallization and is also more friendly to the environment. When ultrasonic vibrations are applied to a homogeneous liquid, chemical reactions can occur. The sonochemical approach has many advantages, including the capacity to split large crystal formations into smaller crystal formations that could be nanoscale, quicker reaction times, and more outcomes, in addition to a simpler process and a quicker reaction path. Intermediate reactions are possible due to low temperatures of reaction and increased energy demands, which promote the following reaction stage. For instance, a catalyst is not required for the calcination or reaction processes.

2.5.2.5. Solvent minimization method:

There are still some problems, such as an excess of imidazole source and a lot of solvent waste during washing, even though the manufacture of ZIFs using an aqueous-based method is more friendly to the environment and doesn't produce any hazardous compounds when compared to organic solvents. As a result, solvent minimization is employed. In this technique, water vapor (or organic solvent-based steam) is applied to Teflon cups holding metal salts as well as organic ligands for 24 hours at 120°C.).
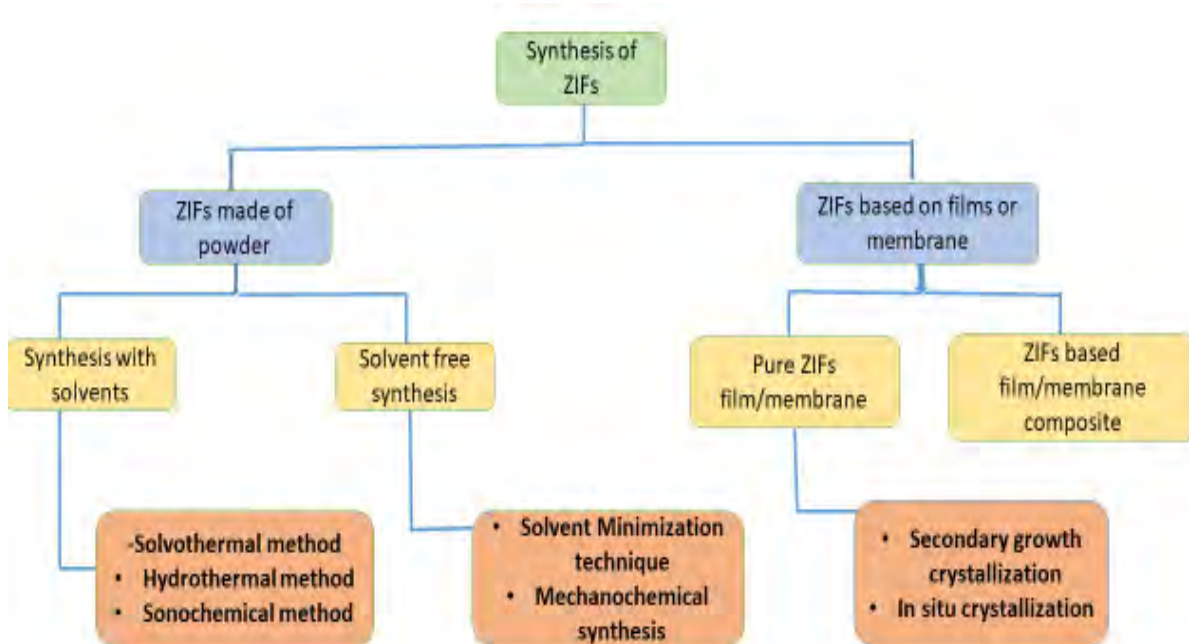
Figure 2.2: An overview of the various ZIF-based materials fabrication methods

2.6. ZIFs synthesis:

The synthesis of ZIFs uses both hydrothermal and solvothermal processes.

2.6.1. Solvothermal method:

This approach involves mixing the reactants with a suitable solvent present before transferring them to a Teflon-lined reactor that is heated to a temperature between 100 and 200ºC. When the temperature rises, the reactants slowly dissolve and react at autogenous pressure above the solvent's boiling point[81]. The final result is obtained as crystals that may be examined using single crystal XRD. This technique gives the user control over the material's size, shape distribution, and crystallinity. By adjusting the experimental parameters, such as reaction temperature, reaction time, solvent type, and precursor type, these properties can be altered.

2.6.2. Hydrothermal method:

Single crystals are created using the hydrothermal process. An autoclave with a steel exterior and a Teflon interior is used to perform the reaction. In a Teflon-lined reactor,

reactants and the solvent are introduced. The growth chamber's opposite ends are separated by a temperature gradient[82]. The capacity to produce crystalline phases gives hydrothermal methods an edge over other sorts of methods. Moreover, hydrothermal methods can be used to create materials that have high vapour pressure close to their boiling temperatures. With this technique, enormous numbers of crystals with adjustable composition can be produced.

Hydrothermal technology can be used in a variety of ways:

1. Temperature-difference technique

2. Temperature-reduction technique

3. Metastable phase approach
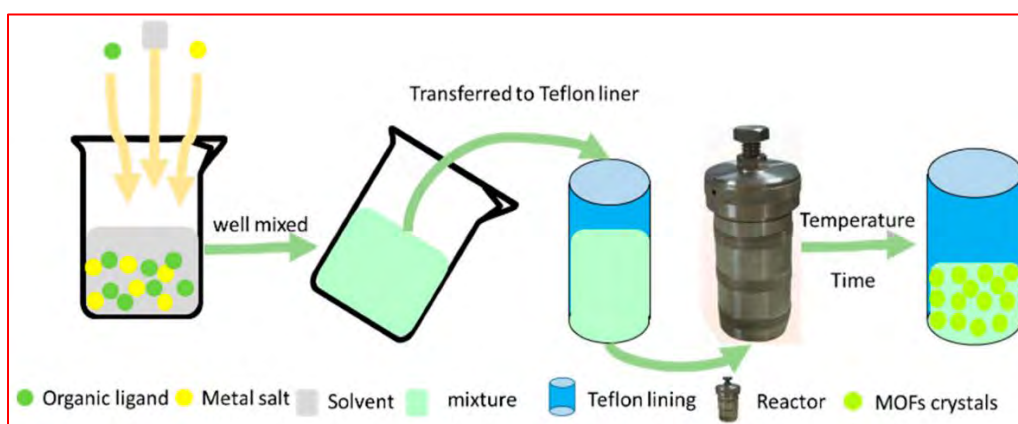
Figure 2.3.illustrate the hydrothermal process utilizing an autoclave

2.7. Synthesis procedure of ZIF-8:

ZIF-8 is synthesized by dissolving 2.38 g of zinc nitrate hexahydrate in 40 mL of methanol. A similar procedure was used to dissolve 2.463g of 2-methyl imidazole in 40 mL of methanol. The two solutions mentioned above were sonicated for the next 30 minutes. The above solutions were mixed together and sonicated for 45 minutes. Without any interruption, the solution was left alone for 24 hours. The result was separated by centrifugation, numerous times rinsed with methanol, and then dried for three hours at 80ºC.[83]

Figure 2.4: A pictorial representation of steps involved in the synthesis of ZIF-8

2.8. Synthesis of Graphene:

Graphene was produced by mixing the 2.78g of maleic acid (MA) and 10.16g of sodium carbonate (Na_2CO_3) together. The above mixture was ground well and placed in a combustion boat, then heated for three hours in a tube furnace to 700°C at a heating rate of 50°C/min in the presence of Argon gas as an inert atmosphere. The next step is to purify the graphene powder by mixing a 1 molar solution of hydrochloric acid with 230 ml of distillate water in a 250 ml beaker. Thereafter, the mixture was left to settle for a day after being stirred for three hours. For the next item, impurities were removed by vacuum filtration three to four times with distillate water. A three-hour drying process at 80°C produced the end product[84].
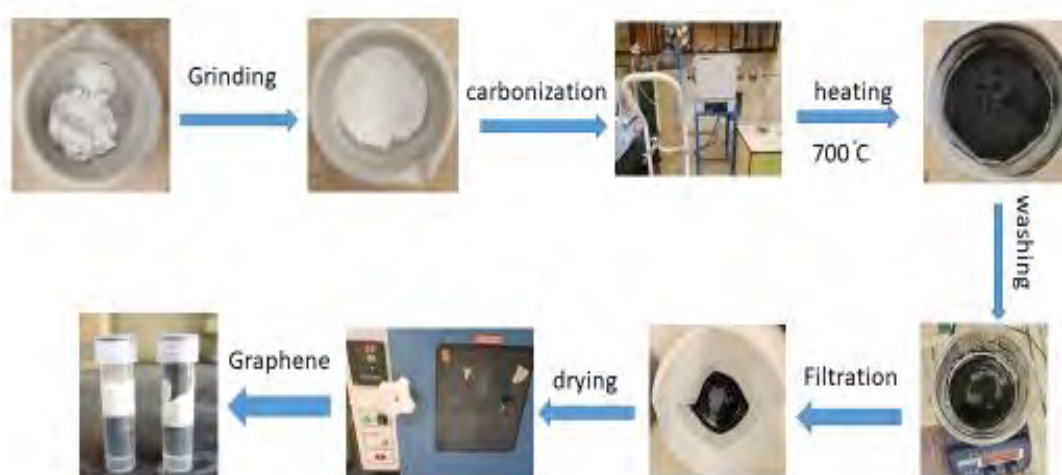
Figure 2.5: represents the synthesis procedure of 3D Graphene

2.9. Synthesis of ZIF-8/3DG composites:

ZIF-8/ 3DG nanocomposites were prepared by dissolving 2.38 g of zinc nitrate hexahydrate in 40 mL of methanol. 2.463 g of 2-methyl imidazole and 0.5wt%, 1wt%, and 2wt% of graphene were dissolved in 40 mL of methanol employing a similar method. The aforementioned two solutions were separately sonicated for the next 30 minutes, subsequently mixed and rapidly stirred for an additional 45 minutes and then left undisturbed for 24 hours. Following centrifugation, the black suspended precipitates were separated, repeatedly washed with methanol, and then lastly dried at 80°C for three hours.
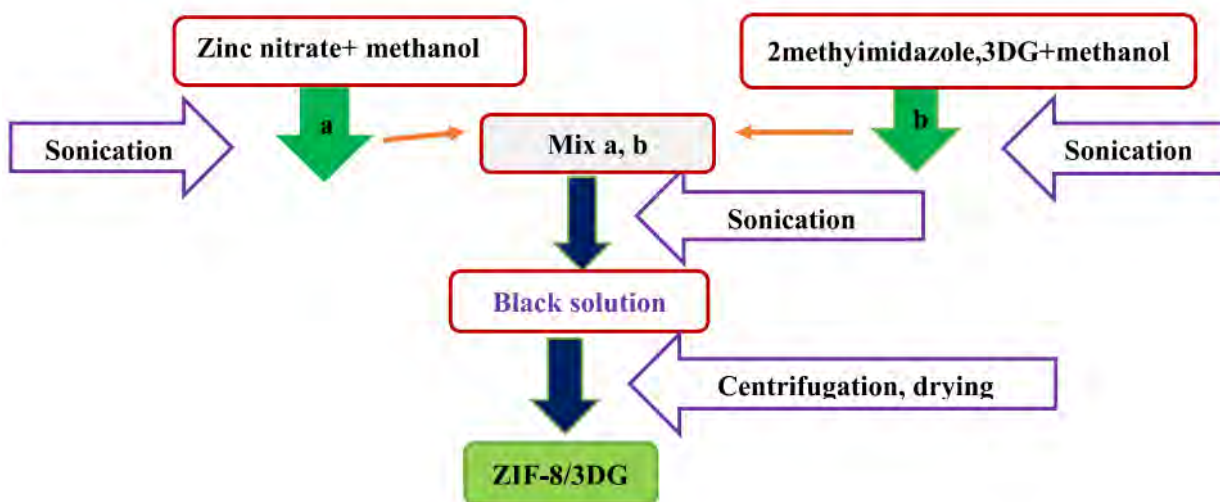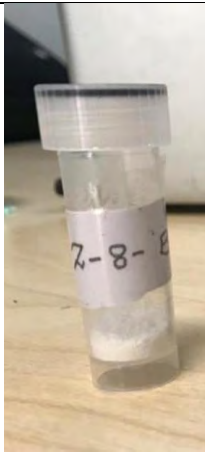
Figure 2.6: Flow chart for the synthesis of ZIF-8/3D Graphene

Table 2.1: as-synthesized nanomaterials

ZIF-8	ZIF-8/3DG

2.10. Membrane synthesis methods:

For the synthesis of membranes, a variety of processes are used in the literature, including phase inversion (PI) and or the electro-spinning, track-etching, or interfacial polymerization (IP), among others. However, the PI is most frequently used for, respectively, preparing the membrane's porous layer and creating the selective layer on the substrate surface.

2.10.1 Support layer synthesis by PI:

PI is one of the regularly used techniques for creating membranes from a range of polymeric building elements or blocks. A polymer is controlled in its transition from a liquid solution to a solid state during this process. Examples of "PI" techniques include immersion precipitation. Immersion precipitation is the process that is most frequently employed for creating membranes. The polymer is dissolved in a suitable solvent, cast on an suitable substrate, and then submerged into a non-solvent containing coagulation solution in this process. The casted polymer mixture as well as the coagulation bath exchange solvent as well as non-solvent, causing in the precipitation of polymer. A variety of polymers are used as substrate materials, including polysulfone (PSf), poly (vinyl

alcohol) (PVA), polyacrylonitrile (PAN), and polytetrafluoroethylene (PTFE). The most popular solvents for phase inversion include DMSO and DMF.

2.11. PSF support preparation:

The TFC and TFN membranes, which had an asymmetric structure, were fabricated on a PSF layer using a wet phase inversion method. To prepare the PSF layer, PSF pellets were subjected to drying in an oven at 110 °C for overnight to remove any moisture present. A solution of PSF (polysulfone) with a concentration of 15 wt% was created by dissolving 1.5 g of PSF pellets in DMF (dimethylformamide) and stirring the mixture on a magnetic stirrer for 6 hours at a temperature of 60 °C. To eliminate any air bubbles, it was taken out and left out overnight. Using a micrometer-adjustable casting-blade or casting knife and maintaining a thickness of 150µm, the polymer solution was casted on a PET support that was firmly supported on a glass plate. For complete phase inversion, the support was submerged in water for 24 hours after casting.
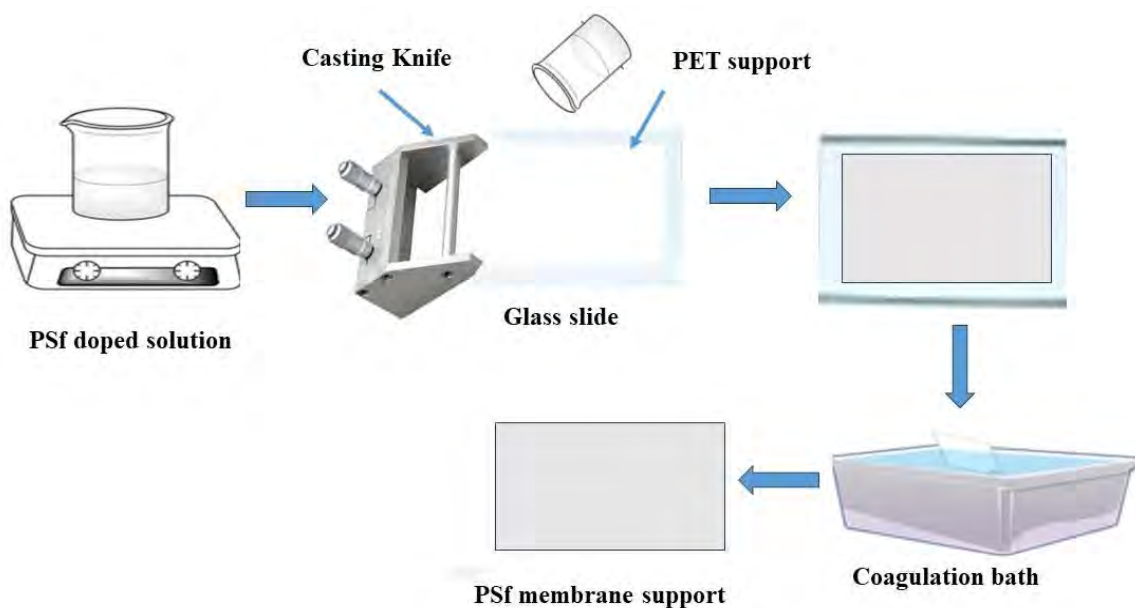
Figure 2.7: Schematic of the PSF support membrane by phase inversion approach

2.12. Solution preparation:

The synthesis of a polyamide active layer by an IP was then carried out using two aqueous as well as non-aqueous (organic) solutions. In order to prevent oxidation of an amine solution, first a 2 wt% MPD solution in DI water was made (without the addition of any additives. DMSO (0.5-2wt%), SLS (0.1-0.5wt%), CSA (0.5-2wt%), and TEA (0.5-2 wt%) were added as additives to the MPD aqueous solution to assess their influence on permeate flux and NaCl rejection. On a magnetic stirrer, the resultant solution was thoroughly stirred until the particles had completely dissolved. To remove any remaining dust or fibrous material, the produced solution was finally filtered using a filtering paper. A 0.1 wt% TMC solution was produced in n-hexane then stirred for 1 hour in an airtight reagent flask to prevent evaporation of the solvent and hydrolysis of TMC from ambient moisture.

2.13. Preparation of polyamide membrane:

The following reaction (Figure 2.8) is how polyamide membrane was created via interfacial polymerization:
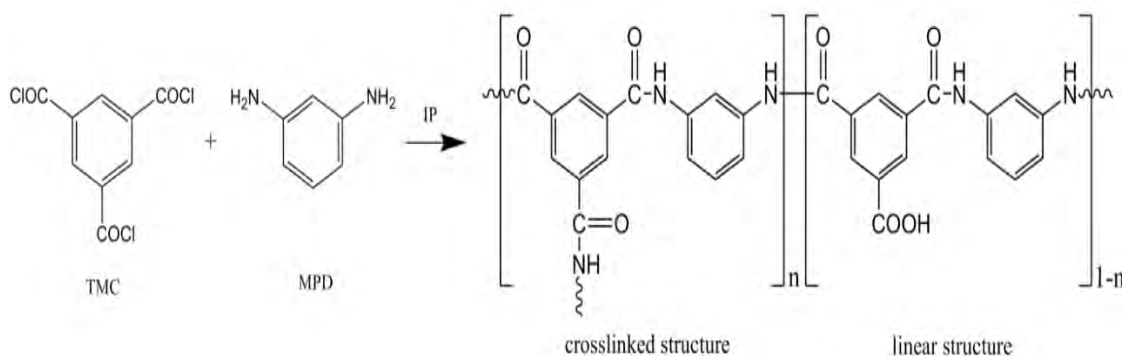
Figure 2.8: Polyamide membrane fabrication

The previously constructed PSF support was placed on a frame in a rectangle shape, and the top surface was exposed to a mixture of above prepared MPD aqueous solution for 10 minutes, allowing the mixture to permeate the PSF's porous structure. A wiper was used to remove the remaining solution from the support's top surface. The above prepared TMC solution was then poured on top of the surface and was allowed to stand for 30 seconds in order to end the reaction and create the TFC polyamide membrane. The above-

mentioned preparation procedures were carried out at room temperature. The Polyamide membrane was then stored in DI water until it was needed.

Figure 2.9 : Thin film composite-PA membrane

2.14. Preparation of ZIF-8 incorporated polyamide membrane:

The TFN membrane was made in the same manner as discussed above with the exception of dispersing ZIF-8 nanoparticles in the TMC solution. Different ZIF-8 concentrations (0.002, 0.008 wt%) were employed, and they were sonicated for 1 hour right before usage. The control polyamide thin -film composite (TFC) PSf@PA-ZIF-8(0wt%) membrane was referred to as M1, while the TFN PSf@PA-ZIF-8 (0.002wt%), PSf@PA-ZIF-8 (0.008wt%) membranes were given the names M2 and M3 respectively. To increase the cross-linking, the membranes were subjected to heating for 10 minutes at 70 °C in the oven. The membrane was then stored in DI water until it was needed.

(a)   (b)
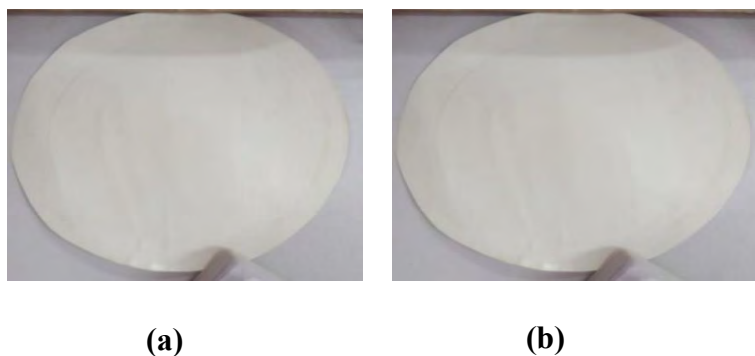
Figure 2.10: TFN-PA membranes with different ZIF-8 concentration (a) PSf@PA-ZIF-8 (0.002wt%) (b) PSf@PA-ZIF-8(0.008wt%)

2.15. Preparation of ZIF-8@3DG /polyamide membrane:

The TFN membrane was made in the same manner as discussed above with the exception of dispersing ZIF-8 and its composite with graphene nanoparticles in the TMC solution. ZIF-8@3DG concentrations (0.002) were employed, and they were sonicated for 1 hour right before usage. The control polyamide thin-film composite (TFC) membranes were referred to as PA, while the TFN membrane PSf@PA-ZIF-8-3DG (0.002wt%), were given the name as M4 respectively. To increase the cross-linking, the membranes were subjected to heating for 10 minutes at 70 °C in the oven. The membrane was then stored in DI water until it was needed.
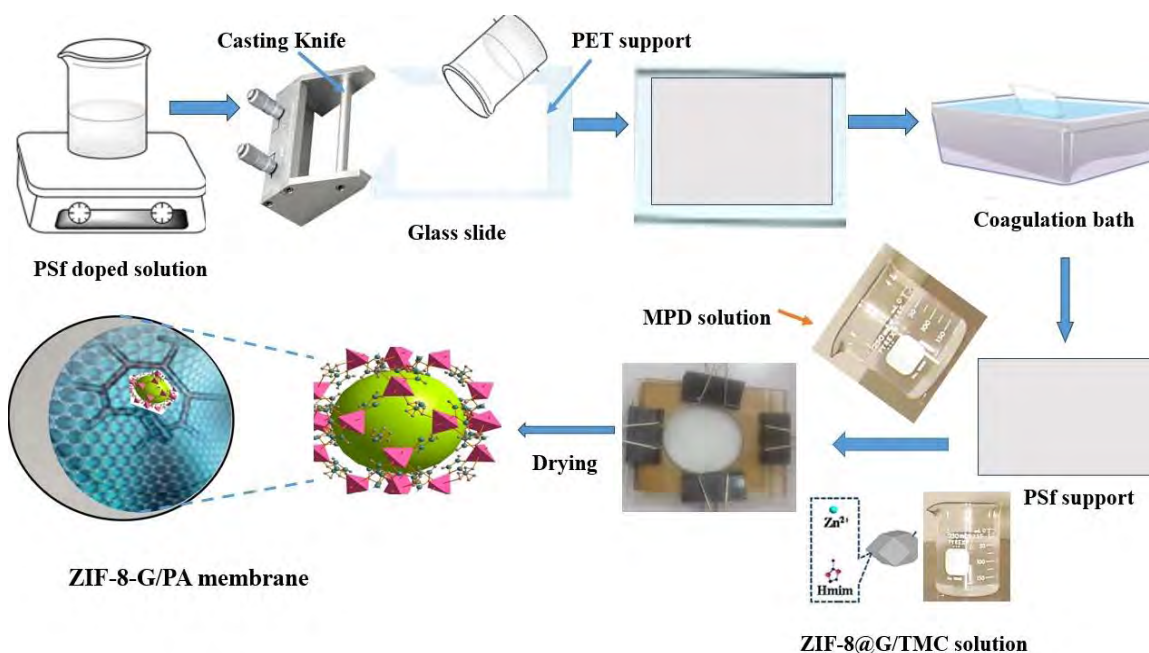
Figure 2.11: Schematic of the PSF@PA-ZIF-8-3DG membrane by Interfacial polymerization reaction.

2.16. Characterization techniques:

Details on characterization techniques will be provided in this chapter. The final section includes the research's findings and conclusions. The produced ZIF-67 and ZIF-8 nanoparticles, as well as their composite with 3D graphene and H-BN, were characterized using a variety of techniques, including XRD, FTIR, TGA, and SEM, RAMAN, BET.

2.16.1.X-ray diffraction (XRD):

Over time, several methodologies and approaches have been employed to investigate the electrical, chemical, and physical structure of various materials in a range of environmental settings. One of the important experimental methods used to characterize materials is X-ray diffraction. This method is applicable for obtaining information on various aspects of materials, including crystalline phase, composition, lattice characteristics, quality, orientation, defects, stress, and strain. A common technique for determining the purity and phase of crystalline materials is XRD, which also provides details on atomic spacing and unit cell dimensions. The crystalline substance and monochromatic x-beam interaction in this method results in constructive interference. The internal orbital of an atom's electrons causes electromagnetic radiation with a relatively short wavelength (0.1–10) known as X-rays. Because it passes through the edges of an object, electromagnetic radiation is mildly bent, causing diffraction. How much bending is involved depends on how large an electromagnetic wave's wavelength is compared to the outlet's size. The bending may be almost imperceptible if the hole is substantially larger than the light wavelength. A crystal can be utilized for the diffraction of x-rays since the space between atoms in one is similar to the wavelength of the radiation. X-rays are diffracted and coherently scattered by the atoms in a crystal's unit cell. Since each crystal is composed of up of parallel planes, it is important that the total distance spanned by the two parallel x-ray beams be an integral multiple that of the wavelength being used for diffraction of X-rays. The term "Bragg's law" is used to describe this phenomenon. Figure 2.12 depicts the schematic diffraction of two parallel sets of planes. All crystals are made of X-rays in the crystal lattice scatter when they come into contact with an atom's electrons. These electrons have been scattered, and this type of scattering is known as elastic scattering. This process results in waves, which are subject to Bragg's law:

$$2\mathrm{dsin}\theta = n\lambda$$

Where d denotes the lattice spacing, θ indicates the incidence angle, denotes the X-ray wavelength, and n is an integer.
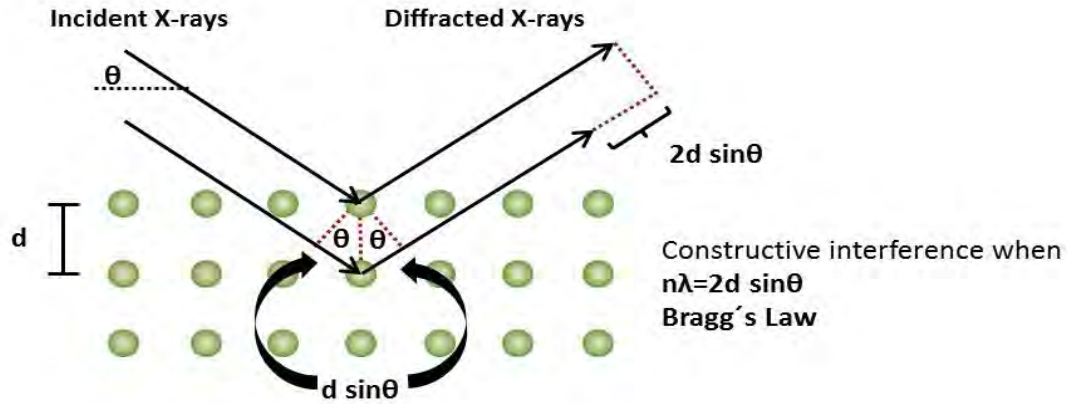
Figure 2.12:X-ray diffraction from crystal surfaces[85]

The following three techniques are usually employed for the diffraction of x-rays from crystal.

- Powder approach
- Laue method
- Rotating-crystal approach

One of the most important methods for examining the structure of materials is XRD analysis. Following the synthesis of the samples, we analyzed them using XRD. With an XRD system based on the powder diffraction technique, we employed the D8 Focus, Bruker model. Cu is utilized as an x-ray source, and the wavelength of the k lines is 1.5406. The utilized range for "2" is 5 to 800. The scan speed is set at 0.8 steps per second. On a computer system, the diffraction data is collected.

2.16.2. Scanning electron microscopy (SEM):

The surface morphology of materials is frequently studied with the scanning electron microscope. When a sample is exposed to radiation, electrons are released from it that reveal details about its topography, composition, and crystalline structure. The foundation of SEM is based on the idea that an image created when electrons interact with the sample's atoms. A variety of signals are generated as a result of this interaction. Such signals are gathered, and an image is created. SEM analysis is carried out. SEM is an outstanding

technique for studying morphology at the nanoscale. This technique frequently allows for the differentiation of features down to 10 nm or less. To prevent the interaction of electrons and free gas molecules, SEM is carried out under vacuum.

The primary elements of a SEM instrument are as follows:

- Electron gun
- Column (objective lens, detector, condenser lens)
- Vacuum
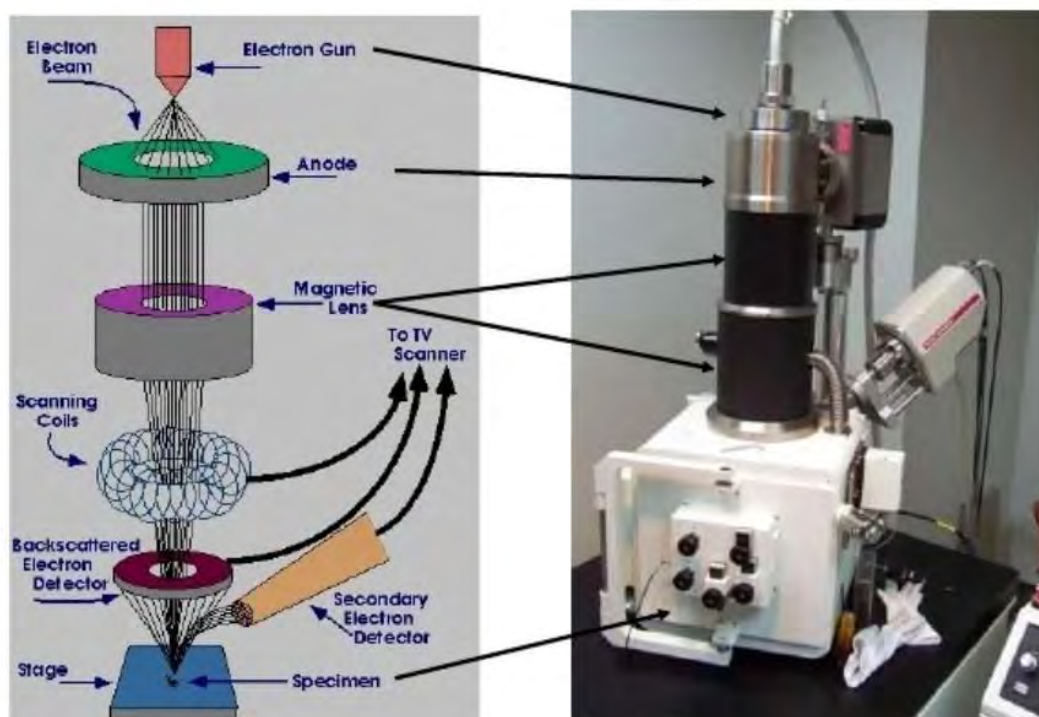
Figure 2.13: Schematic representation of SEM

2.16.3. Fourier transform infrared spectroscopy (FTIR):

One of the most crucial analytical methods used to describe natural, polymeric, and inorganic materials is FTIR spectroscopy. In this method, the sample is subjected to infrared light intervention. The sample must be analyzed using a broad range of near infrared (NIR) to far infrared (FIR) wavelengths. By using FTIR, all possible wavelengths are gathered. As FTIR has a far wider measuring range than traditional spectrophotometers, which have relatively narrow wavelength ranges, it has an advantage.

Radiation source, Michelson interferometer, and detector are the three necessary additives of FTIR. Beam splitter, moving mirror, and constant mirror are the three active components that make up the Michelson interferometer. Two mirrors are placed perpendicular to one another. The typical method for creating a beam splitter, a semi-reflecting device, is to place a thin layer of germanium on a KBr substrate. Radiation originates from the source and is directed at the interferometer. The beam splitter reflects half of the radiation towards the fixed mirror and transmits the other half to the movable mirror. The radiations that are then recombined at the beam splitter were reflected by these two mirrors. An interferogram is the result of the interference between the two reflected radiation beams. The sample, depending on its nature, either absorbs or transmits such radiations, exceeding the interferogram. On a detector, a final interferogram is produced. All of the radiation source's frequencies are present in each interferogram point. Therefore, we need a single intensity value for each frequency for the analysis. As a result, we cannot immediately examine the measured interferogram. To obtain a single frequency value for each absorption measurement, the Fourier transform mathematical technique is applied. Because of this, the method is known as Fourier transform infrared spectroscopy. The following activities can utilize FTIR:

- Identification of unidentified compounds
- Evaluation of a material's quality;
- Determination of additives in a material

In our experimental setup, we used a Nicolet 5700 version spectrometer. We utilized a tiny pellet of KBr for the background spectrum. A little amount of material is combined with KBr powder and pelletized at a pressure lower than 3.8 tons/cm2 after gathering a background spectrum. The spectrometer's sample holder is subsequently filled with the pellet. As 200 scans were performed on each sample, the wave number range of 400 to 700 cm-1 is now available. The raw data is examined using the computer programme Omnic. Ultimately, we look at the vibrational modes of all samples because different vibrational modes are seen for each sample.
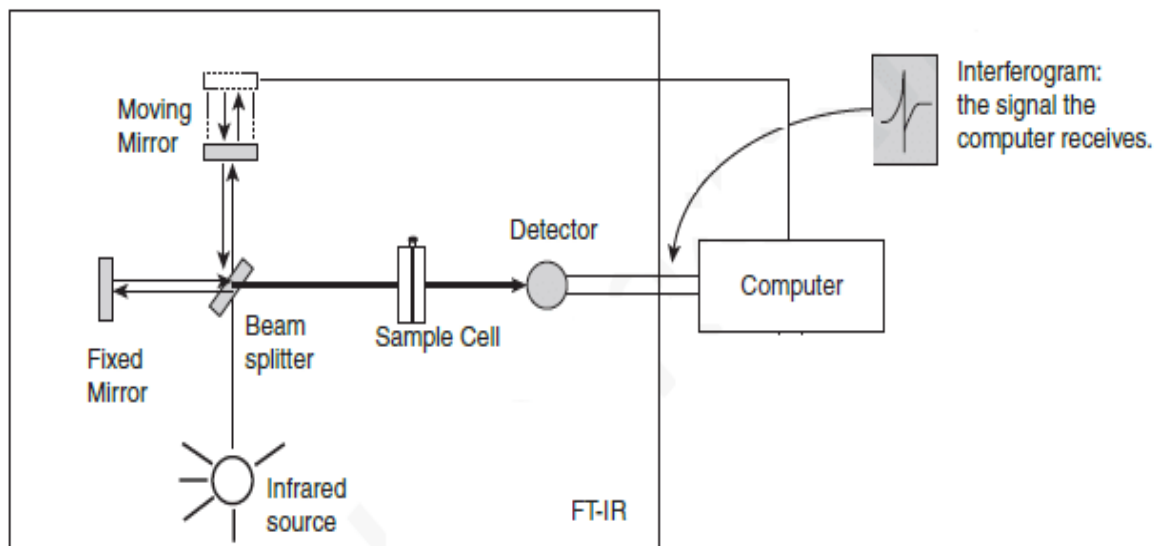
Figure 2.14 : Schematic representation of FTIR instrument[73]

2.16.4. Thermogravimetric analysis (TGA):

The TGA method uses a sample's decomposition pattern to identify the chemicals in the sample. Thermogravimetric analysis can be used to assess the purity of organic substances, inorganic chemicals, and minerals. This method is employed to examine the sample's thermal stability. By adjusting the temperature at a constant rate of heating, TGA entails the study of changes in the physiochemical properties of the materials. The specimen is placed in an inert environment with a regulated temperature that has been programmed. The sample is heated over a period of time until the desired temperature range is reached. The apparatus monitors the weight loss of the sample with regard to time and heat. The curve displayed between the weight loss and temperature can be used to determine the thermal stability for a given sample.

2.16.5. Raman spectroscopy:

Raman spectroscopy, a non-destructive technique for chemical analysis, provides comprehensive information on chemical structure, and phase or molecular vibrations, crystallinity. For the purpose of analyzing the rotational or vibrational modes of molecules, C.V. Raman created the Raman spectroscopy in 1928[86]. Whenever light interacts with molecules in a solid, liquid, or gas, photons are scattered out with an energy equal to that

of the incident photons and this phenomenon is called Rayleigh or Elastic scattering. One of these photons out of every ten million will scatter at a frequency different from the incoming photon. Raman effect, also referred to as inelastic scattering, is the name of this phenomenon. Unlike FTIR spectroscopy, which analyzes variations in dipole moments, Raman spectroscopy analyzes changes in polarizability. As a result of the interaction of light with the molecule, the electron cloud of the molecule may shift or distort.

There are three possible ways for light to be released once an electron absorbed energy:

• The light is emitted again at the same wavelength once an electron comes back to its original ground state as there is no energy difference which is known as Rayleigh scattering.

• When excited, an electron doesn't fall to the ground level; it lowers to a vibrating level, some amount of the energy was absorbed by a molecule, resulting in the emission of light with a wavelength that is longer as the incident light. This is called" Stokes scattering."

•If an electron gets excited from a vibrational level, it will go to a virtual level having more energy. Its wavelength is shorter because it has more energy as the incident photon, which is produced when the   electron strikes the ground. This is known as "Anti-Stokes."
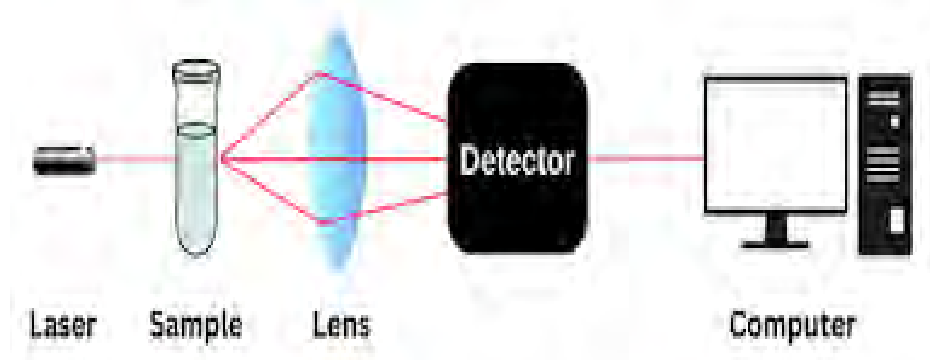
Figure 2.15 : An illustration of Raman spectroscopy equipment

The light source utilized in Raman spectroscopy is a laser. The spectrum of the light is determined by the laser source's bandwidth. Typically, a shorter wavelength causes more Raman scattering. Before going through the filter, the sample is subjected to both elastic or inelastic scattering in the laser-accepting sampling chamber. To discriminate between Raman & Rayleigh scattered light in Raman spectroscopy, a filtering device

is used. This is carried out to acquire high-quality Raman spectra. Long pass, notch, and volume halogen filters are a few types of filters. Dispersed light signal detection is possible by detectors. LCD array detectors are frequently used in modern Raman spectrometers. They are made to detect signals at different wavelengths, even very weak signals. Raman spectra are displayed on computers using appropriate software.

2.16.6. Brunauer –Emmett-Teller (BET):

BET analysis is a method for analyzing solid materials that is used to identify the surface areas as well as pore size distributions. The method relies on the actual adsorption of an inert gas, like nitrogen, upon the solid layer of the sample[87]. The measured particular surface area is expressed in m^2/g. The calculation of surface area should be done at an isothermal temperature. Depending on the inert gas being used (77 K for liquid nitrogen, for instance), a specific temperature must be employed. The appropriate inert gases for the analysis are determined by the characteristics of the sample. Small molecules of gas are drawn to the outermost layer of the solid sample, opening a porous structure to generate an adsorbed gas monolayer[88]. The sample is heated in a non-nitrogen environment once a gaseous layer of molecules has formed. This enables the outermost layer of the sample to release the molecules of adsorbed nitrogen gas. The porosity and surface area of the sample can then be determined, together with the number of released gas molecules. An important step before starting a particular surface area measurement is sample preconditioning. A degassing procedure is required to eliminate any moisture that may be physically bound to the surface. The degassing procedure is carried out for a minimum of 16 hours in a vacuum and at high temperatures. The setup must be calibrated before starting the real BET measurement by carrying out a helium blank run. Normally, the helium cannot be adsorbed onto the solid surface of sample.
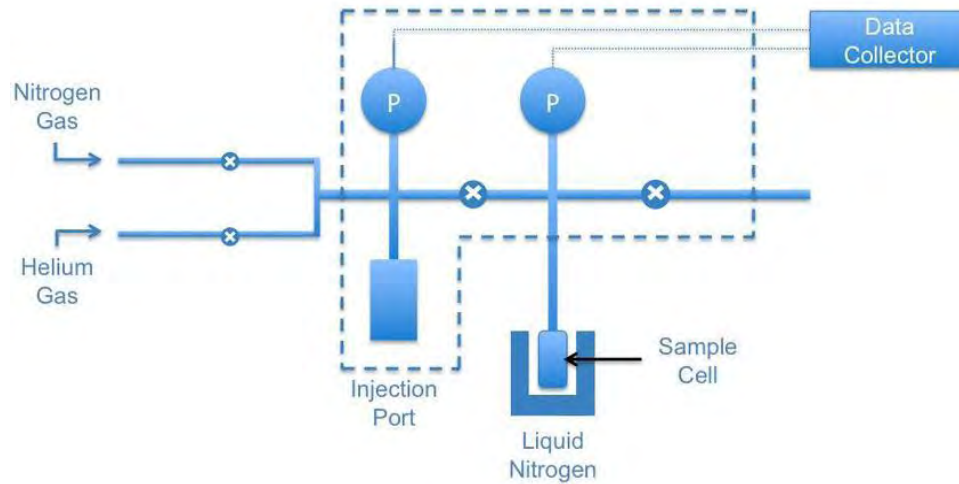
Figure 2.16 : Schematic representation of BET analyzer

2.17.RO membrane tester:

The RO membrane permeation system contained membrane cells, feed tank having deionized water or NaCl solution, flow meter and a bypass valve offers an alternative path for liquid flow, control valve regulates liquid flow and pressure and using thermocouples to control feed temperature, main power supply. The solution was transferred from the feed tank to the membrane module using the feed pump. The stream of rejected concentrate, which is sometimes referred to as retentate, passed through the concentrate's valve: and subsequently recovered back into the feeding solution.
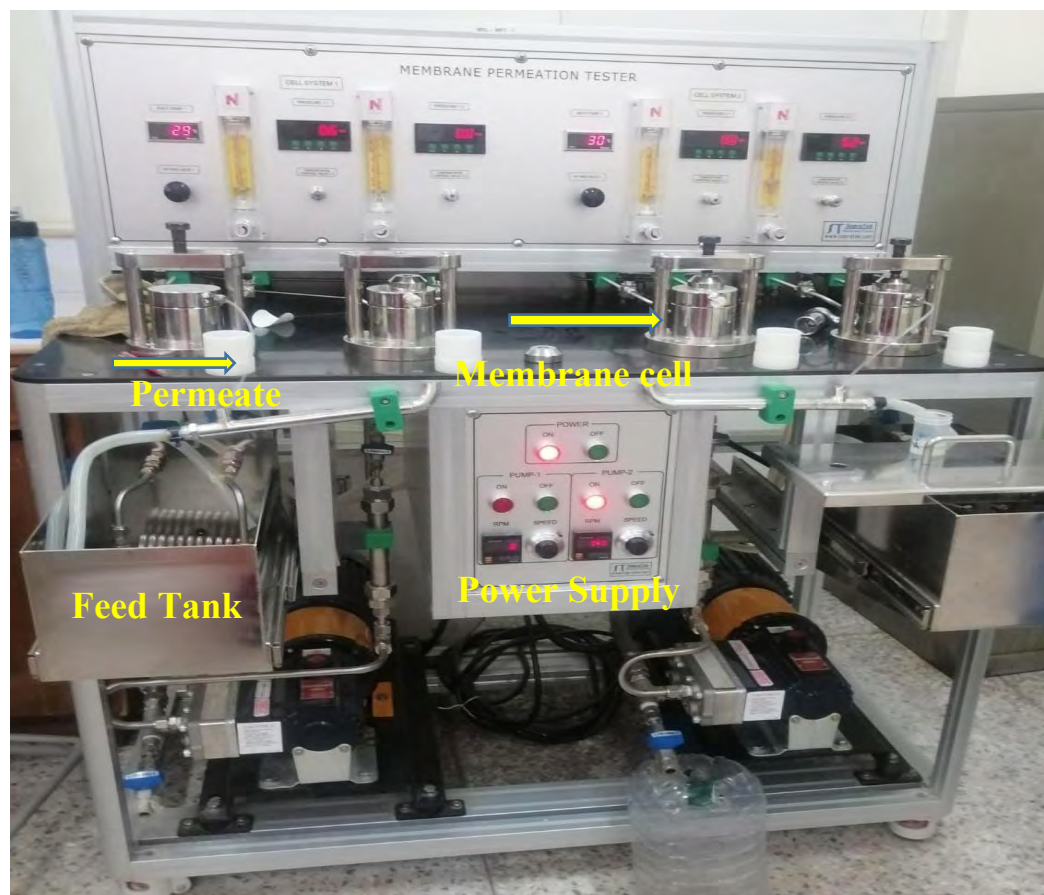
Figure 2.17 : Schematic diagram of RO membrane permeation tester

2.18. Performance test for membrane RO:

The RO performance of prepared TFC and TFN membranes was assessed using a RO experimental setup in order to measure the NaCl rejection and water flux as shown in Figure. 2.19[89]. At first, the 0.0019 m^2 area of TFC-PA membrane that is typically used in a RO setup. The membrane for deionized water performed water permeability testing at room temperature. The concentration of feed remained same in every test experiment. The tests were conducted at a steady operating pressure with a 30-minute interval. The features of the synthesized membrane's water flux and salt rejection were also tested for a 2000 ppm aqueous NaCl mixture at ambient temperature. and the RO performance test was carried out at a cross-flow rate of 2L/min, 20bar feed pressure and 25°C temperature. A standardized digital conductivity metre was used to monitor the electrolyte (NaCl) concentration in both the feed and the permeate. The same procedure was used for thin-film nanocomposite membranes.
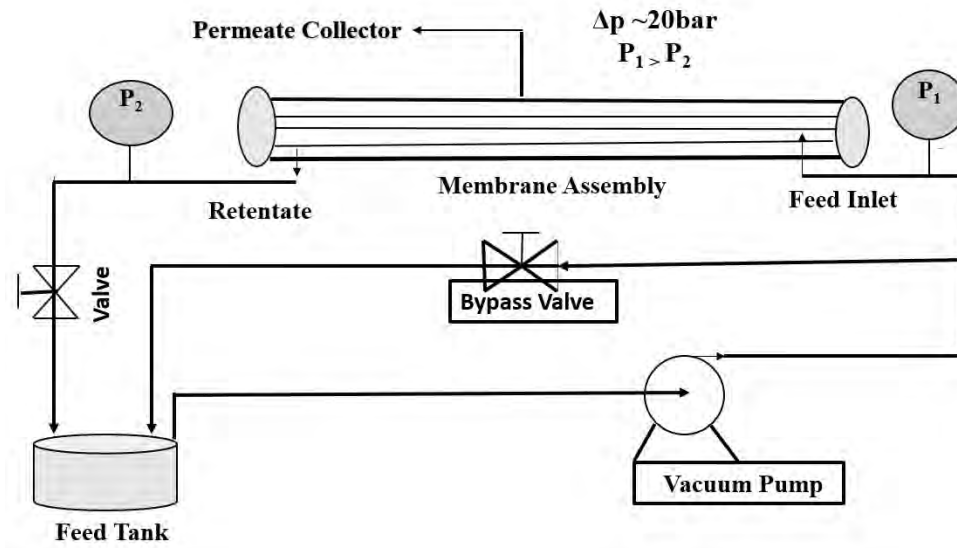
Figure 2.18 : sSchematic representation of RO experimental setup

Salt such as NaCl rejection can be calculated by:

$$R = (1- C_p/C_f) *100\%$$

where C_p is the permeate solution's NaCl concentration

C_f is the feed solution's NaCl concentration.

Pressure-normalized water permeation can be evaluated by:

$$J_w= \Delta v/ \Delta t.A. \Delta P$$

where Δt is the measurement's time (h)

Δp represents pressure at which the device operates (bar)

ΔV is the volume of permeate (L), A is the actual membrane area (m^2).

CHAPTER 3

3.Results and discussion:

 Details on results of characterization techniques will be provided in this chapter. The synthesized ZIF-8 nanoparticles, as well as its composite with 3D graphene and ZIF-8 incorporated polyamide (PA) membranes were characterized using a variety of techniques, including XRD, FTIR, TGA, and SEM, EDX, BET, RAMAN.

3.1. Structural analysis:

The crystalline structure of ZIF-8 and ZIF-67 nanoparticles was examined using XRD. In Figure 3.1a, the distinctive diffraction peaks for the ZIF-8 sample were clearly visible at 2theta = 7.35°, 10.4°, 12.83°, 14.65°, 16.4°, 18.0°, 22.1°, 24.5°, 26.7°, and 29.6°. These peaks can be attributed to the (011), (002), (112), (022), (013), (222), (114), (233), (134), and (044) planes, respectively These peaks show that ZIF-8 has a high degree of crystallinity, and it was successfully synthesized[90]. The crystals show a body-centered cubic crystal structure and the average crystallite size of ZIF-8 is 19.74nm.

Figure3.1: XRD pattern of ZIF-8

Table 3.1 :Structural parameters of ZIF-8 using XRD

Sample Name	Peak position	(hkl)	FWHM	Crystallite size(nm)	D nm(Average)	d(nm)
ZIF-8	7.35	011	0.29347	26.37	19.74	8.019
	10.4	002	0.37552	20.56		5.671
	12.71	112	0.28376	27.16		4.643
	14.69	022	0.71962	10.68		4.020
	16.41	013	0.46921	16.35		3.601
	17.98	222	0.30737	24.92		3.289
	22.49	114	0.52132	14.53		2.423

Figure 3.2. displays the patterns of X-ray diffraction of the three-dimensional graphene in a range of 2Θ from 10° to 50°. The (002) as well as (100) crystalline planes of the graphene sheets were assigned to two distinctive diffraction peaks at $26.5^{\circ}(2\Theta)$ and $43.9^{\circ}(2\Theta)$, respectively, with the former indicating the distance among the layers of graphene and the latter indicating the short-range structure of the stacking graphene nanosheets. The 3D graphene's slightly increased width of the (002) peak refers to a large surface area and better graphitization of the as-prepared three-dimensional graphene frameworks produced by the a single-step carbonization technique, which is comparable with the earlier results.

Figure 3.2: XRD pattern of 3D graphene

Figure 3.3. displays the combined ZIF-8 and Graphene's X-ray diffractogram. The XRD patterns exhibit just one broad peak at 26.5°, which is characteristic of graphitic carbon and correlates with the carbon (002) diffraction. The structural properties of the graphite particles were studied using X-ray diffraction analysis. This analysis shows a distinct peak at position 2 theta = 26.5°; this peak is extremely sharp and intense to support the extremely high crystallinity of graphite powders. These broad peaks are an indication of particular types of amorphous, porous carbon, However the distinctive diffraction peaks for the ZIF-8 sample were clearly visible at 2theta = 7.35°, 10.4°, 12.83°, 14.65°, 16.4°, 18.0°, 22.1°, 24.5°, 26.7°, and 29.6°. These peaks can be attributed to the (011), (002), (112), (022), (013), (222), (114), (233), (134), and (044) planes, respectively. Consequently, this pattern shows graphene peak.

Figure 3.3: XRD pattern of ZIF-8/3DG

XRD analysis was used to describe the crystal structure of the ZIF-8 particles and membranes, as shown in Figure 3.4. The highly crystalline structure or purity of the ZIF-8 particles synthesized in this study are indicated by the ZIF-8 XRD pattern, which is well matched to both simulated and experimental patterns available in literature. The TFC membranes display three diffraction peaks at $2\theta = 17.34°$, $22.54°$, $25.75°$ corresponding to reflections from the (010), (110), and (100) planes, highlighting the semi-crystalline structure of the thin film membrane[91]. The peak strength of the PSf@PA-ZIF-8 membrane are sharper at 5-15º where correlates to the distinctive peaks of ZIF-8 at 7-14º. The XRD spectrum for the PSf@PA-ZIF-8 membranes are identical to the pure PA membrane. The characteristic diffraction peak at 26.5º(2Ө) was ascribed to the (002) crystallographic plane of the graphene sheets. The ZIF-8 nanoparticles were incorporated in PA by interfacial polymerization since the XRD pattern for the PSf@PA-ZIF-8 membrane shows characteristics of both the ZIF-8 nanoparticles as well as pure PA membrane[92].

Figure 3.4:XRD pattern of (a) ZIF-8 ,(b) PSf@PA-ZIF-8(0.00wt%) , PSf@PA-ZIF-8(0.002wt%), (d) PSf@PA-ZIF-8(0.008wt%),(e) PSf@PA-ZIF-8-3DG(0.002wt%)

3.2. Vibrational modes analysis:

Figure 3.5. shows the results of an FTIR analysis to identify the functional groups of the materials produced. The prepared sample ZIF-8 exhibit the main band at ,3141,2929,1635,1585,1446,1381,1178,1146,995,762,687 cm^{-1}. These bands agree with the previously published data. The band at 3455 cm^{-1} may be due to the the oxygen-hydrogen (O-H) stretching vibrations of water following KBr deliquescence and the corresponding N-H stretching vibrations of the remaining Hmim. The aromatic & aliphatic C-H asymmetrical stretching vibrations were linked to the peak at 3135 and 2929 cm^{-1}, respectively. The band at 1585 cm^{-1} corresponded to the C=N stretching vibration, while the band at 1635 cm^{-1} was caused by the C=C stretch mode. While the band at 1146 cm^{-1} was from the aromatic C-N stretching mode, the signals between 1300 and 1460 cm^{-1} were for the whole ring stretching. Similarly, the peak values at 995 and 760 cm^{-1} might be attributed to the vibration of the C-N bending mode and the C-H bending mode, respectively[93]. The band at 694 cm^{-1} was caused by the Hmim's ring out-of-plane bending vibration. Fig 3.7b (b) blue peak representation demonstrates that the C-OH bond which causes the graphene peaks, which are designated at 3430 cm^{-1} and 1572 cm^{-1}.

Table 3.2: FTIR bands observed for ZIF-8

Wave number (cm^{-1})	Bonds
3141	Stretching vibrations of the aromatic C-H
2922	Asymmetric stretching vibrations in the aliphatic C-H ring
1585	C=N stretching vibration
1635	C=C stretching
1146	Aromatic C-N stretch mode
1300-1460	Whole ring stretching
995	C-N bending vibration
762	Bending mode of C-H
687	Hmim's bending vibration
460	Zn-N stretching
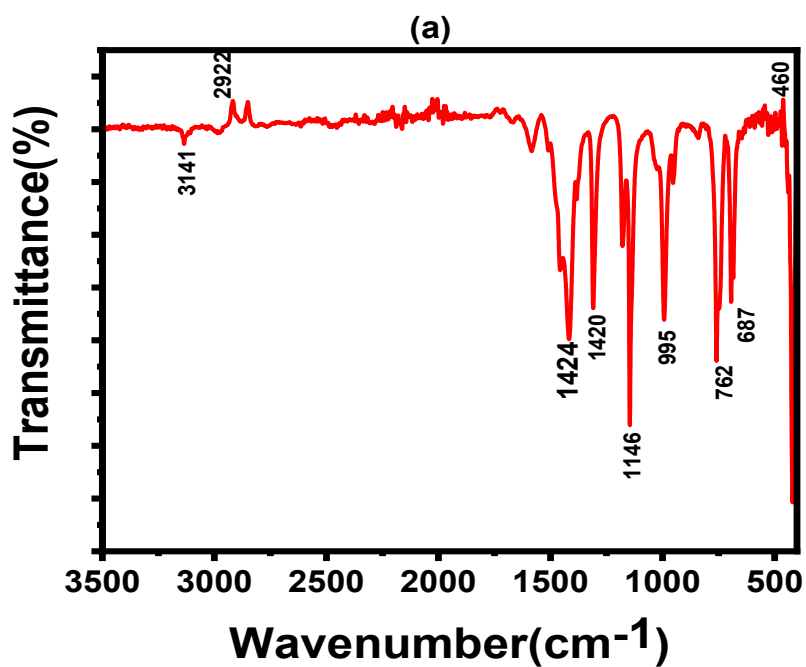
Figure 3.5: FTIR spectra of (a) ZIF-8, (b) ZIF-8/3DG

Figure 3.6 depicts the FTIR spectrum for both neat PA and nanocomposite membranes, and Table 3.9. lists the distinctive functional groups of the membrane. The interconnected PA structures were successfully generated for both the PA and PSf@PA-ZIF-8 membranes, as evidenced by the distinctive PA aromatic rings (C=O bending) around 1639

cm[-1] and the distinctive amide band (N-H bending related to the C=O bending) at 1540 cm^{-1}. Stronger bands were observed in the TFN membrane's spectra at 685,1000 and 1300, 3290 cm^{-1} ,which is consistent with the bands that define ZIF-8. Additionally, more bands within the ZIF-8/polyamide membranes were observed, such as the 1-acyl imidazole derivative-corresponding band at 1360 cm^{-1}. When ZIF-8 was added into the membrane, a band shifting as well as change in intensity in the 600–1600 cm^{-1} range were noticed, indicating a reaction between the activated polyamide layer with the ZIF-8 nanoparticles[95].

Figure 3..6: FTIR spectrum of (a) ZIF-8 ,(b) PSf@PA-ZIF-8(0.00wt%) , (c) PSf@PA-ZIF-8(0.002wt%) , (d) PSf@PA-ZIF-8(0.008wt%),(e)PSf@PA-ZIF-8-3DG(0.002wt%)

Table 3.3; An overview of the membranes' distinctive functional groups

Wavenumber(cm[-1])	Bonds
1660	(C=O bending) Aromatic polyamide
1540	N-H bending paired with C-O bending in the amide II band
1150	C-N stretching

3.3. Surface morphology:

The morphology of the prepared sample was examined using SEM analysis. By adjusting synthesis factors including the solvent choice, the ratio of Zn^{+2} ions to 2-methylimidazole, and the reactivity of the metal salts, ZIF particle sizes can be controlled. The shape of the produced ZIF-8 nanoparticles is shown in (Figure3.7a and b). A common rhombic dodecahedral shape was observed having an apparent uniform size of about 133 nm as shown in Fig.3.8.Smaller nanoparticles have a larger tendency to aggregate or agglomerate because their surface energy is higher, and this tendency persists even after the nanoparticles are subjected to sonication or other processing methods, as seen in SEM[96]. ZIF-8 nanoparticles' small size and evenly distributed size are very advantageous for producing effective mixed matrix membranes without defects. The morphology of synthesized ZIF-8/3DG is shown in (Figure 3.7c and d). The SEM images showed crimps along the outer edges of the walls of the connected three-dimensional porous structure, which were caused by the few thin layers of crumpled graphene nanosheets and also demonstrating that ZIF-8 is distributed almost uniformly across graphene nanosheets.
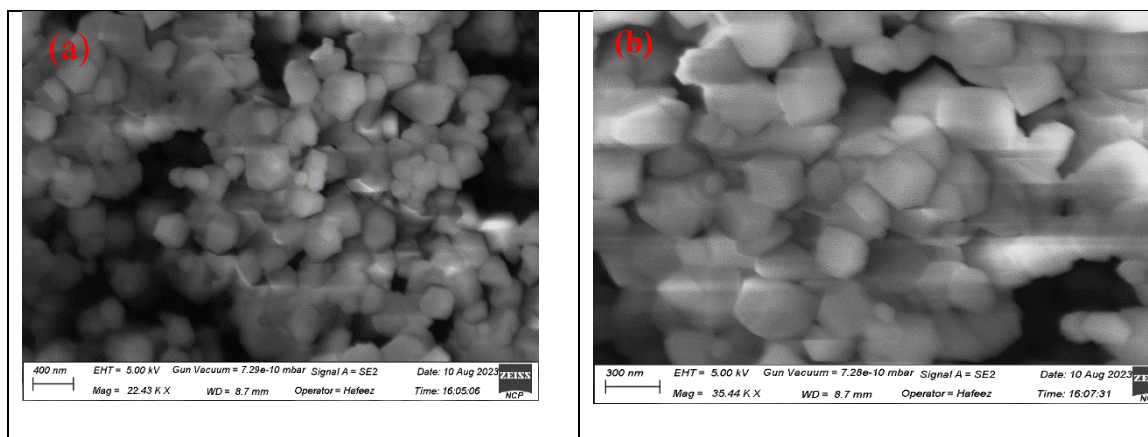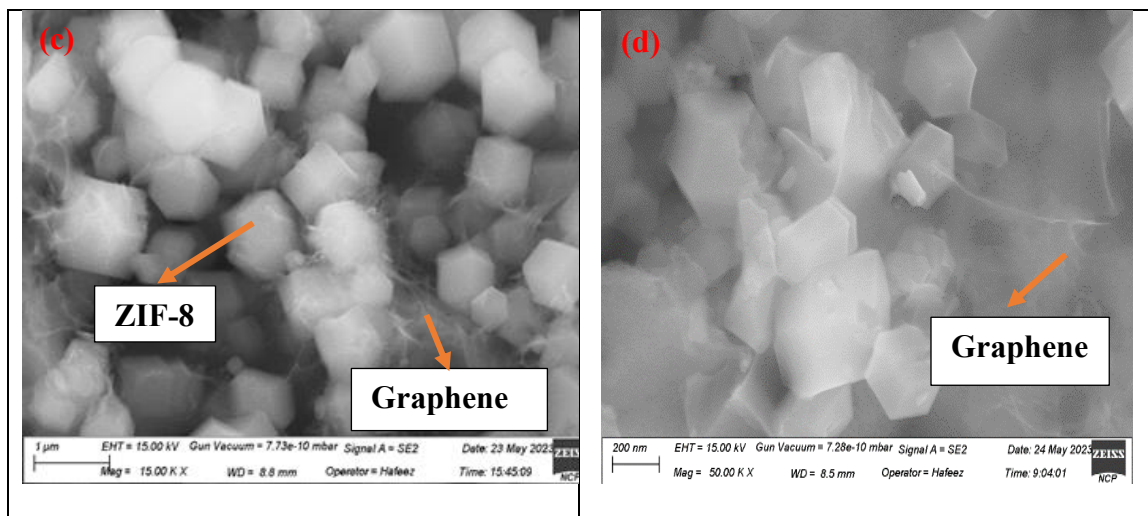
Figure 3.7: -(a, b) SEM images of ZIF-8 and (c, d) shows SEM image of ZIF-8 with graphene at (a) 400nm, (22.43KX) (b) 300nm, (35.44KX) (c) 1µm (15.00KX), (d) 200nm(50.00KX)

Figure 3.8: Distribution of SEM particle sizes of ZIF-8

3.4. Chemical composition of elements:

According to Figure 3.9(a, b), the synthesized sample ZIF-8 and its composite with 3D graphene is composed of up of zinc, nitrogen, and carbon, oxygen components. According to Table 3.4.the chemical composition of the components was determined by EDX analysis.

Table 3.4; displays the concentration (wt.%, at %) of various elements in ZIF-8 and its composite with 3D graphene

Material	Element	Weight (%)	б
ZIF-8	C	52.5	0.9
	N	25.5	1.1
	Zn	18.7	0.4
	O	3.3	0.3
	Total	100	
ZIF-8/3DG	C	58.2	1.6
	N	19.7	1.9
	Zn	17.4	0.7
	O	4.6	0.6
	Total	100	

(a) **(b)**
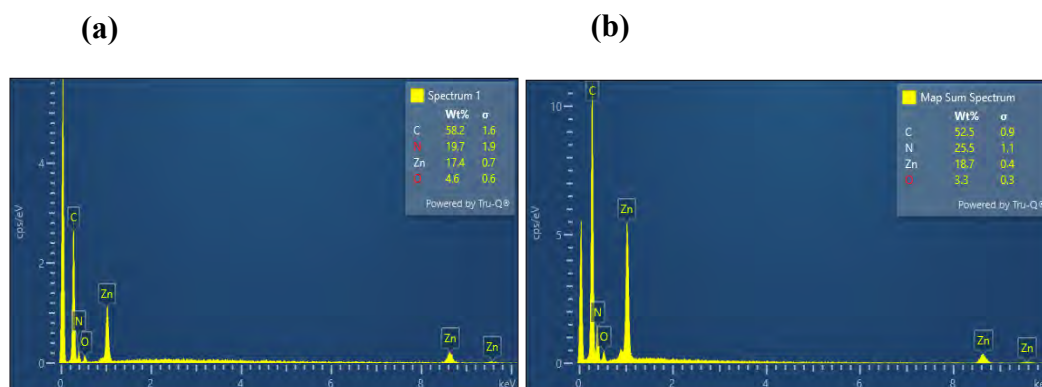
Figure 3..9. (a ,b) creatively demonstrated the analysis of EDS for ZIF-8 and its composite

Scanning electron microscopy (SEM) was used to examine the surface morphology and roughness of the membrane. Figure 3.10. sections a–f, displays the SEM images of the top surfaces of the thin-film composite (TFC/PA) and thin-film nanocomposite (TFN/PA/ZIF-8) membranes. Figure 3.10 (a,c,f) depicts the characteristic ridge and valley type of shape for the polyamide (PA) RO membranes. This kind of morphology is compatible with the literature. On the other hand, the incorporation of ZIF-8 nanocrystals into the polyamide layer did not result in any interfacial defects at the surface for any of the samples. In contrast to the TFC membranes with its nodular surface, the TFN membranes (Figure 3.10 4b and d) exhibits a denser structure throughout the plane. This is due to the fact that the

interfacial polymerization reaction rate affects how quickly the polyamide layer forms over the support layer. The polyamide structure's top layer, which still had ridge and valley structures, did not exhibit any distinctive characteristics. The ZIF-8 particles are hidden beneath the thin polyamide layer, as shown by the polyamide's retained properties. Additionally, it suggests that the ZIF-8 nanoparticles and polymeric matrix indicates good compatibility.
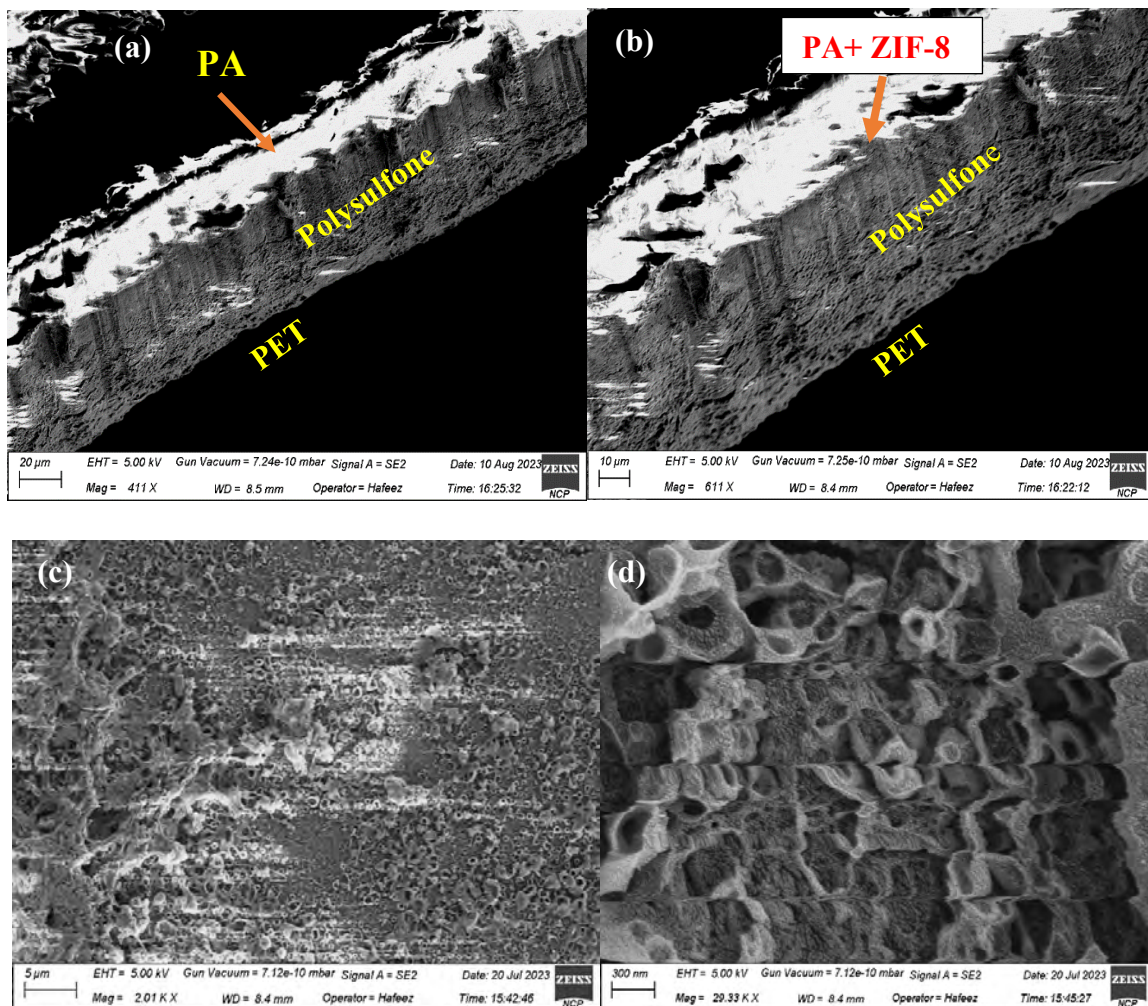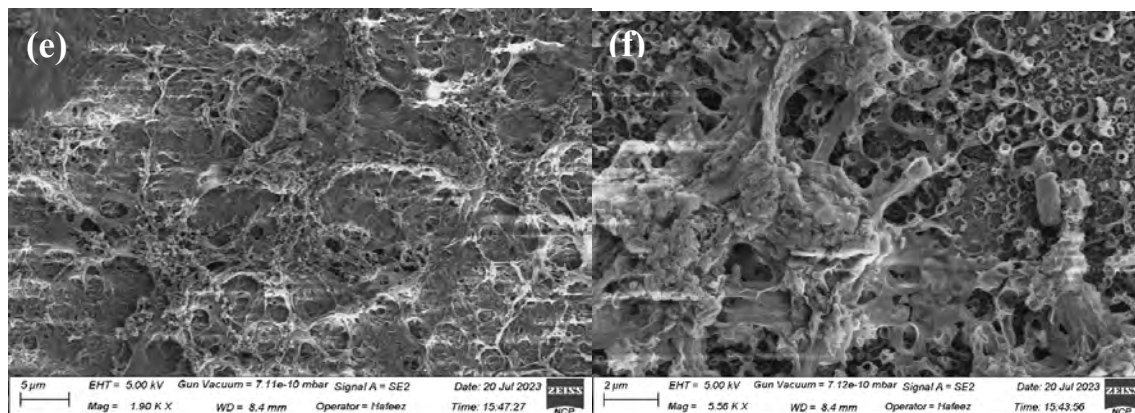
Figure 3.10: SEM micrographs of Polyamide TFC (a, c, f) and TFN (b, d, e) membranes

3.5. Thermal stability:

Finally, TGA of the ZIFs and membranes ware carried out in a N_2 environment as shown in Figure 3.11(a,d) to verify the thermal stability of the materials synthesized in this work. The sample was heated to a maximum of 1200 ºC, starting from ambient temperature. ZIF-8 is stable to a maximum of 490ºC, which is consistent with previous research .The observed weight loss at 490ºC is due to the breakdown of the ZIF-8 framework[97].

Figure 3.11: TGA evaluation (a) ZIF-8, (b)M1, (c) M2 ,(d) M3.

When compared to neat polyamide, which has a temperature of 362°C, the TGA weight loss curve of PSf@PA-ZIF-8 (0.002wt% ,0.008wt%) are shifted towards higher temperatures with a longer plateau, and PSf@PA-ZIF-8(0.08wt%) demonstrated superior thermal stability having a temperature of approximately 450°C[95]. Additionally, the thermogram displays two weight loss stages of breakdown for the neat polyamides, PSf@PA-ZIF-8. The first step results from the elimination of residual solvents , reactant molecules or the dissociation of the functional groups, while the second stage results from the sublimation of the carbon backbone, which denotes the complete disintegration phase of membrane[98].

3.6. Surface area analysis:

The N_2 adsorption-desorption isotherms were used to determine the particular surface area and pore size, and pore volume. The characterized samples showed that all nanocomposites have nano   porous structures. The surface characteristics of the prepared fillers are shown in Table3.5. Pure ZIF-8 possesses a surface area that is comparable to that of reported work.. The parameters of the pore structure, such as its surface area (m^2/g), pore volume (mm^3/g) are shown in Table 3.7.
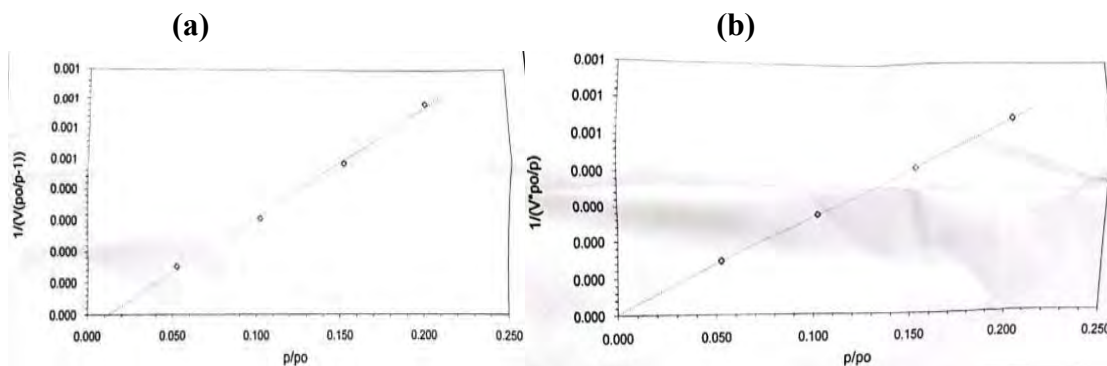
Figure 3.12:(a) BET plot, (b) Langmuir plot

Table 3.5: Characteristics of the pore structure

Material	Surface area(m^2/g)	Micropore volume(mm^3/g)	Micropore area(m^2/g)	Non-microporous Surface area(m^2/g)	Langmuir surface area(m^2/g)
ZIF-8	1242.548	534.004	1515.566	107.234	1622.800

3.7. Raman analysis:

Figure3.13 displays the Raman spectrum of ZIF-8, characterized by strong bands associated with vibrations of the methyl group as well as imidazole ring. The band at 175 cm^{-1} was attributed to Zn-N stretching. As predicted, the Raman spectrum of ZIF-8 contained bands at 647, 680, 837, 948, 1020, 1177, 1379, 1499 cm^{-1}, which were attributed to the methyl group and vibrational modes of the imidazole ring and those at 1450, 1143, and 680 cm^{-1}, which were attributed to methyl bending, C-N stretching, and imidazolium ring puckering, respectively. As shown in Figure 3.14, the 3D Graphene's Raman spectrum has two peaks, the D band (1338 cm^{-1}) as well as the G band (1574 cm^{-1}). The first order scattering of the E_{2g} mode is confirmed by the presence of the graphitic G band, while the disorder D band is explained by the appearance of defects or disorders inside the graphene nanosheets. While the calculated I_D/I_G ratio for D-band to G-band is 0.98, it is comparable to the Raman spectrum of the thermally and chemically reduced three-dimensional graphene oxide.

Table 3.6: Raman bands observed for ZIF-8

Frequency(cm^{-1})	Band assignment
175	stretching of Zn-N
680	Imidazole ring puckering
1143	C-N stretching
1450	methyl bending

Figure 313: Raman spectrum of ZIF-8

Table 3.7: Raman bands observed for 3D Graphene

Raman shift (cm^{-1})	Peak designation	Intensity	Vibrational modes
1338	D band	3710	K photon breathing modes
1574	G band	3760	E$_2$g photons' first order scattering

Figure 3.14: Raman spectrum of 3D Graphene

.

3.8. Performance evaluation of membranes:

Finally, a cross-flow filtering system was used to assess the RO performance of TFC as well as TFN membranes[99]. The ZIF-loaded membranes significantly improved in terms of permeate flux, whereas the pure polyamide membrane having zero loading demonstrated the lowest performance across all studies. NaCl rejection was equivalent for every membrane. Figure 3.15a–c shows that irrespective of the size of the ZIF-8 nanoparticles, the water permeance of TFN membranes gradually increased with ZIF-8 concentration. The pure TFC polyamide membrane (M1) showed a permeate flux of 25.46 $Lm^{-2}.h^{-1.}$ Unexpectedly, the permeate flux was enhanced to 80% with pure water feed by a small loading as low as 0.002 wt% ZIF-8. In our case, a steady rise in flux occurred with increasing loading up to a maximum loading of 0.008 wt%, at which point the permeate flux increased by 95%. Notably, M3 membrane demonstrated a 95% increase in water permeance compared to M1 and M2 and M4 membranes at the various ZIF-8 concentrations (0wt%, 0.002wt% ,0.008wt%), and ZIF-8@3DG(0.002wt%) highlighting the significance of ZIF-8 particles size (Figure3.15d-e).

(a)

(b)

(c)

(d)

(e)   **(f)**

Figure 3.15 (a-d) shows the RO performance of TFN membranes at various ZIF-8 and its composite with 3DG concentrations. (d-e) Comparison of RO results at varied ZIF-8 concentrations and ZIF-8@3DG

The following factors have been shown to influence the reverse osmosis (RO) performance of TFN membranes[100]: (1) physical changes (thickness as well as roughness) in the polyamide layer; (2) chemical modifications (free volume and crosslinking degree) in the polyamide layer; and (3) the addition of a further water transport channels through the intrinsic pores of nanomaterials[101]. The physical morphologies of the TFN membranes, including their thickness or degree of roughness, did not show any discernible modifications. Therefore, it can be claimed that the addition of ZIF-8 has a greater impact on the chemical alterations and the role of extra water transport channels, which improves water permeance[102]. The fact that M3 membrane   revealed the   highest water flux may be due to the highest interface area between polyamide matrix and ZIF-8 nanoparticles. The rise in water flux can be caused by the membrane surface's increased hydrophilicity and the hydrophobic properties of ZIF-8 incorporated into the polyamide layer. The hydrophobic ZIF-8 will speed up transportation through the membrane while the hydrophilic surface will attract more water molecules, thus increasing the permeate flux[103]. Table 3.8. displays the permeate flux and salt rejection for feed conditions with pure water (J_w) as well as brackish water (J_s).

Table 3.8: Rejection and permeation flux of membranes under brackish water circumstances

Membrane	J_w (L/m^2.h)	J_S (L/m^2.h)	R (%)	Permeance(L/m^2.h.bar)
M1	29.84	25.46	95.28	1.49
M2	47.79	45.95	97.26	2.39
M3	56.89	49.80	95.56	2.84
M4	44.40	42.61	97.36	2.22

In contrast to employing water that is pure as a feed, the flux of permeate is significantly lower when brackish water is utilized as a feed. Salt molecules have a tendency to gather on the feed side of the membrane surface, which can be explained through the concentration polarization phenomenon. By raising the osmotic pressure, this salt concentration will reduce the total driving force towards mass transfer.

4.Conclusion:

The solvothermal approach was successfully employed to synthesize pure ZIF-8 and its combined nanostructures containing 3D graphene. By using XRD, SEM, IR, TGA, and BET, the synthesized materials were identified and examined. The purity and crystalline structure of the material are confirmed by XRD. Functional groups are identified by IR. TGA and BET both provide information on the material's surface area and thermal stability. All of these characteristics ensure the synthesis of our substance. The rhombic dodecahedral architecture of ZIF-8 nanoparticles in SEM images showed an apparent uniform size of roughly 133nm .Using the interfacial polymerization (IP) method, ZIF-8 nanoparticles incorporated polyamide membranes are utilized as the top layer, which is subsequently coated on polysulfone (as the middle layer) and then overlaid on PET support (the bottom layer). To successfully construct TFN-RO membranes enabling water desalination, three distinct weight percentages of ZIF-8 nanomaterials (0.00wt%, 0.002wt%, and 0.008wt%) were added to organic solutions. The TFN membranes are synthesized and characterised using a variety of experimental techniques throughout the research process. Three diffraction peaks are visible in the TFC membranes, revealing the semi-crystalline nature of the thin film membrane at 2Θ = 17.34º, 22.54º, and 25.75º.In comparison to other TFN membranes, PSf@PA-ZIF-8(0.08wt%) showed higher thermal stability at a temperature of about 450°C and membrane images showed the typical ridge and valley structure of aromatic polyamide (PA). The distinctive PA aromatic rings (C=O bending) about 1639 cm^{-1} and the distinctive amide band (N-H bending related to the C=O bending) at 1540cm^{-1} demonstrate the successful generation of the interconnected PA structures for both the PA and PSf@PA-ZIF-8 membranes. Stronger bands were seen in the spectra of the TFN membrane at 460,1000 and 1300cm^{-1}, which is compatible with the bands that characterize ZIF-8. On the membrane surface, no structural changes appeared, but an interaction among the two phases may have occurred based on band shifting and intensity variations in the FTIR spectra. As a result, when compared to the pristine TFC and others wt.% of PSf@PA-ZIF-8 TFN membranes, PSf@PA-ZIF-8(0.008wt%) TFN membranes had the greatest water permeance of 2.84 L/m^2.h.bar and the highest NaCl rejection of 95.56%. The improved distinctive aperture as well as extremely porous structure of ZIF-8 were responsible for the better performance of TFN membranes. To our

knowledge, this is the unique study to demonstrate the significance of particle deposition based on varying weight percentages prior to the interfacial polymerization, eventually influencing the RO performances. Future TFN membrane research should take this unexpected factor into consideration. In addition to illuminating the complex interactions among materials at the nanoscale, the outcomes of this study also provide a feasible strategy for enhancing water desalination systems. The ZIF-8-polyamide composite's enhanced permeability, salt rejection, as well as stability have opened up new design and development options for subsequent-generation desalination membranes.

5. References

[1]   G. Férey, "Hybrid porous solids: Past, present, future," *Chem. Soc. Rev.*, vol. 37, no. 1, pp. 191–214, 2008, doi: 10.1039/b618320b.

[2]   P. L. Sallinger, "The Role of Water Resources in the Arab-Israeli Conflict," *Syria*, vol. 5, no. Xii, pp. 1–18, 2010.

[3]   A. Vinu, T. Mori, and K. Ariga, "New families of mesoporous materials," *Sci. Technol. Adv. Mater.*, vol. 7, no. 8, pp. 753–771, 2006, doi: 10.1016/j.stam.2006.10.007.

[4]   H. Furukawa, K. E. Cordova, M. O'Keeffe, and O. M. Yaghi, "The chemistry and applications of metal-organic frameworks," *Science (80-.).*, vol. 341, no. 6149, 2013, doi: 10.1126/science.1230444.

[5]   S. H. Jhung, N. A. Khan, and Z. Hasan, "Analogous porous metal-organic frameworks: Synthesis, stability and application in adsorption," *CrystEngComm*, vol. 14, no. 21, pp. 7099–7109, 2012, doi: 10.1039/c2ce25760b.

[6]   D. D. Zu, L. Lu, X. Q. Liu, D. Y. Zhang, and L. B. Sun, "Improving hydrothermal stability and catalytic activity of metal-organic frameworks by graphite oxide incorporation," *J. Phys. Chem. C*, vol. 118, no. 34, pp. 19910–19917, 2014, doi: 10.1021/jp506335x.

[7]   I. Ahmed, Z. Hasan, N. A. Khan, and S. H. Jhung, "Adsorptive denitrogenation of model fuels with porous metal-organic frameworks (MOFs): Effect of acidity and basicity of MOFs," *Appl. Catal. B Environ.*, vol. 129, pp. 123–129, 2013, doi: 10.1016/j.apcatb.2012.09.020.

[8]   K. Y. A. Lin, S. Y. Chen, and A. P. Jochems, "Zirconium-based metal organic frameworks: Highly selective adsorbents for removal of phosphate from water and urine," *Mater. Chem. Phys.*, vol. 160, pp. 168–176, 2015, doi: 10.1016/j.matchemphys.2015.04.021.

[9]   J. T. Fitzsimons, "Angiotensin, thirst, and sodium appetite," *Physiol. Rev.*, vol. 78, no. 3, pp. 583–686, 1998, doi: 10.1152/physrev.1998.78.3.583.

[10] G. A. Tularam and M. Ilahee, "Environmental concerns of desalinating seawater using reverse osmosis," *J. Environ. Monit.*, vol. 9, no. 8, pp. 805–813, 2007, doi: 10.1039/b708455m.

[11] C. Fritzmann, J. Löwenberg, T. Wintgens, and T. Melin, "State-of-the-art of reverse osmosis desalination," *Desalination*, vol. 216, no. 1–3, pp. 1–76, 2007, doi: 10.1016/j.desal.2006.12.009.

[12] T. V. Luong, S. Schmidt, S. A. Deowan, J. Hoinkis, A. Figoli, and F. Galiano, "Membrane Bioreactor and Promising Application for Textile Industry in Vietnam," *Procedia CIRP*, vol. 40, pp. 419–424, 2016, doi: 10.1016/j.procir.2016.01.083.

[13] M. Z. Rong, M. Q. Zhang, and W. H. Ruan, "Surface modification of nanoscale fillers for improving properties of polymer nanocomposites: A review," *Mater. Sci. Technol.*, vol. 22, no. 7, pp. 787–796, 2006, doi: 10.1179/174328406X101247.

[14] B. A. Buzzanga, "Precipitation and Sea Level Rise Impacts on Groundwater Levels in Virginia Beach, Virginia Recommended Citation," no. October, 2017, doi: 10.25777/qsft-gq17.

[15] F. Sanchez and K. Sobolev, "Nanotechnology in concrete - A review," *Constr. Build. Mater.*, vol. 24, no. 11, pp. 2060–2071, 2010, doi: 10.1016/j.conbuildmat.2010.03.014.

[16] W. J. Lau, S. Gray, T. Matsuura, D. Emadzadeh, J. Paul Chen, and A. F. Ismail, "A review on polyamide thin film nanocomposite (TFN) membranes: History, applications, challenges and approaches," *Water Res.*, vol. 80, pp. 306–324, 2015, doi: 10.1016/j.watres.2015.04.037.

[17] D. L. Zhao *et al.*, "Engineering metal–organic frameworks (MOFs) based thin-film nanocomposite (TFN) membranes for molecular separation," *Chem. Eng. J.*, vol. 454, 2023, doi: 10.1016/j.cej.2022.140447.

[18] A. R. Smith and J. Klosek, "A review of air separation technologies and their integration with energy conversion processes," *Fuel Process. Technol.*, vol. 70, no.

2, pp. 115–134, 2001, doi: 10.1016/S0378-3820(01)00131-X.

[19]   E. P. Favvas, F. K. Katsaros, S. K. Papageorgiou, A. A. Sapalidis, and A. C. Mitropoulos, "A review of the latest development of polyimide based membranes for CO2 separations," *React. Funct. Polym.*, vol. 120, pp. 104–130, 2017, doi: 10.1016/j.reactfunctpolym.2017.09.002.

[20]   M. Zajda and U. Aleksander-Kwaterczak, "Wastewater treatment methods for effluents from the confectionery industry-An overview," *J. Ecol. Eng.*, vol. 20, no. 9, pp. 293–304, 2019, doi: 10.12911/22998993/112557.

[21]   M. Younas and M. Rezakazemi, "Introduction to Membrane Technology," *Membr. Contactor Technol.*, pp. 1–16, 2022, doi: 10.1002/9783527831036.ch1.

[22]   CHOQUETTE PW and PRAY LC, "Geologic Nomenclature and Classification of Porosity in Sedimentary Carbonates," *Am. Assoc. Pet. Geol. Bull.*, vol. 54, no. 2, pp. 207–250, 1970, doi: 10.1306/5d25c98b-16c1-11d7-8645000102c1865d.

[23]   M. Thommes *et al.*, "Physisorption of gases, with special reference to the evaluation of surface area and pore size distribution (IUPAC Technical Report)," *Pure Appl. Chem.*, vol. 87, no. 9–10, pp. 1051–1069, 2015, doi: 10.1515/pac-2014-1117.

[24]   S. P. Nunes *et al.*, "Thinking the future of membranes: Perspectives for advanced and new membrane materials and manufacturing processes," *J. Memb. Sci.*, vol. 598, 2020, doi: 10.1016/j.memsci.2019.117761.

[25]   X. Kong and M. M. Ohadi, "Applications of micro and nano technologies in the oil and gas industry-an overview of the recent progress," *Soc. Pet. Eng. - 14th Abu Dhabi Int. Pet. Exhib. Conf. 2010, ADIPEC 2010*, vol. 3, pp. 1703–1713, 2010, doi: 10.2118/138241-ms.

[26]   J. Dechnik, C. J. Sumby, and C. Janiak, "Enhancing Mixed-Matrix Membrane Performance with Metal-Organic Framework Additives," *Cryst. Growth Des.*, vol. 17, no. 8, pp. 4467–4488, 2017, doi: 10.1021/acs.cgd.7b00595.

[27]   M. S. Dresselhaus, G. Dresselhaus, and R. Saito, "Physics of carbon nanotubes,"

Carbon N. Y., vol. 33, no. 7, pp. 883–891, 1995, doi: 10.1016/0008-6223(95)00017-8.

[28] G. Liang, N. Neophytou, M. S. Lundstrom, and D. E. Nikonov, "Ballistic graphene nanoribbon metal-oxide-semiconductor field-effect transistors: A full real-space quantum transport simulation," *J. Appl. Phys.*, vol. 102, no. 5, 2007, doi: 10.1063/1.2775917.

[29] Y. Wu, J. Zhu, and L. Huang, "A review of three-dimensional graphene-based materials: Synthesis and applications to energy conversion/storage and environment," *Carbon N. Y.*, vol. 143, pp. 610–640, 2019, doi: 10.1016/j.carbon.2018.11.053.

[30] L. Zhang *et al.*, "Porous 3D graphene-based bulk materials with exceptional high surface area and excellent conductivity for supercapacitors," *Sci. Rep.*, vol. 3, no. March, 2013, doi: 10.1038/srep01408.

[31] E. M. Flanigen, "Plenary Paper—Technology: Molecular sieve zeolite technology - the first twenty-five years," *Pure Appl. Chem.*, vol. 52, no. 9, pp. 2191–2211, 1980, doi: 10.1351/pac198052092191.

[32] G. Dong, H. Li, and V. Chen, "Challenges and opportunities for mixed-matrix membranes for gas separation," *J. Mater. Chem. A*, vol. 1, no. 15, pp. 4610–4630, 2013, doi: 10.1039/c3ta00927k.

[33] P. S. Goh, A. F. Ismail, S. M. Sanip, B. C. Ng, and M. Aziz, "Recent advances of inorganic fillers in mixed matrix membrane for gas separation," *Sep. Purif. Technol.*, vol. 81, no. 3, pp. 243–264, 2011, doi: 10.1016/j.seppur.2011.07.042.

[34] F. Qi *et al.*, "Tunable Interaction between Metal-Organic Frameworks and Electroactive Components in Lithium–Sulfur Batteries: Status and Perspectives," *Adv. Energy Mater.*, vol. 11, no. 20, 2021, doi: 10.1002/aenm.202100387.

[35] R. B. Lin, Z. Zhang, and B. Chen, "Achieving High Performance Metal-Organic Framework Materials through Pore Engineering," *Acc. Chem. Res.*, vol. 54, no. 17, pp. 3362–3376, 2021, doi: 10.1021/acs.accounts.1c00328.

[36] R. Li, N. N. Adarsh, H. Lu, and M. Wriedt, "Metal-organic frameworks as platforms for the removal of per- and polyfluoroalkyl substances from contaminated waters," *Matter*, vol. 5, no. 10, pp. 3161–3193, 2022, doi: 10.1016/j.matt.2022.07.028.

[37] Y. Zhou *et al.*, "Bimetallic metal–organic frameworks and MOF-derived composites: Recent progress on electro- and photoelectrocatalytic applications," *Coord. Chem. Rev.*, vol. 451, 2022, doi: 10.1016/j.ccr.2021.214264.

[38] J. Zhang, Z. Li, X. L. Qi, and D. Y. Wang, "Recent Progress on Metal–Organic Framework and Its Derivatives as Novel Fire Retardants to Polymeric Materials," *Nano-Micro Lett.*, vol. 12, no. 1, 2020, doi: 10.1007/s40820-020-00497-z.

[39] M. M. Zagho, M. K. Hassan, M. Khraisheh, M. A. A. Al-Maadeed, and S. Nazarenko, "A review on recent advances in CO2 separation using zeolite and zeolite-like materials as adsorbents and fillers in mixed matrix membranes (MMMs)," *Chem. Eng. J. Adv.*, vol. 6, 2021, doi: 10.1016/j.ceja.2021.100091.

[40] S. A. Mazari *et al.*, "Nanomaterials: Applications, waste-handling, environmental toxicities, and future challenges - A review," *J. Environ. Chem. Eng.*, vol. 9, no. 2, 2021, doi: 10.1016/j.jece.2021.105028.

[41] H. Wang *et al.*, "Advances and perspectives of ZIFs-based materials for electrochemical energy storage: Design of synthesis and crystal structure, evolution of mechanisms and electrochemical performance," *Energy Storage Mater.*, vol. 43, pp. 531–578, 2021, doi: 10.1016/j.ensm.2021.09.023.

[42] E. Jang *et al.*, "Formation of ZIF-8 membranes inside porous supports for improving both their H2/CO2 separation performance and thermal/mechanical stability," *J. Memb. Sci.*, vol. 540, pp. 430–439, 2017, doi: 10.1016/j.memsci.2017.06.072.

[43] Y. Y. Zhao, Y. L. Liu, X. M. Wang, X. Huang, and Y. F. Xie, "Impacts of Metal-Organic Frameworks on Structure and Performance of Polyamide Thin-Film Nanocomposite Membranes," *ACS Appl. Mater. Interfaces*, vol. 11, no. 14, pp.

13724–13734, 2019, doi: 10.1021/acsami.9b01923.

[44] S. Zhang, K. Wang, F. Li, and S. H. Ho, "Structure-mechanism relationship for enhancing photocatalytic H2 production," *Int. J. Hydrogen Energy*, vol. 47, no. 88, pp. 37517–37530, 2022, doi: 10.1016/j.ijhydene.2021.10.139.

[45] R. Krishna and S. T. Sie, "Strategies for multiphase reactor selection," *Chem. Eng. Sci.*, vol. 49, no. 24 PART A, pp. 4029–4065, 1994, doi: 10.1016/S0009-2509(05)80005-3.

[46] F. A. Vicente, I. Plazl, S. P. M. Ventura, and P. Žnidaršič-Plazl, "Separation and purification of biomacromolecules based on microfluidics," *Green Chem.*, vol. 22, no. 14, pp. 4391–4410, 2020, doi: 10.1039/c9gc04362d.

[47] R. Mahdavi Far, B. Van der Bruggen, A. Verliefde, and E. Cornelissen, "A review of zeolite materials used in membranes for water purification: history, applications, challenges and future trends," *J. Chem. Technol. Biotechnol.*, vol. 97, no. 3, pp. 575–596, 2022, doi: 10.1002/jctb.6963.

[48] C. H. Lau, P. Li, F. Li, T. S. Chung, and D. R. Paul, "Reverse-selective polymeric membranes for gas separations," *Prog. Polym. Sci.*, vol. 38, no. 5, pp. 740–766, 2013, doi: 10.1016/j.progpolymsci.2012.09.006.

[49] S. Sridhar, B. Smitha, and T. M. Aminabhavi, "Separation of carbon dioxide from natural gas mixtures through polymeric membranes - A review," *Sep. Purif. Rev.*, vol. 36, no. 2, pp. 113–174, 2007, doi: 10.1080/15422110601165967.

[50] A. Ozcan, C. Perego, M. Salvalaglio, M. Parrinello, and O. Yazaydin, "Concentration gradient driven molecular dynamics: A new method for simulations of membrane permeation and separation," *Chem. Sci.*, vol. 8, no. 5, pp. 3858–3865, 2017, doi: 10.1039/c6sc04978h.

[51] A. Azaïs, J. Mendret, E. Petit, and S. Brosillon, "Evidence of solute-solute interactions and cake enhanced concentration polarization during removal of pharmaceuticals from urban wastewater by nanofiltration," *Water Res.*, vol. 104, pp. 156–167, 2016, doi: 10.1016/j.watres.2016.08.014.

[52] H. B. Park, J. Kamcev, L. M. Robeson, M. Elimelech, and B. D. Freeman, "Maximizing the right stuff: The trade-off between membrane permeability and selectivity," *Science (80-.).*, vol. 356, no. 6343, pp. 1138–1148, 2017, doi: 10.1126/science.aab0530.

[53] N. N. Bui, M. L. Lind, E. M. V. Hoek, and J. R. McCutcheon, "Electrospun nanofiber supported thin film composite membranes for engineered osmosis," *J. Memb. Sci.*, vol. 385–386, no. 1, pp. 10–19, 2011, doi: 10.1016/j.memsci.2011.08.002.

[54] I. Wenten, "Ultrafiltration in Water Treatment and Its Evaluation as Pretreatment for Reverse Osmosis System," *Dept. Chem. Eng. - Inst. Teknol. Bandung*, no. June 2008, 1996, [Online]. Available: http://www.ultra-flo.com.sg/images/wenton.pdf

[55] C. Y. Feng, K. C. Khulbe, T. Matsuura, and A. F. Ismail, "Recent progresses in polymeric hollow fiber membrane preparation, characterization and applications," *Sep. Purif. Technol.*, vol. 111, pp. 43–71, 2013, doi: 10.1016/j.seppur.2013.03.017.

[56] A. G. Fane, R. Wang, and M. X. Hu, "Synthetic membranes for water purification: Status and future," *Angew. Chemie - Int. Ed.*, vol. 54, no. 11, pp. 3368–3386, 2015, doi: 10.1002/anie.201409783.

[57] H. A. Shawky, "Performance of aromatic polyamide RO membranes synthesized by interfacial polycondensation process in a water-tetrahydrofuran system," *J. Memb. Sci.*, vol. 339, no. 1–2, pp. 209–214, 2009, doi: 10.1016/j.memsci.2009.04.052.

[58] H. D. Lee, H. W. Kim, Y. H. Cho, and H. B. Park, "Experimental evidence of rapid water transport through carbon nanotubes embedded in polymeric desalination membranes," *Small*, vol. 10, no. 13, pp. 2653–2660, 2014, doi: 10.1002/smll.201303945.

[59] L. Lin, H. Yang, and X. Xu, "Effects of Water Pollution on Human Health and Disease Heterogeneity: A Review," *Front. Environ. Sci.*, vol. 10, 2022, doi: 10.3389/fenvs.2022.880246.

[60]   B. Feng, K. Xu, and A. Huang, "Synthesis of graphene oxide/polyimide mixed matrix membranes for desalination," *RSC Adv.*, vol. 7, no. 4, pp. 2211–2217, 2017, doi: 10.1039/c6ra24974d.

[61]   I. Salahshoori, A. Seyfaee, and A. Babapoor, "Recent advances in synthesis and applications of mixed matrix membranes," *Synth. Sinter.*, vol. 1, no. 1, pp. 1–27, 2021, doi: 10.53063/synsint.2021.116.

[62]   D. N. Chakkaravarthy, "Water Scarcity- Challenging the Future," *Int. J. Agric. Environ. Biotechnol.*, vol. 12, no. 3, 2019, doi: 10.30954/0974-1712.08.2019.2.

[63]   G. Wu, H. Kang, X. Zhang, H. Shao, L. Chu, and C. Ruan, "A critical review on the bio-removal of hazardous heavy metals from contaminated soils: Issues, progress, eco-environmental concerns and opportunities," *J. Hazard. Mater.*, vol. 174, no. 1–3, pp. 1–8, 2010, doi: 10.1016/j.jhazmat.2009.09.113.

[64]   N. Abdullah, M. A. Rahman, M. H. D. Othman, J. Jaafar, and A. F. Ismail, "Membranes and Membrane Processes: Fundamentals," *Curr. Trends Futur. Dev. Membr. Photocatalytic Membr. Photocatalytic Membr. React.*, pp. 45–70, 2018, doi: 10.1016/B978-0-12-813549-5.00002-5.

[65]   B. Van Der Bruggen, C. Vandecasteele, T. Van Gestel, W. Doyen, and R. Leysen, "A review of pressure-driven membrane processes in wastewater treatment and drinking water production," *Environ. Prog.*, vol. 22, no. 1, pp. 46–56, 2003, doi: 10.1002/ep.670220116.

[66]   A. Joyce, D. Loureiro, C. Rodrigues, and S. Castro, "Small reverse osmosis units using PV systems for water purification in rural places," *Desalination*, vol. 137, no. 1–3, pp. 39–44, 2001, doi: 10.1016/S0011-9164(01)00202-8.

[67]   N. Akther, A. Sodiq, A. Giwa, S. Daer, H. A. Arafat, and S. W. Hasan, "Recent advancements in forward osmosis desalination: A review," *Chem. Eng. J.*, vol. 281, pp. 502–522, 2015, doi: 10.1016/j.cej.2015.05.080.

[68]   M. Q. Seah, W. J. Lau, P. S. Goh, H. H. Tseng, R. A. Wahab, and A. F. Ismail, "Progress of interfacial polymerization techniques for polyamide thin film

(Nano)composite membrane fabrication: A comprehensive review," *Polymers (Basel).*, vol. 12, no. 12, pp. 1–39, 2020, doi: 10.3390/polym12122817.

[69] M. Qasim, M. Badrelzaman, N. N. Darwish, N. A. Darwish, and N. Hilal, "Reverse osmosis desalination: A state-of-the-art review," *Desalination*, vol. 459, pp. 59–104, 2019, doi: 10.1016/j.desal.2019.02.008.

[70] B. Robert and E. B. Brown, "No 主観的健康感を中心とした在宅高齢者における 健康関連指標に関する共分散構造分析Title," no. 1, pp. 1–14, 2004, doi: http://hdl.handle.net/1828/5207.

[71] A. Al-Karaghouli and L. L. Kazmerski, "Energy consumption and water production cost of conventional and renewable-energy-powered desalination processes," *Renew. Sustain. Energy Rev.*, vol. 24, pp. 343–356, 2013, doi: 10.1016/j.rser.2012.12.064.

[72] K. P. Lee, T. C. Arnot, and D. Mattia, "A review of reverse osmosis membrane materials for desalination-Development to date and future potential," *J. Memb. Sci.*, vol. 370, no. 1–2, pp. 1–22, 2011, doi: 10.1016/j.memsci.2010.12.036.

[73] D. T. F. D. F. Erlangen-nürnberg, "Low Temperature Processing Route of Silicon Nanoparticle Layers for Solar Cell Application," pp. 45–46, [Online]. Available: https://www.researchgate.net/publication/328447517_Low_Temperature_Processing_Route_of_Silicon_Nanoparticle_Layers_for_Solar_Cell_Application

[74] E. Maynard and C. Whapham, "Quality and supply of water used in hospitals," *Decontam. Hosp. Healthc.*, pp. 45–69, 2019, doi: 10.1016/B978-0-08-102565-9.00003-0.

[75] J. Schwinge, P. R. Neal, D. E. Wiley, D. F. Fletcher, and A. G. Fane, "Spiral wound modules and spacers: Review and analysis," *J. Memb. Sci.*, vol. 242, no. 1–2, pp. 129–153, 2004, doi: 10.1016/j.memsci.2003.09.031.

[76] A. J. Karabelas, M. Kostoglou, and C. P. Koutsou, "Modeling of spiral wound membrane desalination modules and plants - review and research priorities," *Desalination*, vol. 356, pp. 165–186, 2015, doi: 10.1016/j.desal.2014.10.002.

[77]   A. Pron and P. Rannou, "Processible conjugated polymers: From organic semiconductors to organic metals and superconductors," *Prog. Polym. Sci.*, vol. 27, no. 1, pp. 135–190, 2002, doi: 10.1016/S0079-6700(01)00043-0.

[78]   H. Mokarizadeh, S. Moayedfard, M. S. Maleh, S. I. G. P. Mohamed, S. Nejati, and M. R. Esfahani, "The role of support layer properties on the fabrication and performance of thin-film composite membranes: The significance of selective layer-support layer connectivity," *Sep. Purif. Technol.*, vol. 278, 2022, doi: 10.1016/j.seppur.2021.119451.

[79]   M. Baghbanzadeh, L. Carbone, P. D. Cozzoli, and C. O. Kappe, "Microwave-assisted synthesis of colloidal inorganic nanocrystals," *Angew. Chemie - Int. Ed.*, vol. 50, no. 48, pp. 11312–11359, 2011, doi: 10.1002/anie.201101274.

[80]   G. Zhan and H. C. Zeng, "Alternative synthetic approaches for metal-organic frameworks: transformation from solid matters," *Chem. Commun.*, vol. 53, no. 1, pp. 72–81, 2017, doi: 10.1039/c6cc07094a.

[81]   J. Mittal, "Recent progress in the synthesis of Layered Double Hydroxides and their application for the adsorptive removal of dyes: A review," *J. Environ. Manage.*, vol. 295, 2021, doi: 10.1016/j.jenvman.2021.113017.

[82]   T. H. Lin *et al.*, "Unveiling the surface precipitation effect of Ag ions in Ag-doped TiO2 nanofibers synthesized by one-step hydrothermal method for photocatalytic hydrogen production," *J. Taiwan Inst. Chem. Eng.*, vol. 120, pp. 291–299, 2021, doi: 10.1016/j.jtice.2021.03.011.

[83]   B. Robert and E. B. Brown, "No 主観的健康感を中心とした在宅高齢者における 健康関連指標に関する共分散構造分析Title," no. 1, pp. 1–14, 2004, doi: https://doi.org/10.1016/j.surfin.2023.103163.

[84]   Z. Bano *et al.*, "Synthesis, characterization and applications of 3D porous graphene hierarchical structure by direct carbonization of maleic acid," *Ceram. Int.*, vol. 48, no. 6, pp. 8409–8416, 2022, doi: 10.1016/j.ceramint.2021.12.048.

[85]   S. Nasir, M. Z. Hussein, Z. Zainal, N. A. Yusof, S. A. Mohd Zobir, and I. M.

Alibe, "Potential valorization of by-product materials from oil palm: A review of alternative and sustainable carbon sources for carbon-based nanomaterials synthesispotential valorization of by-product materials from oil palm: A review of alternative and sustainable carbon sources for carbon-based nanomaterials synthesis," *BioResources*, vol. 14, no. 1, pp. 2352–2388, 2019, doi: 10.15376/biores.14.1.Nasir.

[86] M. L. Frezzotti, F. Tecce, and A. Casagli, "Raman spectroscopy for fluid inclusion analysis," *J. Geochemical Explor.*, vol. 112, pp. 1–20, 2012, doi: 10.1016/j.gexplo.2011.09.009.

[87] A. Shaji and A. K. Zachariah, "Surface Area Analysis of Nanomaterials," *Therm. Rheol. Meas. Tech. Nanomater. Charact.*, vol. 3, pp. 197–231, 2017, doi: 10.1016/B978-0-323-46139-9.00009-8.

[88] "Recommendations for the characterization of porous solids (Technical Report)," *Pure Appl. Chem.*, vol. 66, no. 8, pp. 1739–1758, 1994, doi: 10.1351/pac199466081739.

[89] D. Emadzadeh, W. J. Lau, T. Matsuura, A. F. Ismail, and M. Rahbari-Sisakht, "Synthesis and characterization of thin film nanocomposite forward osmosis membrane with hydrophilic nanocomposite support to reduce internal concentration polarization," *J. Memb. Sci.*, vol. 449, pp. 74–85, 2014, doi: 10.1016/j.memsci.2013.08.014.

[90] A. M. Aboraia *et al.*, "Structural characterization and optical properties of zeolitic imidazolate frameworks (ZIF-8) for solid-state electronics applications," *Opt. Mater. (Amst).*, vol. 100, 2020, doi: 10.1016/j.optmat.2019.109648.

[91] M. M. Said, A. H. M. El-Aassar, Y. H. Kotp, H. A. Shawky, and M. S. A. A. Mottaleb, "Performance assessment of prepared polyamide thin film composite membrane for desalination of saline groundwater at Mersa Alam-Ras Banas, Red Sea Coast, Egypt," *Desalin. Water Treat.*, vol. 51, no. 25–27, pp. 4927–4937, 2013, doi: 10.1080/19443994.2013.795208.

[92] L. Wang *et al.*, "The influence of dispersed phases on polyamide/ZIF-8 nanofiltration membranes for dye removal from water," *RSC Adv.*, vol. 5, no. 63, pp. 50942–50954, 2015, doi: 10.1039/c5ra06185g.

[93] E. G. Masibi, T. A. Makhetha, and R. M. Moutloali, "Effect of the Incorporation of ZIF-8@GO into the Thin-Film Membrane on Salt Rejection and BSA Fouling," *Membranes (Basel).*, vol. 12, no. 4, 2022, doi: 10.3390/membranes12040436.

[94] M. Ghafoor, Z. U. Khan, M. H. Nawaz, N. Akhtar, A. Rahim, and S. Riaz, "In-situ synthesized ZIF-67 graphene oxide (ZIF-67/GO) nanocomposite for efficient individual and simultaneous detection of heavy metal ions," *Environ. Monit. Assess.*, vol. 195, no. 3, 2023, doi: 10.1007/s10661-023-10966-8.

[95] I. H. Aljundi, "Desalination characteristics of TFN-RO membrane incorporated with ZIF-8 nanoparticles," *Desalination*, vol. 420, pp. 12–20, 2017, doi: 10.1016/j.desal.2017.06.020.

[96] I. H. Aljundi, "Desalination characteristics of TFN-RO membrane incorporated with ZIF-8 nanoparticles," *Desalination*, vol. 420, no. December 2016, pp. 12–20, 2017, doi: 10.1016/j.desal.2017.06.020.

[97] W. Sun, X. Zhai, and L. Zhao, "Synthesis of ZIF-8 and ZIF-67 nanocrystals with well-controllable size distribution through reverse microemulsions," *Chem. Eng. J.*, vol. 289, pp. 59–64, 2016, doi: 10.1016/j.cej.2015.12.076.

[98] H. Yin, H. Kim, J. Choi, and A. C. K. Yip, "Thermal stability of ZIF-8 under oxidative and inert environments: A practical perspective on using ZIF-8 as a catalyst support," *Chem. Eng. J.*, vol. 278, pp. 293–300, 2015, doi: 10.1016/j.cej.2014.08.075.

[99] F. Wang, T. Zheng, R. Xiong, P. Wang, and J. Ma, "Strong improvement of reverse osmosis polyamide membrane performance by addition of ZIF-8 nanoparticles: Effect of particle size and dispersion in selective layer," *Chemosphere*, vol. 233, pp. 524–531, 2019, doi: 10.1016/j.chemosphere.2019.06.008.

[100] G. M. Geise, D. R. Paul, and B. D. Freeman, "Fundamental water and salt transport properties of polymeric materials," *Prog. Polym. Sci.*, vol. 39, no. 1, pp. 1–42, 2014, doi: 10.1016/j.progpolymsci.2013.07.001.

[101] M. You, J. Yin, R. Sun, X. Cao, and J. Meng, "Water/salt transport properties of organic/inorganic hybrid films based on cellulose triacetate," *J. Memb. Sci.*, vol. 563, pp. 571–583, 2018, doi: 10.1016/j.memsci.2018.06.035.

[102] J. Duan, Y. Pan, F. Pacheco, E. Litwiller, Z. Lai, and I. Pinnau, "High-performance polyamide thin-film-nanocomposite reverse osmosis membranes containing hydrophobic zeolitic imidazolate framework-8," *J. Memb. Sci.*, vol. 476, pp. 303–310, 2015, doi: 10.1016/j.memsci.2014.11.038.

[103] I. Wan Azelee *et al.*, "Enhanced desalination of polyamide thin film nanocomposite incorporated with acid treated multiwalled carbon nanotube-titania nanotube hybrid," *Desalination*, vol. 409, pp. 163–170, 2017, doi: 10.1016/j.desal.2017.01.029.